Exploring miRNA Function and Host Response to *Coxiella burnetii* Infection

by

Madhur Sachan

A dissertation submitted in partial fulfillment of the
requirements for the degree of

Doctor of Philosophy
in
Biology

Dissertation Committee:
Kenneth Stedman, Chair
Rahul Raghavan
Brooke Ann Napier
Anna-Louise Reysenbach

Portland State University
2021

ABSTRACT

Alveolar macrophages attempt to control bacterial infection through a spectrum of defense processes, including induction of apoptosis, autophagy, inflammatory response, and nutrient sequestration. MicroRNAs (miRNAs), a class of small non-coding RNAs, are involved in a spectrum of physiological processes, including immune response to intracellular infections. However, whether microRNAs have any functions in host response to *Coxiella burnetii* infection is unknown. *Coxiella burnetii* is a highly infectious intracellular pathogen that causes Q fever, a zoonosis with a worldwide occurrence. In this work, I investigated the functions of miRNAs in host response to *C. burnetii* infection and found that miRNAs are an integral component of macrophages' stage-specific response to *C. burnetii* infection, and inhibition of miR-143-3p likely facilitates the pathogen's intracellular growth. I also examined how different isolates of *C. burnetii* impact host inflammatory responses, and using single-cell analysis discovered that certain subpopulations of infected macrophages are likely more pathogen friendly than others. Additionally, I determined that gallium-protoporphyrin IX (GaPPIX), a heme analog, inhibits *C. burnetii*'s axenic and intracellular growth, and could potentially be used as a therapeutic agent. Together, these results could contribute to the development of novel miRNA- or GaPPIX-based therapeutic agents and could be applied to better understand the virulence strategies of other intracellular pathogens.

ACKNOWLEDGEMENTS

I sincerely thank my mentor, Dr. Rahul Raghavan, for his continual support. I am grateful to him for letting me acquire skills that have shaped my ability to design and conduct independent experiments. I am indebted to my committee members – Drs. Kenneth Stedman, Brooke Napier, and Anna-Louise Reysenbach, for their support and guidance throughout the last four years. My lab mates and friends, including Amanda Brenner, Madeline Krieger, Abe Moses, Jim Archuleta, Max Schreyer, Jess Millar, Canan Schumann, and Anna St Lorenz for a wonderful learning environment. I am grateful to have constant support from the people and facilities at Portland State University and Oregon Health & Science University. I am thankful to Dr. Dan Voth and his lab group at the University of Arkansas for Medical Sciences for providing the lung biopsy samples. I dedicate this work to my parents for their faith in my abilities.

TABLE OF CONTENTS

LIST OF TABLES

LIST OF FIGURES

Chapter I

Introduction to *Coxiella burnetii*, host response, and microRNAs

I. Discovery of *Coxiella burnetii*

Coxiella burnetii is the etiological agent of Q (query) fever (1). This zoonotic disease can manifest either as a self-limiting acute flu-like illness or as more serious chronic diseases such as infective endocarditis or granulomatous hepatitis (2). Unlike acute infections that may require 2-3 weeks of antibiotic treatment, chronic *C. burnetii* infections are very difficult to treat and requires 1.5-3 years of combination antibiotic therapy (2).

Discovery

The first descriptions of Q fever were published in the late 1930s by Edward Derrick and Macfarlane Burnet in Australia (3, 4). This illness was named Query fever due to its unclear origin. Meanwhile, at the Rocky Mountain Laboratory (RML) in the United States, Herald Cox and Gordon Davis identified a infectious agent that passed through filters by feeding *Dermacentor andersoni* ticks on guinea pigs (5). The causal link between this unidentified agent and Q fever was discovered serendipitously due to a laboratory-acquired infection by this agent (6). Due to its "rickettsial nature" the bacterium was initially placed in the order *Rickettsiales*. However, 16S rRNA analysis later showed that the bacterium belonged to the order *Legionallales* and was hence placed

in the phylum *Proteobacteria*, class γ-Proteobacteria, order *Legionellales*, family *Coxiellaceae*, under the genus "*Coxiella*" and species "*burnetii*" (3, 7).

II. Epidemiology and disease

C. burnetii has a worldwide geographical distribution and infects mammals (mainly cattle, goats, and sheep), birds, reptiles, and arthropods (8). *C. burnetii* is typically transmitted from animals to humans by aerosols derived from infected excreta and birth products (9). In addition, ticks such as *Dermacentor andersoni* could serve as vectors for transmission to human hosts (10). In contrast to most other intracellular pathogens, *C. burnetii* is resistant to environmental stressors such as elevated temperature, osmotic pressure, and ultraviolet radiation (11, 12). Due to its environmental stability, low aerosol infectious dose (<10 bacteria can cause disease), and ability to cause influenza-like illness, the CDC has classified *Coxiella* as a category B select agent (13).

Q fever typically remains undiagnosed due to its non-specific flu-like symptoms that are common to many respiratory infections. One study suggests that the seroprevalence of Q fever in the United States is ~3.1% higher than the cases reported to the CDC (14). The largest reported outbreak of Q fever occurred between 2007-2010 in the Netherlands (15). During this period, approximately 4,000 individuals contracted acute Q fever, particularly in intensive goat farming areas. The outbreak was controlled by vaccination and culling of more than 50,000 goats and sheep, but it highlighted the need for effective diagnosis and treatment.

Diagnosis

The diagnosis of Q fever includes polymerase chain reaction (PCR) and serological methods such as immunofluorescence assays (IFA), complement fixation test (CFT), and enzyme-linked immunosorbent assay (ELISA) to assess immunoglobulin G (IgG) titer (16). The immune response induces antibodies against *C. burnetii* phase I (virulent reference isolate) or phase II (clonal derivative of phase I isolate) antigen, and elevated phase I or phase II IgG titers indicate a Q fever infection (1).

Symptoms, treatment, and vaccine

Q fever is an acute febrile illness with flu-like symptoms such as high fever, headaches, cough, and vomiting that may develop weeks after exposure (16). Almost half of the infected individuals remain asymptomatic in primary infection. Acute infection can be self-limiting or may require 2-3 weeks of doxycycline treatment (17). Acute infection has been shown to present as pneumonia and hepatitis whereas chronic Q fever can present as endocarditis, lymphadenitis, vascular and osteoarticular infections (16). It has been hypothesized that chronic Q fever may occur due to the reactivation of bacteria from a previous infection (18). Chronic infection is very difficult to treat and requires a combination of doxycycline and hydroxychloroquine (1.5-3 years), or doxycycline and fluoroquinolone (3-4 years) (19, 20). In addition, strains of *C. burnetii* resistant to doxycycline have been reported and necessitate an effective therapeutic against this pathogen (21). There is no approved Q fever vaccine in the United States, however, Q-

Vax, an inactivated whole-cell phase I strain of *C. burnetii* (Henzerling RSA334), is licensed in Australia (22, 23).

III. Bacteriology

C. burnetii is an obligate intracellular Gram-negative bacillus that has a biphasic lifestyle. The environmentally stable small cell variant (SCV) form is less than 0.2 μM in size that transitions into a metabolically active form known as large cell variant (LCV) within a host cell **(Figure 1)** (24, 25). The genome of *C. burnetii* isolates ranges from 1.9 to 2.2 megabases (Mb) with a single plasmid or an integrated plasmid sequence within the chromosome (26, 27). *C. burnetii* has a reduced genome rich in mobile elements and genes encoding eukaryotic domain-containing proteins, suggesting that transition to its intracellular lifestyle is a relatively recent event in its evolution (26).

Different isolates or strains of *C. burnetii* have been placed into eight groups (28–31). Of these, notable isolates are: (1) Nine Mile RSA493 Phase I (NMI), a reference isolate from group I that typically causes acute disease and contains the full length lipopolysaccharide (LPS); (2) Nine Mile RSA439 Phase II, clone 4 (NMII) is a clonal derivative of NMI from group I with a truncated LPS that does not cause disease and is a traditional lab strain of *C. burnetii* for use under biosafety level-2 conditions; (3) Graves Phase I/Q212 (Graves) is a group V isolate associated with chronic disease conditions such as endocarditis; and (4) Dugway 7E9-12 (Dugway) is group VI isolate isolated from rodents in Dugway, Utah that shows attenuated virulence in animal models.

The development of an axenic growth medium, termed acidified citrate cysteine medium (ACCM) has transformed *C. burnetii* research (32). The doubling time of

exponential growing *C. burnetii* is 9.1 h under axenic conditions, which is ~2 h less than its generation time in Vero cells (32). The currently known determinants of *C. burnetii*'s virulence are LPS, a Dot/Icm type IV secretion system (T4SS), and effector proteins secreted through the T4SS (33). The unique LPS of this pathogen facilitates immune evasion by shielding bacterial surface proteins from immune recognition by Toll-like receptors (TLRs) (34, 35). However, after repeated passaging in eukaryotic cells, LPS was shown to be truncated, lacking the terminal O antigen sugars, and was associated with loss of the disease-causing ability in immunocompetent hosts (35). Although T4SS facilitates the translocation of more that 100 effectors proteins into the host cytoplasm, the functions of only a few of them have been characterized (36). Among these effectors, AnkG, CaeA, CaeB are known to prevent host apoptosis, and Cig2, CvpF participates in the manipulation of autophagy (37–42). CstK and AnkF contributes the establishment of *Coxiella*-containing vacuole (CCV) (43, 44). IcaA inhibits the activation of host inflammasome and NopA reduces the nuclear import of transcription factors involved in the innate immune sensing of pathogens (45, 46).

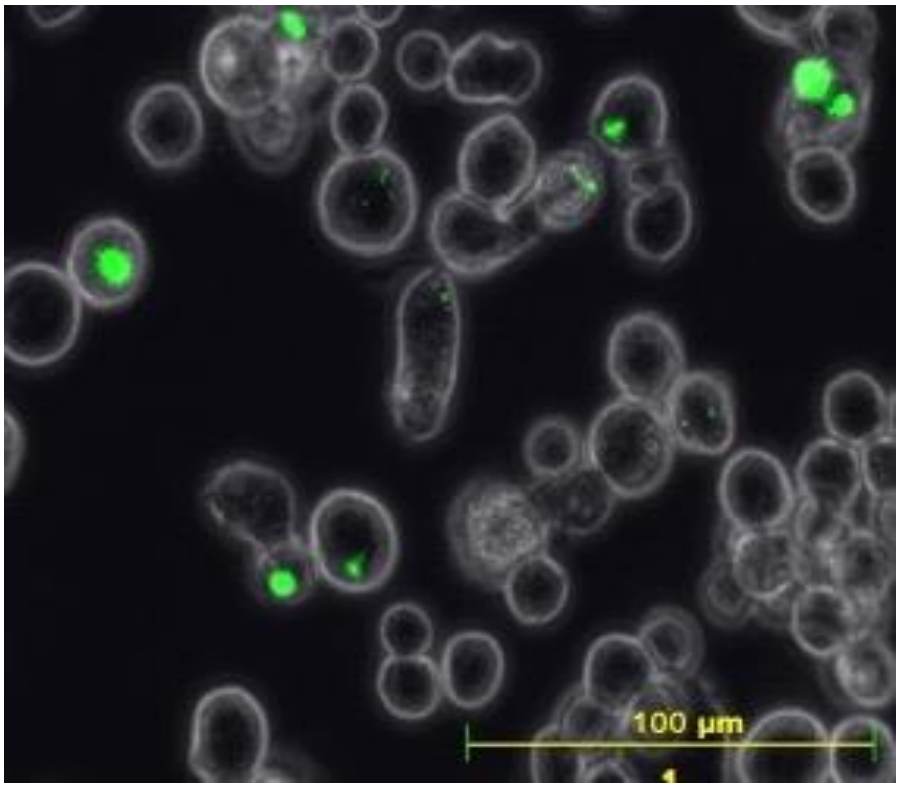

Figure 1. Fluorescent micrograph of THP-1 cells infected with green-fluorescent protein (GFP)-tagged *Coxiella burnetii.* The green color shows *Coxiella burnetii* growing inside *Coxiella*-containing vacuole at 72 hours post-infection. The image was taken at 400× magnification using FITC filter in a fluorescence microscope (Keyence).

IV. Intracellular life and host response

Shortly after uptake into eukaryotic cells, typically by alveolar macrophages, *C. burnetii*-harboring phagosomes mature through a series of coordinated fusion events with endolysosomal, autophagic, and secretory vesicles **(Figure 2)** (47). Initially, *C. burnetii* binds to $\alpha_v\beta_3$ integrin and associated proteins that promote actin-dependent phagocytosis (48–50). After internalization, the nascent CCV acquires markers EEA1 (early endosome antigen 1) and small GTPase Rab5 (Ras-related protein Rab-5A) typical to normal phagosomal development (33, 51–53). Rab5 elicits fusion of nascent phagosome with early endosomes, resulting in acidification of nascent CCV to approximately pH 5.4 (33). However, the nascent CCV also acquires autophagosomal marker LC3 (microtubule-associated protein 1A/1B-light chain 3), which is dependent on bacterial protein synthesis (53, 54). This nascent CCV matures through fusion and fission events with endosomes resulting in the acquisition of proteins LAMP1 (lysosomal associated membrane protein 1) and Rab7 (Ras-related protein Rab-7A) and forming the early CCV. From 8 hours to 2 days post-internalization, the expansion of the early CCV occurs inside the host cytoplasm, which is dependent on bacterial protein synthesis and acquisition of Rho-GTPase, and Rab1B proteins to the CCV membrane. During this process, vacuolar ATPase pumps protons into the maturing phagosome leading to decreased pH inside the early CCV to about pH 5 (33). Some proteins such as Rho-GTPase, and Rab1B acquired by the early CCV facilitate CCV maintenance and gain of additional membranes to create the spacious mature CCV (51). The mature CCV (pH 4.5-5) further gets decorated with additional proteins, including anti-apoptotic protein Bcl-2 that participates in the anti-apoptotic activity of *C. burnetii* (55). Each CCV maturation stage is associated with

acquiring specific host proteins on the CCV membrane as shown in **Table 1** (51). These proteins belong to diverse host processes such as endolysosomal, autophagy, secretory, and apoptosis signaling.

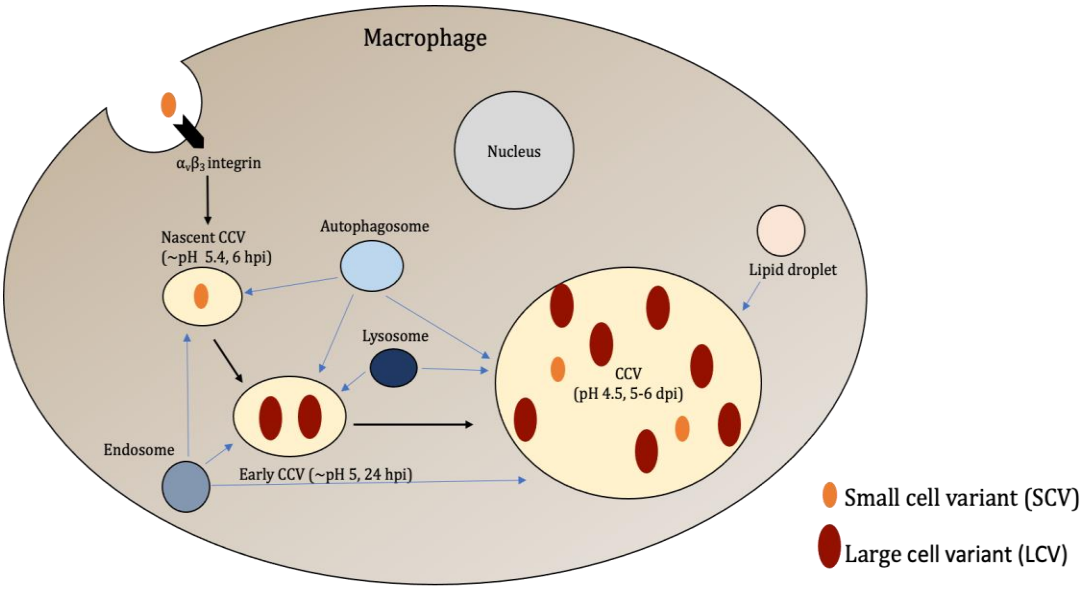

Figure 2. Maturation of *Coxiella*-containing vacuole (CCV). *C. burnetii* (orange) binds to $\alpha_v\beta_3$ integrin that promotes phagocytosis to internalize the bacteria. Within 6 hours post-infection (hpi), the bacteria reside in nascent CCVs. Within 24 hpi, an early CCV is formed after fusion with endosome, autophagosome, and lysosome. Here, bacterial small cell variant (SCV) transitions into metabolically active large cell variant (LCV) that secrete effector proteins through a type 4 secretion system (T4SS). This early CCV subsequently expands in a T4SS-dependent manner through continuous fusion with endosomes, autophagosomes, lysosomes, and acquires lipid droplets. Around 5-6 days post-infection (dpi), LCV can switch to SCV to maintain both forms of bacteria. Each CCV maturation stage is associated with acidification and the acquisition of specific host proteins on the CCV membrane that support *C. burnetii* growth.

Table 1. CCV maturation stage and acquired host proteins

Stage[a]	Acquired host proteins[b]
Nascent CCV	LC3, p62, Beclin-1, EEA1, Rab5, NDP52, PI(3)P, VAMP-3, VAMP-7, VAMP-8, Vti1a, Vti1b, Synaptotagmin VII, Clathrin
Early CCV	nascent CCV associated proteins and PS, LAMP1, LAMP2, LAMP3, v-ATPase, Cathepsin D, Rab7, Rab1β, Rab24, RhoA, VASP, HOPS, ORP1L, Flotillin 1, Flotillin 2, Galectin 3, Galectin 8
Late CCV	early CCV associated proteins and mTORC1, Cathepsin B, Arl8, p150, Arp3, WASH, FAM21, VPS35, Cortactin, Calnexin, Bad, 14-3-3β, Bcl-2, PKA, Syntaxin 8, Filipin

[a]CCV, *Coxiella*-containing vacuole

[b]LC3, microtubule-associated protein 1A/1B-light chain 3; p62, sequestosome 1; EEA1, early endosome antigen 1; Rab5, Ras-related protein Rab-5A; NDP52, calcium binding and coiled-coil domain 2; PI(3)P, phosphatidylinositol 3-phosphate; VAMP-3, vesicle associated membrane protein 3; Vti1a, vesicle transport through interaction with T-SNAREs 1A; PS, phosphatidylserine; LAMP1, lysosomal associated membrane protein 1; RhoA, Ras homolog family member A; VASP, vasodilator stimulated phosphoprotein; HOPS, homotypic fusion and protein-sorting; ORP1L, oxysterol binding protein like 1A; mTORC1, mammalian target of rapamycin complex 1; Arl8, ADP-ribosylation factor-like protein 8; p150, chromatin assembly factor 1 subunit A; Arp3, actin-related protein 3; WASH, Wiskott–Aldrich syndrome protein; FAM21, WASH complex subunit FAM21; VPS35, VPS35 retromer complex component; Bad, Bcl2-associated agonist of cell death; Bcl-2, B-cell lymphoma-2; PKA, protein kinase A.

Experimental models

The animal models useful to understanding the host immune response to *C. burnetii* infection include guinea pigs, *Galleria mellonella*, *Drosophila melanogaster*, severe combined immunodeficient (SCID) mice, and primates (rhesus and cynomolgus macaques) (56–58). In *ex vivo* human lung tissue platforms, *C. burnetii* preferentially replicates in human alveolar macrophage (hAMs); and *in vitro* models such as epithelial, fibroblast, trophoblast, macrophage, and endothelial cell lines and primary cells are also reliable to model host-*C. burnetii* interactions (59–62).

Innate and adaptive immune responses

Both innate and adaptive arms of the host immune response respond to *C. burnetii* infection. The LPS of *C. burnetii* subverts receptor-mediated phagocytosis by interfering with the interplay between integrins, CR3 (complement receptor-3), actin remodeling, and activating protein tyrosine kinases (35, 48). The LPS mediated interference results in low internalization of the virulent strain compared to the avirulent *C. burnetii*, which contains a truncated LPS (35). In addition, LPS of virulent strain is recognized by TLR4 (toll-like receptor 4), but unlike the avirulent strain, virulent *C. burnetii* LPS seems to mask its recognition by TLR2. It has been predicted that virulent bacterial LPS breaks a potential physical link between TLR-4 and TLR-2 that leads to inactivation of p38α mitogen-activated protein kinase (MAPK) and reduced inflammatory response compared to avirulent *C. burnetii* (34, 35).

Macrophage polarization likely plays a role in controlling *C. burnetii* replication, and *C. burnetii* attempts to convert the proinflammatory M1 activation state to an atypical anti-inflammatory M2 state associated with a hospitable environment (35). These atypically polarized macrophages exhibit induced expression of M2 activation-related genes (such as transforming growth factor-β1, IL-1 receptor antagonist, CCL18, the mannose receptor, and arginase-1) as well as M1 activation-related genes (such as IL-6 and CXCL8) (63). In acute Q fever, *C. burnetii* stimulates an M1 polarization in monocytes that can control the infection (64). However, in macrophages, the atypical M2 polarization cannot prevent *C. burnetii* infection. In chronic Q fever, M2 cytokines such as IL-10 or ingestion of apoptotic cells trigger polarization of infected monocytes and macrophages towards an M2 phenotype that allows bacterial growth. A few M1 associated proteins such as IFN-γ (interferon gamma) and TNF-α (tumor necrosis factor) have been experimentally shown to be critical for the early control of infection (65). In addition, chemokines (CCL2 and CCL5) can directly interfere with granuloma formation associated with the resolution of Q fever (66).

Both T cells and B cells of the adaptive immune response contribute to control *C. burnetii* infection. CD8+ T cells play a significant role than CD4+ T cells in controlling *C. burnetii* infection due to their ability to produce IFN-γ (67). IFN-γ promotes an antimicrobial response by mechanisms including phagosome maturation, apoptosis, production of cytokines such as TNF-α, and nutrient regulation such as iron or tryptophan (65, 68–71). Further, it has been suggested that contribution of antibodies against *C. burnetii* infection is complicated and antibodies may remain dispensable for pathogen clearance (70). Indeed, during acute Q fever, cell-mediated immunity, IFN-γ, and

granuloma protect against *C. burnetii*. However, defective granuloma formation, cell-mediated immunity, and overproduction of IL-10 are characteristics of chronic infection (70).

V. Manipulation of host signaling

Several signaling pathways in the host cell are perturbed in *C. burnetii* infection, including apoptosis, autophagy, inflammatory pathways, intracellular trafficking, and kinase signaling. To facilitate its intracellular survival and replication, *C. burnetii* manipulates these signaling through the effector proteins secreted by its T4SS (51).

Apoptosis

Certain intracellular pathogens induce apoptosis, a type of regulated cell death, to invade surrounding cells, whereas others inhibit this process for successful infection (72). *C. burnetii* prevents host apoptosis modalities to prolong viability of the host cell before exiting by an unknown mechanism. It has been shown that *C. burnetii* inhibits staurosporine-induced intrinsic apoptosis and TNF-α mediated extrinsic apoptosis of human macrophages (73). *C. burnetii* reduces cleavage of caspase-3, caspase-9, poly(ADP-ribose) polymerase (PARP) and prevents the release of mitochondrial cytochrome c to antagonize apoptosis. In addition, this pathogen promotes a pro-survival signaling pathway by activating Akt, Erk1/2, and PKA, recruits Bcl-2 to the CCV,

inactivates Bad, and stimulates expression of Mcl-1 in neutrophils (51, 74–76). As mentioned earlier, a few T4SS-secreted effector proteins such as AnkG, CaeA, and CaeB are also known to be involved in apoptosis inhibition by an unknown mechanism (37–41). AnkG binds to host p32 and enters the nucleus to prevent apoptosis, and CaeA and CaeB prevent mitochondrial-dependent intrinsic apoptosis.

Autophagy

Autophagy is an evolutionarily conserved process induced by metabolic and infection-mediated stresses that results in lysosomal degradation of unwanted cytoplasmic entities (77). Macroautophagy (herein referred to as autophagy) is the best-characterized form of autophagy that involves a specialized double-membrane vesicle, known as autophagosome. Intracellular pathogens engage with autophagy to gain nutrients or prevent lysosomal degradation (78). Lysosomal degradation does not happen for *C. burnetii*, and when CCV engages with the autophagosomes, autophagy-related proteins such as LC3 and p62 get recruited to CCVs in a T4SS-dependent manner (79). Recently, a T4SS effector termed CvpF has been shown to interact with the host GTPase RAB26, resulting in the acquisition of LC3 to CCVs and proper vacuole biogenesis (42). In addition, *C. burnetii* inhibits mTORC1, an autophagy-inhibiting protein, and its localization to endolysosomal membranes (80). Inhibition of components of autophagy thus culminates in reduced *C. burnetii* replication (52, 80). Together, induction of autophagy is critical for proper CCV development and *C. burnetii* replication.

Inflammatory pathways

After confronting the intracellular pathogens, alveolar macrophages typically promote a proinflammatory response and recruits immune cells to the site of infection as an innate defense response against the pathogen (81). Although the inflammatory response to *C. burnetii* is not well defined, studies have shown that avirulent *C. burnetii* stimulates IL-1β production, NLRP3 inflammasome, and caspase-1-dependent pyroptosis, a form of regulated cell death (45, 60, 82). In contrast, virulent isolates suppress the IL-1β, inflammasome response, and do not promote pyroptosis in human macrophages, probably due to different LPS composition or secreted effectors than avirulent isolates. The disparity in the inflammatory response to *C. burnetii* appears to depend on the type of host cells as well as the nature of bacterial isolate.

VI. MicroRNAs

MicroRNAs (miRNAs) are a class of single-stranded small (~22 nucleotides), non-coding RNAs (ncRNAs) that contribute to the post-transcriptional gene regulation in a wide range of eukaryotes and some viruses (83). More than 2500 mature miRNAs are currently annotated in miRBase, a depository of published miRNA sequences (84). miRNAs can regulate more than 60% of the human transcriptome (85), typically by inhibiting target gene expression that combines translation repression and messenger RNA (mRNA) degradation (86, 87).

Evolution, biogenesis, and nomenclature

miRNAs have emerged multiple times in eukaryotes from an ancestral RNA silencing pathway called RNA interference (RNAi) (88). RNAi is considered to have been present in the last common ancestor of eukaryotes to defend against viruses and transposable elements (88). The formation of miRNA is a multistep process that regulates miRNA maturation (89, 90) **(Figure 3)**. Canonically, miRNA genes are transcribed by RNA polymerase II, resulting in a primary miRNA transcript or pri-miRNAs. Each pri-miRNA forms at least one distinct hairpin structure that is cleaved at the double-stranded stem region by the Microprocessor, a complex of Drosha endonuclease and dimeric RNA-binding protein DGCR8, to release a precursor miRNA (pre-miRNA). The pre-miRNA is then exported to the cytoplasm by the action of Exportin 5 and RAN–GTP for further processing by the endonuclease Dicer. Dicer cleaves off the loop region of the hairpin to generate the approximately 22 to 23 nt miRNA duplex, which contains the miRNA paired to its passenger strand (miRNA*). This miRNA duplex is then loaded into the RNA-induced silencing complex (RISC) that consists of Argonaute (AGO) and associated proteins. Here, the seed sequences (nucleotides at positions 2–8 from 5' end) of the guide miRNA (a strand of the miRNA duplex, which incorporates into RISC and silences the gene expression) strand complementarily base-pairs with mRNA and other targets, whereas the passenger strand is usually degraded.

The standard nomenclature for miRNAs uses a specific convention maintained by miRBase (91). For example, in hsa-miR-121, the first three letters specify the organism (such as *Homo sapiens*), followed by mature miRNA as “miR”. The gene encoding miRNA or stem-loop portion in the primary transcript is depicted as “mir”. Distinct

precursor sequences and genomic loci expressing identical mature sequences are depicted as hsa-mir-121-1 and hsa-mir-121-2. Closely related mature sequences are depicted by lettered suffixes such as hsa-miR-121a and hsa-miR-121b. In addition, sometimes two different ~22nt sequences miRNAs originate from the same precursor, in which the mature sequences are assigned as miR-56 (the predominantly expressed product) and miR-56* (from the opposite arm of the precursor) but if the expression data for such sequences are insufficient to determine the predominantly expressed product, names such as miR-143-5p (from the 5' arm) and miR-143-3p (from the 3' arm) are assigned.

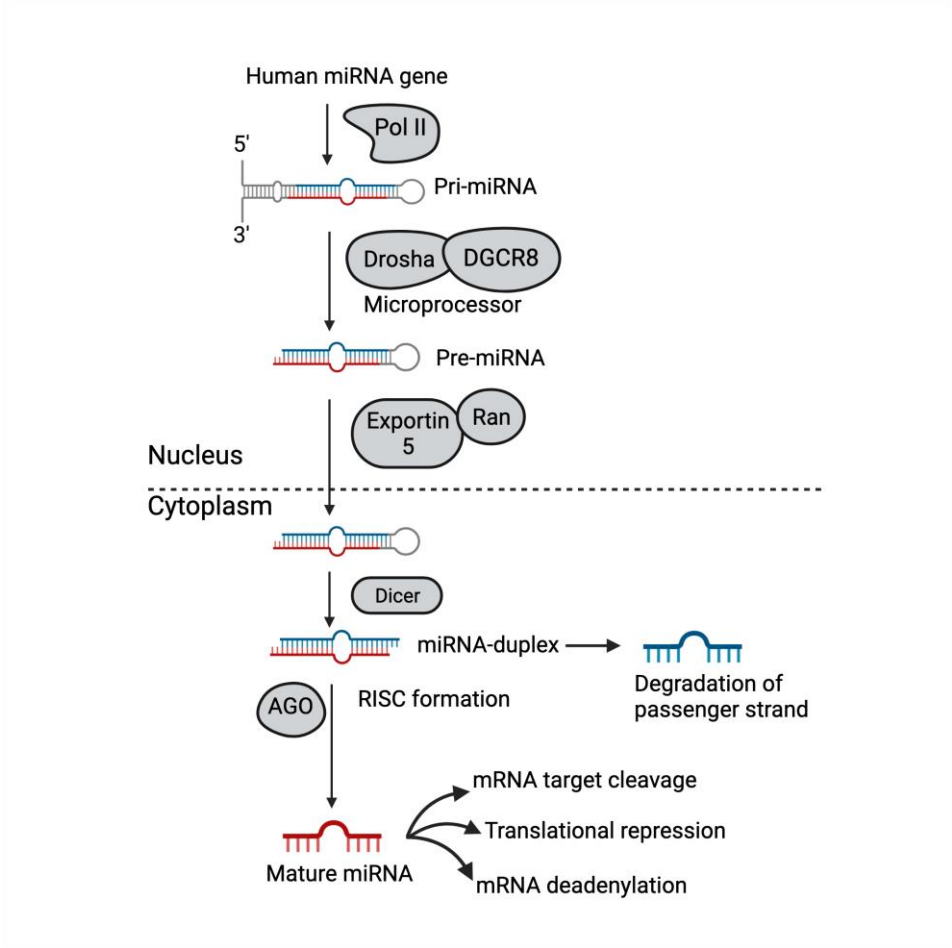

Figure 3. miRNA processing pathway. Primary miRNA transcript (pri-miRNA) is produced by RNA polymerase II (pol II) in the nucleus. pri-miRNA is cleaved by the microprocessor complex Drosha–DGCR8 resulting in precursor miRNA (pre-miRNA), which is exported into the cytoplasm by Exportin-5 and Ran-GTP. In the cytoplasm, the endonuclease Dicer cleaves the hairpin of pre-miRNA, and the one strand of the mature miRNA duplex, mature miRNA (red), gets loaded with Argonaute (AGO) proteins into the RNA-induced silencing complex (RISC). This guide strand directs the RNA-induced silencing complex (RISC) to the target mRNA cleavage, translational repression, or deadenylation, and the passenger strand (blue) is degraded.

Functional regulation and target prediction

miRNAs have transcriptionally regulated tissue-specific expression patterns (86). miRNA target sites are typically present in the 3' untranslated region (UTR) of mRNAs **(Figure 4)**. These target sites possess complementarity to the seed region, a conserved sequence that is typically situated at positions 2-8 from the miRNA 5'-end. Animal miRNAs bound to AGO protein in RISC recognize their mRNA targets by base-pairing to partially complementary binding sites. AGO proteins interact with a GW182 protein that results in deadenylation of the mRNA target, which is followed by decapping and 5'-to-3' exonucleolytic decay of the mRNA. In addition, miRNAs can inhibit translation initiation by interfering with the activity and/or assembly of the eukaryotic initiation factor 4F (eIF4F) complex. Based on the similarity in their seed sequences, which are primarily responsible for targeting mRNA, these molecules are grouped into different families.

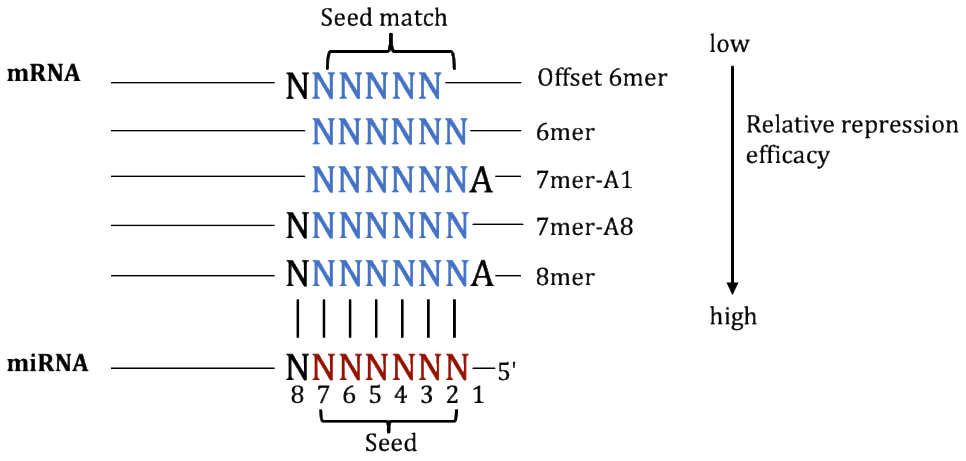

Figure 4. MicroRNA target sites. In a canonical mRNA target, the strongest seed match is considered to be an 8mer that includes perfect Watson–Crick (WC) complementarity from nucleotides 2–8 of the miRNA seed in addition to an adenine across from the miRNA. The 7mer-m8 site shows perfect WC complementarity to nucleotides 2-8 of the mature miRNA (the seed + match at position 8), whereas the 7mer-A1 site consists of perfect WC complementarity to nucleotides 2-7 of the mature miRNA (seed) followed by an adenine residue. A 6mer generally shows the least repression efficacy.

Despite the expanding knowledge about the miRNA-target interactions, identifying potential miRNA targets in the human genome is still difficult (92). In contrast with plant miRNAs that bind to their targets with perfect complementarity, animal miRNAs show partial sequence complementarity or seed match (93). Therefore, miRNA targeting specificity and repression efficiency are determined by multiple sequence-specific and cell-specific variables (94):

(1) Seed match: A strong Watson–Crick (WC) pairing between a miRNA and mRNA is very critical for targeting (94). The strongest seed match is considered to be 8mer that includes a perfect WC complementarity from nucleotides 2–8 of the miRNA seed in addition to an adenine across from the miRNA followed by 7mer-m8, 7mer-A1 as described in **Figure 4.** Sometimes, noncanonical sites with no six adjacent WC pairs to the seed region (miRNA positions 2-8) can additionally have compensatory sites that base pairs with the miRNA to compensate for the imperfect seed match.

(2) Thermodynamic stability: Thermodynamic stability of the miRNA–mRNA duplex is measured by calculating the free energy of the putative binding (94). If the free energy is low, the pairing between miRNA–mRNA strands is considered strong and thereby a strongly predicted target.

(3) Sequence conservation: Conservation of target sequence in closely related species in orthologous 3' UTR sequences can reduce the false positive predictions (94). Compared to the other regions, miRNA seed regions show higher conservation probably due to the evolutionary conservation of microRNA regulatory circuits (95).

(4) Target site accessibility: Both the miRNA and the 3' UTR of target should be accessible in the region that corresponds to the seed to facilitate interaction (94).

Therefore, calculation of free energy required to make the complementary site accessible by the miRNA can improve the target prediction.

(5) Multiple binding sites: miRNAs form complex networks of interactions as one miRNA can target multiple mRNAs, and one mRNA can be regulated by multiple miRNAs in an additive, cooperative or competitive manner depending on their target site proximity (94). The target repression efficacy varies according to the number of miRNAs that bind to a target gene. Therefore, predictions based on multitargeting can increase the probability of finding true targets.

Despite relying on the features mentioned above and additional features such as increased local AU content, existing bioinformatic algorithms show a high false-positive or negative rate in predicting the targeting efficiency of miRNAs (96, 97). Therefore, a functional validation of miRNA-target-pathway networks is vital (92).

VII. miRNAs: Host defense or pathogen offense?

In the last decade, miRNAs have emerged as an integral part of the host immune response to bacterial pathogens (98). Eukaryotes employ these ncRNAs to regulate critical processes such as cell death, autophagy, and inflammation to neutralize infection (98, 99). Conversely, intracellular bacterial pathogens such as *Mycobacterium tuberculosis*, *Legionella pneumophila*, and *Chlamydia trachomatis* subvert miRNA expression to promote survival, replication, and persistence (100–104).

For example, macrophages infected with *M. tuberculosis* induce production of miR-142-3p that leads to the downregulation of N-Wasp, an actin-binding protein (105). N-Wasp downregulation limits the amount of actin required for the actin filament

formation in the early phagosome. Consequently, miR-142-3p induction results in reduced uptake of this pathogen as a host defense strategy. On the other hand, *M. tuberculosis*-infected macrophages show induction of miR-125a-3p that leads to downregulation of an autophagy inducer protein UVRAG (UV radiation resistance-associated gene) (106). Therefore, induction of miR-125a-3p in *infected macrophages* results in inhibition of autophagy and phagosomal maturation that favors intracellular *survival of M. tuberculosis.*

Collectively, such observations suggest that miRNAs could either serve to control infection or to promote intracellular survival of pathogens in a cell-specific context; however, whether miRNAs have a role in *C. burnetii* infection is unknown. The present study aims to elucidate the contribution of miRNAs in *C. burnetii* infection.

REFERENCES

1. Anderson A, Bijlmer H, Fournier P-E, Graves S, Hartzell J, Kersh GJ, Limonard G, Marrie TJ, Massung RF, McQuiston JH, Nicholson WL, Paddock CD, Sexton DJ. 2013. Diagnosis and management of Q fever--United States, 2013: recommendations from CDC and the Q Fever Working Group. *MMWR Recomm Rep* 62:1–30.
2. Angelakis E, Raoult D. 2010. Q Fever. *Vet Microbiol* 140:297–309.
3. Hechemy KE. 2012. History and prospects of *Coxiella burnetii* research. *Adv Exp Med Biol* 984:1–11.
4. Burnet FM, Freeman M. 1983. Experimental studies on the virus of "Q" fever. *Rev Infect Dis* 5:800–808.
5. Davis GE, Cox HR, Parker RR, Dyer RE. 1938. A filter-passing infectious agent isolated from ticks. *Public Health Reports* (1896-1970) 53:2259.
6. Dyer RE. 1939. Similarity of Australian "Q" Fever and a disease caused by an infectious agent isolated from ticks in Montana. *Public Health Reports* (1896-1970) 54:1229.
7. Weisburg WG, Dobson ME, Samuel JE, Dasch GA, Mallavia LP, Baca O, Mandelco L, Sechrest JE, Weiss E, Woese CR. 1989. Phylogenetic diversity of the *Rickettsiae*. *J Bacteriol* 171:4202–4206.
8. Knap N, Žele D, Glinšek Biškup U, Avšič-Županc T, Vengušt G. 2019. The prevalence of *Coxiella burnetii* in ticks and animals in Slovenia. *BMC Vet Res* 15:368.

9. Honarmand H. 2012. Q Fever: an old but still a poorly understood disease. *Interdiscip Perspect Infect Dis* 2012:131932.
10. Körner S, Makert GR, Mertens-Scholz K, Henning K, Pfeffer M, Starke A, Nijhof AM, Ulbert S. 2020. Uptake and fecal excretion of *Coxiella burnetii* by *Ixodes ricinus* and *Dermacentor marginatus* ticks. *Parasit Vectors* 13:75.
11. Burgdorfer W, Anacker RL, 1981. *Rickettsiae* and rickettsial diseases. *Academic Press.*
12. Minnick MF, Raghavan R. 2011. Genetics of *Coxiella burnetii*: on the path of specialization. *Future Microbiol* 6:1297–1314.
13. Oyston PCF, Davies C. 2011. Q fever: the neglected biothreat agent. *J Med Microbiol* 60:9–21.
14. Anderson AD, Kruszon-Moran D, Loftis AD, McQuillan G, Nicholson WL, Priestley RA, Candee AJ, Patterson NE, Massung RF. 2009. Seroprevalence of Q fever in the United States, 2003-2004. *Am J Trop Med Hyg* 81:691–694.
15. Dijkstra F, van der Hoek W, Wijers N, Schimmer B, Rietveld A, Wijkmans CJ, Vellema P, Schneeberger PM. 2012. The 2007–2010 Q fever epidemic in The Netherlands: characteristics of notified acute Q fever patients and the association with dairy goat farming. *FEMS Immunol Med Microbiol* 64:3–12.
16. Eldin C, Mélenotte C, Mediannikov O, Ghigo E, Million M, Edouard S, Mege J-L, Maurin M, Raoult D. 2017. From Q fever to *Coxiella burnetii* infection: a paradigm change. *Clin Microbiol Rev* 30:115–190.
17. Kersh GJ. 2013. Antimicrobial therapies for Q fever. *Expert Rev Anti Infect Ther* 11:1207–1214.

18. Zeman DH, Kirkbride CA, Leslie-Steen P, Duimstra JR. 1989. Ovine abortion due to *Coxiella burnetti* infection. *J Vet Diagn Invest* 1:178–180.

19. Raoult D, Houpikian P, Tissot Dupont H, Riss JM, Arditi-Djiane J, Brouqui P. 1999. Treatment of Q fever endocarditis: comparison of 2 regimens containing doxycycline and ofloxacin or hydroxychloroquine. *Arch Intern Med* 159:167–173.

20. Levy PY, Drancourt M, Etienne J, Auvergnat JC, Beytout J, Sainty JM, Goldstein F, Raoult D. 1991. Comparison of different antibiotic regimens for therapy of 32 cases of Q fever endocarditis. *Antimicrob Agents Chemother* 35:533–537.

21. Rolain J-M, Lambert F, Raoult D. 2005. Activity of telithromycin against thirteen new isolates of *C. burnetii* including three resistant to doxycycline. *Ann N Y Acad Sci* 1063:252–256.

22. Marmion BP, Ormsbee RA, Kyrkou M, Wright J, Worswick D, Cameron S, Esterman A, Feery B, Collins W. 1984. Vaccine prophylaxis of abattoir-associated Q fever. *Lancet* 2:1411–1414.

23. Zhang G, Samuel JE. 2004. Vaccines against *Coxiella* infection. *Expert Rev Vaccines* 3:577–584.

24. Minnick MF, Raghavan R. 2012. Developmental biology of *Coxiella burnetii*. *Adv Exp Med Biol* 984:231–248.

25. Heinzen RA, Hackstadt T, Samuel JE. 1999. Developmental biology of *Coxiella burnetii*. *Trends Microbiol* 7:149–154.

26. Seshadri R, Paulsen IT, Eisen JA, Read TD, Nelson KE, Nelson WC, Ward NL, Tettelin H, Davidsen TM, Beanan MJ, Deboy RT, Daugherty SC, Brinkac LM, Madupu R, Dodson RJ, Khouri HM, Lee KH, Carty HA, Scanlan D, Heinzen RA,

Thompson HA, Samuel JE, Fraser CM, Heidelberg JF. 2003. Complete genome sequence of the Q-fever pathogen *Coxiella burnetii*. *Proc Natl Acad Sci USA* 100:5455–5460.

27. Beare PA, Unsworth N, Andoh M, Voth DE, Omsland A, Gilk SD, Williams KP, Sobral BW, Kupko JJ, Porcella SF, Samuel JE, Heinzen RA. 2009. Comparative genomics reveal extensive transposon-mediated genomic plasticity and diversity among potential effector proteins within the genus *Coxiella*. *Infect Immun* 77:642–656.

28. Hendrix LR, Samuel JE, Mallavia LP. 1991. Differentiation of *Coxiella burnetii* isolates by analysis of restriction-endonuclease-digested DNA separated by SDS-PAGE. *J Gen Microbiol* 137:269–276.

29. Long CM, Beare PA, Cockrell DC, Larson CL, Heinzen RA. 2019. Comparative virulence of diverse *Coxiella burnetii* strains. *Virulence* 10:133–150.

30. McLaughlin HP, Cherney B, Hakovirta JR, Priestley RA, Conley A, Carter A, Hodge D, Pillai SP, Weigel LM, Kersh GJ, Sue D. 2017. Phylogenetic inference of *Coxiella burnetii* by 16S rRNA gene sequencing. *PLoS One* 12:e0189910.

31. Hornstra HM, Priestley RA, Georgia SM, Kachur S, Birdsell DN, Hilsabeck R, Gates LT, Samuel JE, Heinzen RA, Kersh GJ, Keim P, Massung RF, Pearson T. 2011. Rapid typing of *Coxiella burnetii. PLoS One* 6:e26201.

32. Omsland A, Cockrell DC, Howe D, Fischer ER, Virtaneva K, Sturdevant DE, Porcella SF, Heinzen RA. 2009. Host cell-free growth of the Q fever bacterium *Coxiella burnetii*. *Proc Natl Acad Sci USA* 106:4430–4434.

33. van Schaik EJ, Chen C, Mertens K, Weber MM, Samuel JE. 2013. Molecular pathogenesis of the obligate intracellular bacterium *Coxiella burnetii*. *Nat Rev Microbiol* 11:561–573.

34. Conti F, Boucherit N, Baldassarre V, Trouplin V, Toman R, Mottola G, Mege J-L, Ghigo E. 2014. *Coxiella burnetii* lipopolysaccharide blocks p38α-MAPK activation through the disruption of TLR-2 and TLR-4 association. *Front Cell Infect Microbiol* 4:182.

35. Abnave P, Muracciole X, Ghigo E. 2017. *Coxiella burnetii* Lipopolysaccharide: What Do We Know? *Int J Mol Sci* 18:2509.

36. Weber MM, Chen C, Rowin K, Mertens K, Galvan G, Zhi H, Dealing CM, Roman VA, Banga S, Tan Y, Luo Z-Q, Samuel JE. 2013. Identification of *Coxiella burnetii* type IV secretion substrates required for intracellular replication and *Coxiella*-containing vacuole formation. *J Bacteriol* 195:3914–3924.

37. Eckart RA, Bisle S, Schulze-Luehrmann J, Wittmann I, Jantsch J, Schmid B, Berens C, Lührmann A. 2014. Antiapoptotic activity of *Coxiella burnetii* effector protein AnkG is controlled by p32-dependent trafficking. *Infect Immun* 82:2763–2771.

38. Schäfer W, Eckart RA, Schmid B, Cagköylü H, Hof K, Muller YA, Amin B, Lührmann A. 2017. Nuclear trafficking of the anti-apoptotic *Coxiella burnetii* effector protein AnkG requires binding to p32 and Importin-α1. *Cell Microbiol* 19(1), e12634.

39. Bisle S, Klingenbeck L, Borges V, Sobotta K, Schulze-Luehrmann J, Menge C, Heydel C, Gomes JP, Lührmann A. 2016. The inhibition of the apoptosis pathway

by the *Coxiella burnetii* effector protein CaeA requires the EK repetition motif, but is independent of survivin. *Virulence* 7:400–412.

40. Klingenbeck L, Eckart RA, Berens C, Lührmann A. 2013. The *Coxiella burnetii* type IV secretion system substrate CaeB inhibits intrinsic apoptosis at the mitochondrial level. *Cell Microbiol* 15:675–687.

41. Latomanski EA, Newton HJ. 2018. Interaction between autophagic vesicles and the *Coxiella*-containing vacuole requires CLTC (clathrin heavy chain). *Autophagy* 14:1710–1725.

42. Siadous FA, Cantet F, Van Schaik E, Burette M, Allombert J, Lakhani A, Bonaventure B, Goujon C, Samuel J, Bonazzi M, Martinez E. 2021. *Coxiella* effector protein CvpF subverts RAB26-dependent autophagy to promote vacuole biogenesis and virulence. *Autophagy* 17:706–722.

43. Martinez E, Huc-Brandt S, Brelle S, Allombert J, Cantet F, Gannoun-Zaki L, Burette M, Martin M, Letourneur F, Bonazzi M, Molle V. 2020. The secreted protein kinase CstK from *Coxiella burnetii* influences vacuole development and interacts with the GTPase-activating host protein TBC1D5. *J Biol Chem* 295:7391-7403

44. Pechstein J, Schulze-Luehrmann J, Bisle S, Cantet F, Beare PA, Ölke M, Bonazzi M, Berens C, Lührmann A. 2020. The *Coxiella burnetii* T4SS Effector AnkF Is Important for Intracellular Replication. *Front Cell Infect Microbiol* 10:559915.

45. Cunha LD, Ribeiro JM, Fernandes TD, Massis LM, Khoo CA, Moffatt JH, Newton HJ, Roy CR, Zamboni DS. 2015. Inhibition of inflammasome activation

by *Coxiella burnetii* type IV secretion system effector IcaA. *Nat Commun* 6:10205.

46. Burette M, Allombert J, Lambou K, Maarifi G, Nisole S, Di Russo Case E, Blanchet FP, Hassen-Khodja C, Cabantous S, Samuel J, Martinez E, Bonazzi M. 2020. Modulation of innate immune signaling by a *Coxiella burnetii* eukaryotic-like effector protein. *Proc Natl Acad Sci USA* 117:13708-13718.

47. Larson CL, Martinez E, Beare PA, Jeffrey B, Heinzen RA, Bonazzi M. 2016. Right on Q: genetics begin to unravel *Coxiella burnetii* host cell interactions. *Future Microbiol* 11:919–939.

48. Capo C, Lindberg FP, Meconi S, Zaffran Y, Tardei G, Brown EJ, Raoult D, Mege JL. 1999. Subversion of monocyte functions by *Coxiella burnetii*: impairment of the cross-talk between alphavbeta3 integrin and CR3. *J Immunol* 163:6078–6085.

49. Dellacasagrande J, Ghigo E, Hammami SM, Toman R, Raoult D, Capo C, Mege JL. 2000. alpha(v)beta(3) integrin and bacterial lipopolysaccharide are involved in *Coxiella burnetii*-stimulated production of tumor necrosis factor by human monocytes. *Infect Immun* 68:5673–5678.

50. Raoult D, Marrie T, Mege J. 2005. Natural history and pathophysiology of Q fever. *Lancet Infect Dis* 5:219–226.

51. Dragan AL, Voth DE. 2019. *Coxiella burnetii:* International pathogen of mystery. *Microbes Infect* 22:100-110.

52. Gutierrez MG, Vázquez CL, Munafó DB, Zoppino FCM, Berón W, Rabinovitch M, Colombo MI. 2005. Autophagy induction favours the generation and maturation of the *Coxiella*-replicative vacuoles. *Cell Microbiol* 7:981–993.

53. Romano PS, Gutierrez MG, Berón W, Rabinovitch M, Colombo MI. 2007. The autophagic pathway is actively modulated by phase II *Coxiella burnetii* to efficiently replicate in the host cell. *Cell Microbiol* 9:891–909.

54. Berón W, Gutierrez MG, Rabinovitch M, Colombo MI. 2002. *Coxiella burnetii* localizes in a Rab7-labeled compartment with autophagic characteristics. *Infect Immun* 70:5816–5821.

55. Lührmann A, Roy CR. 2007. *Coxiella burnetii* inhibits activation of host cell apoptosis through a mechanism that involves preventing cytochrome c release from mitochondria. *Infect Immun* 75:5282–5289.

56. Norville IH, Hartley MG, Martinez E, Cantet F, Bonazzi M, Atkins TP. 2014. *Galleria mellonella* as an alternative model of *Coxiella burnetii* infection. *Microbiology (Reading, Engl)* 160:1175–1181.

57. Bastos RG, Howard ZP, Hiroyasu A, Goodman AG. 2017. Host and bacterial factors control susceptibility of *Drosophila melanogaster* to *Coxiella burnetii* Infection. *Infect Immun* 85:e00218-17.

58. Bewley KR. 2013. Animal models of Q fever (*Coxiella burnetii*). *Comp Med* 63:469–476.

59. Graham JG, Winchell CG, Kurten RC, Voth DE. 2016. Development of an *ex vivo* tissue platform to study the human lung response to *Coxiella burnetii*. *Infect Immun* 84:1438–1445.

60. Graham JG, MacDonald LJ, Hussain SK, Sharma UM, Kurten RC, Voth DE. 2013. Virulent *Coxiella burnetii* pathotypes productively infect primary human alveolar macrophages. *Cell Microbiol* 15:1012–1025.

61. Dragan AL, Kurten RC, Voth DE. 2019. Characterization of early stages of human alveolar infection by the Q fever agent *Coxiella burnetii*. *Infect Immun* 87.

62. Mori M, Boarbi S, Michel P, Bakinahe R, Rits K, Wattiau P, Fretin D. 2013. *In vitro* and *in vivo* infectious potential of *Coxiella burnetii*: a study on Belgian livestock isolates. *PLoS One* 8:e67622.

63. Benoit M, Barbarat B, Bernard A, Olive D, Mege J-L. 2008. *Coxiella burnetii*, the agent of Q fever, stimulates an atypical M2 activation program in human macrophages. *Eur J Immunol* 38:1065–1070.

64. Benoit M, Desnues B, Mege J-L. 2008. Macrophage polarization in bacterial infections. *J Immunol* 181:3733–3739.

65. Dellacasagrande J, Capo C, Raoult D, Mege JL. 1999. IFN-gamma-mediated control of *Coxiella burnetii* survival in monocytes: the role of cell apoptosis and TNF. *J Immunol* 162:2259–2265.

66. Faugaret D, Ben Amara A, Alingrin J, Daumas A, Delaby A, Lépolard C, Raoult D, Textoris J, Mège J-L. 2014. Granulomatous response to *Coxiella burnetii*, the agent of Q fever: the lessons from gene expression analysis. *Front Cell Infect Microbiol* 4:172.

67. Read AJ, Erickson S, Harmsen AG. 2010. Role of CD4+ and CD8+ T cells in clearance of primary pulmonary infection with *Coxiella burnetii*. *Infect Immun* 78:3019–3026.

68. Ghigo E, Capo C, Tung C-H, Raoult D, Gorvel J-P, Mege J-L. 2002. *Coxiella burnetii* survival in THP-1 monocytes involves the impairment of phagosome

maturation: IFN-gamma mediates its restoration and bacterial killing. *J Immunol* 169:4488–4495.

69. Ghigo E, Capo C, Raoult D, Mege JL. 2001. Interleukin-10 stimulates *Coxiella burnetii* replication in human monocytes through tumor necrosis factor down-modulation: role in microbicidal defect of Q fever. *Infect Immun* 69:2345–2352.

70. Capo C, Mege J-L. 2012. Role of innate and adaptive immunity in the control of Q fever. *Adv Exp Med Biol* 984:273–286.

71. Ganesan S, Roy CR. 2019. Host cell depletion of tryptophan by IFNγ-induced Indoleamine 2,3-dioxygenase 1 (IDO1) inhibits lysosomal replication of *Coxiella burnetii*. *PLoS Pathog* 15:e1007955.

72. Labbé K, Saleh M. 2008. Cell death in the host response to infection. *Cell Death Differ* 15:1339–1349.

73. Voth DE, Howe D, Heinzen RA. 2007. *Coxiella burnetii* inhibits apoptosis in human THP-1 cells and monkey primary alveolar macrophages. *Infect Immun* 75:4263–4271.

74. Macdonald LJ, Graham JG, Kurten RC, Voth DE. 2014. *Coxiella burnetii* exploits host cAMP-dependent protein kinase signalling to promote macrophage survival. *Cell Microbiol* 16:146–159.

75. Vázquez CL, Colombo MI. 2010. *Coxiella burnetii* modulates Beclin 1 and Bcl-2, preventing host cell apoptosis to generate a persistent bacterial infection. *Cell Death Differ* 17:421–438.

76. Voth DE, Heinzen RA. 2009. Sustained activation of Akt and Erk1/2 is required for *Coxiella burnetii* antiapoptotic activity. *Infect Immun* 77:205–213.

77. Kaur J, Debnath J. 2015. Autophagy at the crossroads of catabolism and anabolism. *Nat Rev Mol Cell Biol* 16:461–472.

78. Deretic V, Levine B. 2009. Autophagy, immunity, and microbial adaptations. *Cell Host Microbe* 5:527–549.

79. Winchell CG, Graham JG, Kurten RC, Voth DE. 2014. *Coxiella burnetii* type IV secretion-dependent recruitment of macrophage autophagosomes. *Infect Immun* 82:2229–2238.

80. Larson CL, Sandoz KM, Cockrell DC, Heinzen RA. 2019. Noncanonical inhibition of mTORC1 by *Coxiella burnetii* promotes replication within a phagolysosome-like vacuole. *mBio* 10.

81. Allard B, Panariti A, Martin JG. 2018. Alveolar macrophages in the resolution of inflammation, tissue repair, and tolerance to infection. *Front Immunol* 9:1777.

82. Schoenlaub L, Cherla R, Zhang Y, Zhang G. 2016. *Coxiella burnetii* avirulent Nine Mile phase II induces caspase-1-dependent pyroptosis in murine peritoneal B1a B cells. *Infect Immun* 84:3638–3654.

83. Bartel DP. 2018. Metazoan MicroRNAs. *Cell* 173:20–51.

84. Kozomara A, Birgaoanu M, Griffiths-Jones S. 2019. miRBase: from microRNA sequences to function. *Nucleic Acids Res* 47:D155–D162.

85. Friedman RC, Farh KK-H, Burge CB, Bartel DP. 2009. Most mammalian mRNAs are conserved targets of microRNAs. *Genome Res* 19:92–105.

86. Gebert LFR, MacRae IJ. 2019. Regulation of microRNA function in animals. *Nat Rev Mol Cell Biol* 20:21–37.

87. Vasudevan S, Tong Y, Steitz JA. 2007. Switching from repression to activation: microRNAs can up-regulate translation. *Science* 318:1931–1934.

88. Shabalina SA, Koonin EV. 2008. Origins and evolution of eukaryotic RNA interference. *Trends Ecol Evol (Amst)* 23:578–587.

89. Bartel DP. 2004. MicroRNAs: genomics, biogenesis, mechanism, and function. *Cell* 116:281–297.

90. McCreight JC, Schneider SE, Wilburn DB, Swanson WJ. 2017. Evolution of microRNA in primates. *PLoS One* 12:e0176596.

91. Ambros V, Bartel B, Bartel DP, Burge CB, Carrington JC, Chen X, Dreyfuss G, Eddy SR, Griffiths-Jones S, Marshall M, Matzke M, Ruvkun G, Tuschl T. 2003. A uniform system for microRNA annotation. *RNA* 9:277–279.

92. Steinkraus BR, Toegel M, Fulga TA. 2016. Tiny giants of gene regulation: experimental strategies for microRNA functional studies. *Wiley Interdiscip Rev Dev Biol* 5:311–362.

93. Li Z, Xu R, Li N. 2018. MicroRNAs from plants to animals, do they define a new messenger for communication? *Nutr Metab (Lond)* 15:68.

94. Akhtar MM, Micolucci L, Islam MS, Olivieri F, Procopio AD. 2019. A practical guide to miRNA target prediction. *Methods Mol Biol* 1970:1–13.

95. Barbash S, Shifman S, Soreq H. 2014. Global coevolution of human microRNAs and their target genes. *Mol Biol Evol* 31:1237–1247.

96. Agarwal V, Bell GW, Nam J-W, Bartel DP. 2015. Predicting effective microRNA target sites in mammalian mRNAs. *Elife* 4:e05005.

97. Chen L, Heikkinen L, Wang C, Yang Y, Sun H, Wong G. 2019. Trends in the development of miRNA bioinformatics tools. *Brief Bioinformatics* 20:1836–1852.

98. Aguilar C, Mano M, Eulalio A. 2019. MicroRNAs at the host-bacteria interface: host defense or bacterial offense. *Trends Microbiol* 27:206–218.

99. Zhou X, Li X, Wu M. 2018. miRNAs reshape immunity and inflammatory responses in bacterial infection. *Signal Transduct Target Ther* 3:14.

100. Tamgue O, Gcanga L, Ozturk M, Whitehead L, Pillay S, Jacobs R, Roy S, Schmeier S, Davids M, Medvedeva YA, Dheda K, Suzuki H, Brombacher F, Guler R. 2019. Differential Targeting of c-Maf, Bach-1, and Elmo-1 by microRNA-143 and microRNA-365 promotes the intracellular growth of *Mycobacterium tuberculosis* in alternatively IL-4/IL-13 activated macrophages. *Front Immunol* 10:421.

101. Li M, Wang J, Fang Y, Gong S, Li M, Wu M, Lai X, Zeng G, Wang Y, Yang K, Huang X. 2016. microRNA-146a promotes mycobacterial survival in macrophages through suppressing nitric oxide production. *Sci Rep* 6:23351.

102. Herkt CE, Caffrey BE, Surmann K, Blankenburg S, Gesell Salazar M, Jung AL, Herbel SM, Hoffmann K, Schulte LN, Chen W, Sittka-Stark A, Völker U, Vingron M, Marsico A, Bertrams W, Schmeck B. 2020. A microRNA network controls *Legionella pneumophila* replication in human macrophages via LGALS8 and MX1. *mBio* 11.

103. Benyeogor I, Simoneaux T, Wu Y, Lundy S, George Z, Ryans K, McKeithen D, Pais R, Ellerson D, Lorenz WW, Omosun T, Thompson W, Eko FO, Black CM,

Blas-Machado U, Igietseme JU, He Q, Omosun Y. 2019. A unique insight into the MiRNA profile during genital chlamydial infection. *BMC Genomics* 20:143.

104. Das K, Garnica O, Dhandayuthapani S. 2016. Modulation of host miRNAs by intracellular bacterial pathogens. *Front Cell Infect Microbiol* 6:79.

105. Bettencourt P, Marion S, Pires D, Santos LF, Lastrucci C, Carmo N, Blake J, Benes V, Griffiths G, Neyrolles O, Lugo-Villarino G, Anes E. 2013. Actin-binding protein regulation by microRNAs as a novel microbial strategy to modulate phagocytosis by host cells: the case of N-Wasp and miR-142-3p. Front *Cell Infect Microbiol* 3:19.

106. Kim JK, Yuk J-M, Kim SY, Kim TS, Jin HS, Yang C-S, Jo E-K. 2015. MicroRNA-125a inhibits autophagy activation and antimicrobial responses during mycobacterial infection. *J Immunol* 194:5355–5365.

Chapter II

MicroRNAs contribute to host response to *Coxiella burnetii* infection

Madhur Sachan[1], Katelynn Doiron[2], Daniel E Voth[2], Rahul Raghavan[1,3]*

[1]Department of Biology, Portland State University, Portland, OR, 97201, USA.

[2]Department of Microbiology and Immunology, University of Arkansas for Medical Sciences, Little Rock, AR, 72205, USA.

[3]Department of Biology, The University of Texas at San Antonio, San Antonio, TX, 78249, USA.

Key words: *Coxiella burnetii*, miRNA, macrophage, apoptosis, infection

ABSTRACT

MicroRNAs (miRNAs), a class of small non-coding RNAs, are implicated in a spectrum of physiological processes, including immune response to intracellular infections. However, no information is available about miRNAs' roles during infection by *C. burnetii*, a bacterial pathogen that suppresses host apoptosis during infection. We investigated the expression of miRNAs in *C. burnetii*-infected THP-1 cells and identified several potential microRNA-target interactions and cell signaling pathways that showed an infection-stage-specific response. A pathway enrichment analysis of genes targeted by miRNAs indicated that miRNAs likely contribute to apoptosis inhibition during infection. Among these apoptosis-related miRNAs, we conducted functional studies on miR-143-3p, which was downregulated during infection. Our data showed that overexpression of miR-143-3p down-regulates the expression of pro-survival proteins such as Akt1 and Bcl-2, promotes apoptosis and inflammation, and inhibits the host's autophagic response. Interestingly, during infection, despite *C. burnetii* appearing to neutralize the effect of miR-143-3p overexpression, this miRNA could still inhibit bacterial growth. Taken together, the present study show that miRNAs are an integral component of macrophages' stage-specific response to *C. burnetii* infection, and inhibition of miR-143-3p might facilitate the pathogen's intracellular growth.

INTRODUCTION

The highly infectious intracellular pathogen *Coxiella burnetii* is the etiological agent of Q fever (1). It has a unique biphasic life cycle where the bacterium alternates between a dormant small cell variant (SCV) and a metabolically active form called the large cell variant (LCV) (1). After its uptake by a host cell, typically an alveolar macrophage, *C. burnetii* establishes a *Coxiella*-containing vacuole (CCV) that matures by fusing with endolysosomal, autophagic, and secretory vesicles (2–4). Alveolar macrophages utilize an arsenal of innate defense responses, including induction of apoptosis, inflammation, and modified vesicular trafficking to control *C. burnetii* infection (2, 5–8). In response, the pathogen actively disrupts many of these host defense networks; for example, by recruiting anti-apoptotic Bcl-2 to the CCV, inactivating pro-apoptotic Bad, and promoting a pro-survival response by activating Erk1/2, Akt, and PKA signaling (9–11). This subversion is critical to *Coxiella*'s intracellular growth and virulence, and effector proteins secreted through a type IV secretion system (T4SS) have been shown to contribute to this process (6, 12).

MicroRNAs (miRNAs) are a class of single-stranded, small (~22 nucleotides), non-coding RNAs that orchestrate post-transcriptional gene regulation in a wide range of eukaryotes and some viruses (13). In humans, miRNAs regulate a large number of genes, primarily by inhibiting target gene expression via translation repression and mRNA degradation (14–16). Studies have shown that miRNAs are integral to host response to bacterial, viral, and parasitic infections; however, miRNAs could either promote or inhibit infection (17–24).

We have shown previously that expression of miRNAs is perturbed in macrophages infected with *C. burnetii* (25), but the function, if any, of miRNAs are unclear. In this study, we show that miRNAs are a major component of the host response to *C. burnetii* and demonstrate that miR-143-3p could promote apoptosis, inhibit autophagy, and induce the production of pro-inflammatory cytokines. These data indicate that the downregulation of miR-143-3p expression observed during *C. burnetii* infection likely contributes to the pathogen's intracellular growth.

RESULTS

Host gene expression correlates with the stage of infection

To identify infection-associated miRNAs and their potential targets, we measured miRNA and mRNA expression in THP-1 cells infected (or uninfected) with *C. burnetii* Nine Mile RSA439 Phase II (NMII). The total number of miRNAs and mRNAs that were differentially expressed (log2 fold-change ≥ 0.75, Padj ≤ 0.05) in NMII-infected cells in comparison to uninfected cells increased from 1 to 3-day post-infection (dpi) **(Figure 1, Table 1 and S1)**. But by day 5, the number of protein-coding and miRNA genes that were up- or down-regulated in *Coxiella*-infected cells has reduced considerably **(Figure 1, Table 1 and S1)**. These data indicate that the magnitude of host cell response to *Coxiella* infection increases as the bacterium replicates (days 1-3), and as actively growing LCVs transition into metabolically less active SCVs (day 5) (26), the host response becomes muted in tandem.

Table 1. Number of differentially expressed (log2 fold-change ≥ 0.75, Padj ≤ 0.05) miRNAs and mRNAs in NMII-infected cells in comparison to uninfected cells at respective hours post-infection (hpi).

	miRNA			**mRNA**		
Time	Total	Down	Up	Total	Down	Up
8 hpi	25	12	13	454	220	234
24 hpi	25	16	9	1160	665	495
48 hpi	35	23	12	1742	445	1297
72 hpi	60	43	17	6525	3236	3289
120 hpi	34	18	16	211	80	131

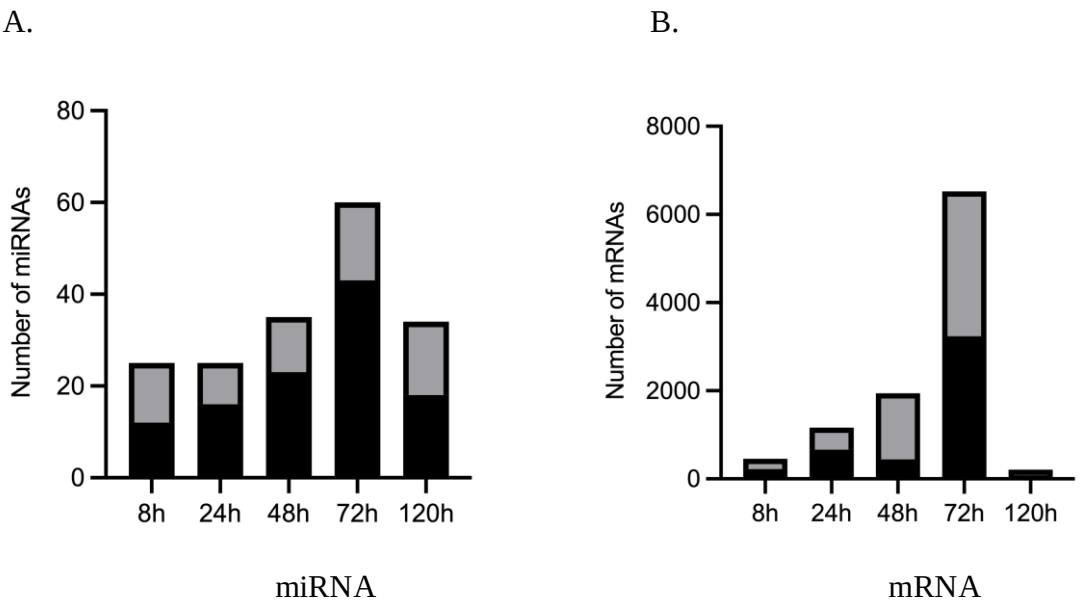

Figure 1. Host gene expression during *C. burnetii* infection. The total number of (A) miRNAs and (B) mRNAs that were differentially expressed in NMII-infected cells in comparison to uninfected cells. Gray bars denote upregulated genes while black corresponds to downregulated ones (log2 fold-change ≥ 0.75, Padj ≤ 0.05; n = 3).

miRNAs likely regulate apoptosis signaling during *Coxiella* infection

To identify the genes and signaling pathways potentially targeted by miRNAs, we performed inverse-expression pairing and core pathway analyses using the Ingenuity Pathway Analysis (IPA) tool (27). In the case of inverse-expression pairing, we selected miRNAs and their known and predicted targets to find an inverse pattern of expression, i.e., if the miRNA expression is upregulated, the target gene expression is down-regulated, and vice versa **(Table S2)**. To perform core pathway analysis, we focused on host pathways that are enriched for genes that are potentially targeted by miRNAs, where the target gene and miRNA show an inverse pattern of expression. These analyses revealed 215 pathways, including apoptosis signaling, PI3K/AKT, autophagy, and IL-17 signaling, that are likely regulated by miRNAs **(Figure 2, Table S3)**. To begin to investigate a potential role for miRNAs in regulating host cell apoptosis during *Coxiella* infection, we measured the expression of 84 apoptosis-regulating miRNAs using a qRT-PCR array (Qiagen). This assay showed that 12 miRNAs were up-or down-regulated in *Coxiella*-infected cells (**Table 2**), suggesting their involvement in host response to *C. burnetii* infection.

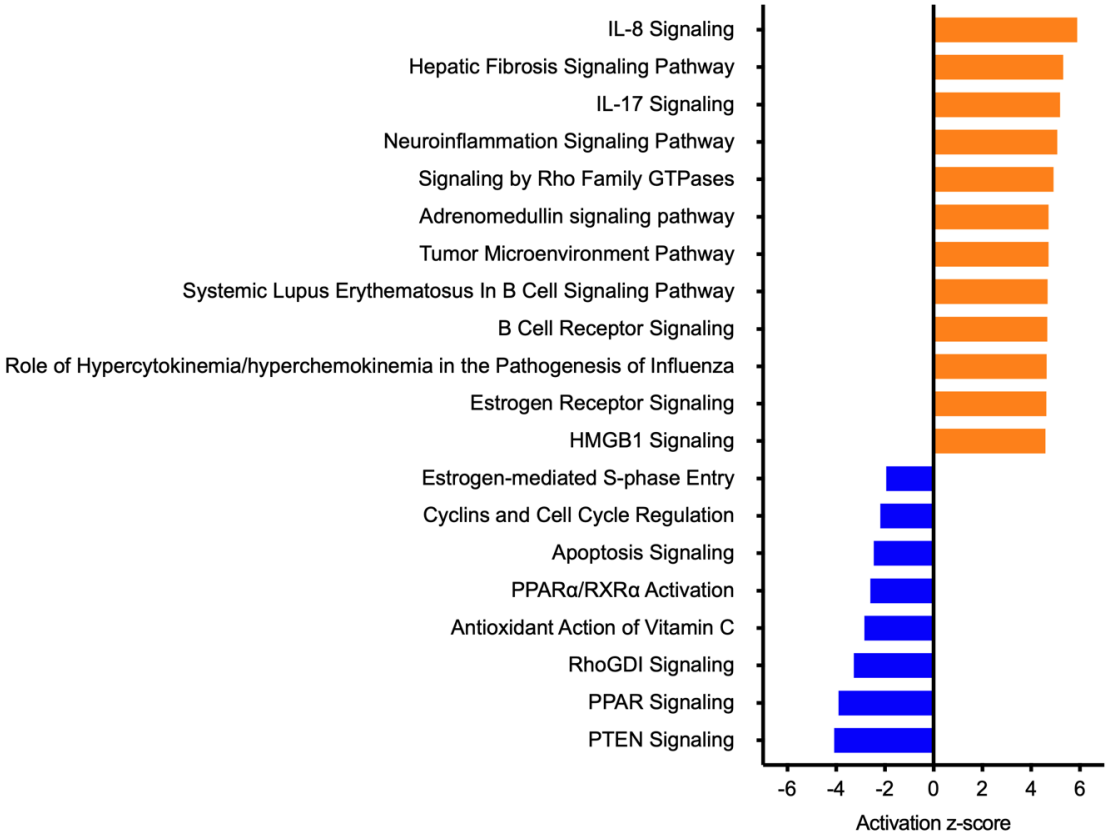

Figure 2. Host pathways potentially controlled by miRNAs during *Coxiella* infection. Top 20 significantly affected (z-score ≥ 1.5 or ≤1.5) miRNA-targeted pathways based on IPA. Orange bars show pathways with positive z-score (activation), while blue corresponds to a negative z-score (inhibition) in ingenuity pathway analysis (IPA).

Table 2. Differentially expressed ($p \leq 0.05$, $n = 3$) miRNAs in NMII-infected THP-1 cells compared to uninfected controls were confirmed through qRT-PCR array.

miRNA	**Fold Change**	**p-value**
hsa-miR-708-5p	0.6225	0.037471
hsa-miR-145-5p	0.6312	0.006722
hsa-miR-143-3p	0.6535	0.007199
hsa-miR-106b-5p	0.7386	0.032799
hsa-miR-181d-5p	0.7611	0.028265
hsa-miR-16-5p	0.8026	0.024211
hsa-miR-222-3p	0.8804	0.014724
hsa-miR-365b-3p	1.1015	0.016939
hsa-miR-218-5p	1.5832	0.013546
hsa-miR-125a-5p	1.5868	0.010438
hsa-miR-192-5p	1.7689	0.03232
hsa-miR-146a-5p	5.9635	0.000006

miR-143-3p is downregulated during *C. burnetii* infection

Among the apoptosis-related miRNAs that were differentially expressed during *C. burnetii* infection, in this study we focused on miR-143-3p, that was significantly downregulated in NMII-infected cells (**Figure 3B and C, Table 2**). To further confirm the low expression of miR-143-3p during *C. burnetii* infection, we quantified the miRNA expression using qRT-PCR in human alveolar macrophages (hAMs) infected with either NMII or with *C. burnetii* Nine Mile RSA 493 (NMI), the fully virulent isolate. Expression of miR-143-3p was significantly downregulated in hAMs infected with either isolate of *C. burnetii* (**Figure 3A**), suggesting that the miRNA has a role in host response during natural infections. Intriguingly, the expression of miR-143-3p was significantly lower in NMI-infected than in NMII-infected hAMs. While the cause for this disparity is unknown, the full-length lipopolysaccharide (LPS) present in NMI might have a role in the differential repression of host miR-143-3p.

We further assessed the impact of miR-143-3p on *Coxiella*'s intracellular growth. As shown in **Figure 4**, *Coxiella* growth was significantly lower in miR-143-3p-transfected HeLa cells in comparison to untransfected cells and to cells transfected with a miRNA negative control. Thus, based on these data, we surmise that downregulation of miR-143-3p that occurs during *Coxiella* infection in macrophages could be advantageous to the Q fever pathogen.

A.

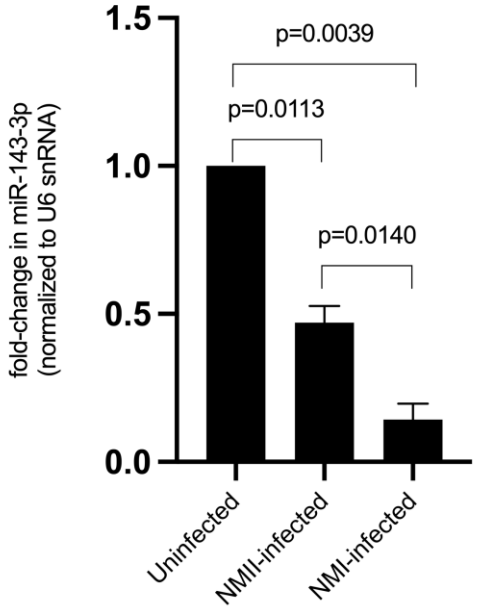
1.5
1.0
0.5
0.0
fold-change in miR-143-3p
(normalized to U6 snRNA)
p=0.0039
p=0.0113
p=0.0140
Uninfected
NMII-infected
NMI-infected

B.

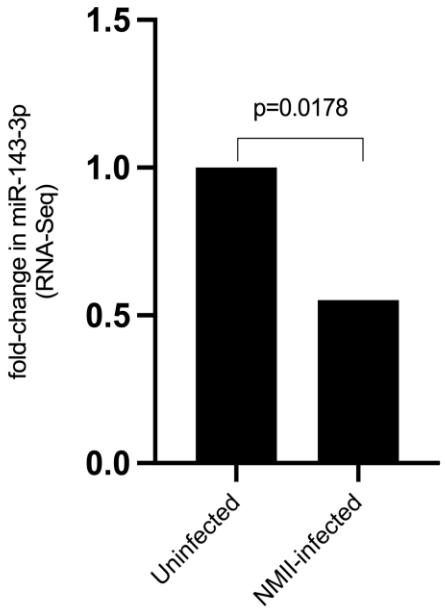
1.5
1.0
0.5
0.0
fold-change in miR-143-3p
(RNA-Seq)
p=0.0178
Uninfected
NMII-infected

C.

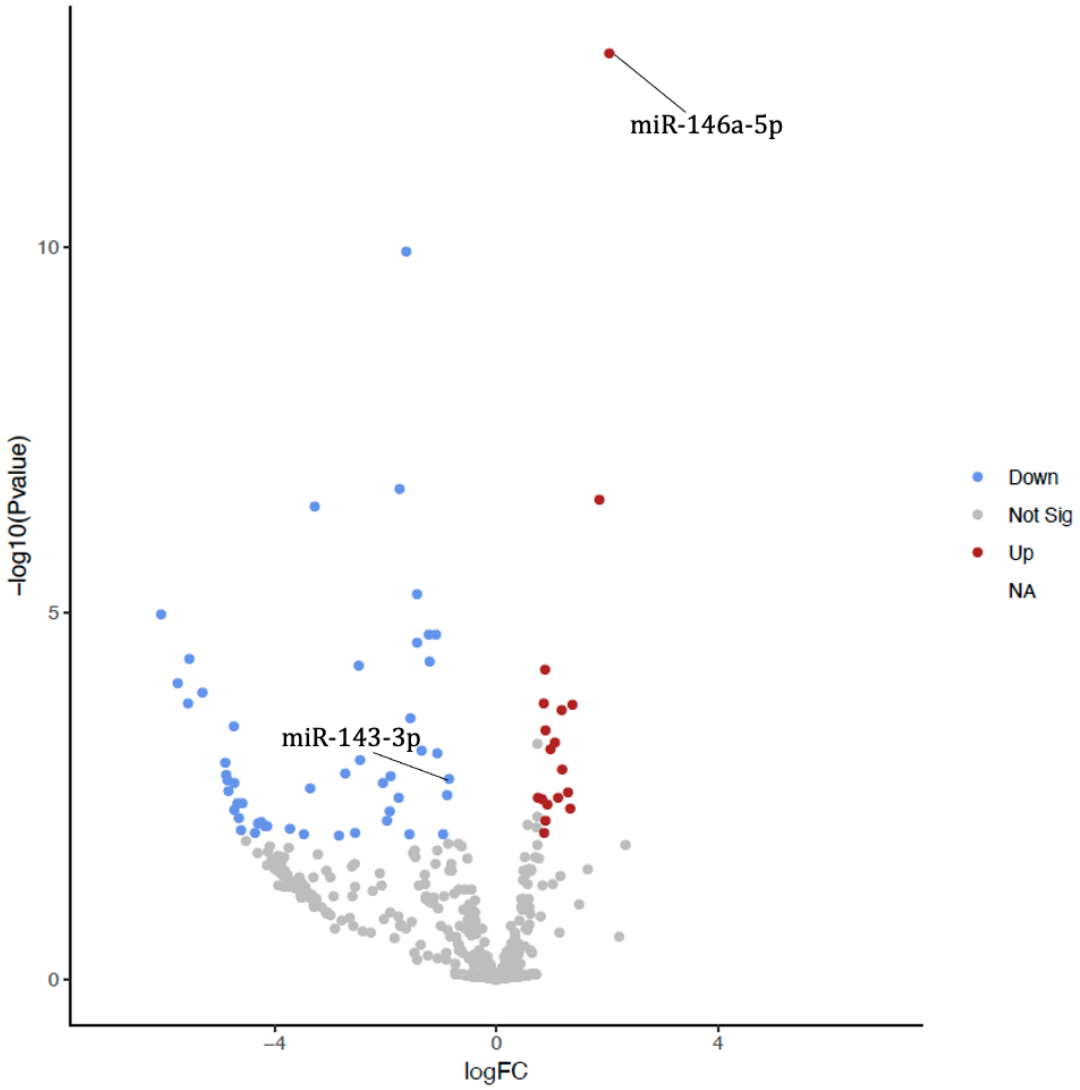
miR-146a-5p
miR-143-3p
10
5
0
−log10(Pvalue)
−4
0
4
logFC
Down
Not Sig
Up
NA

D.

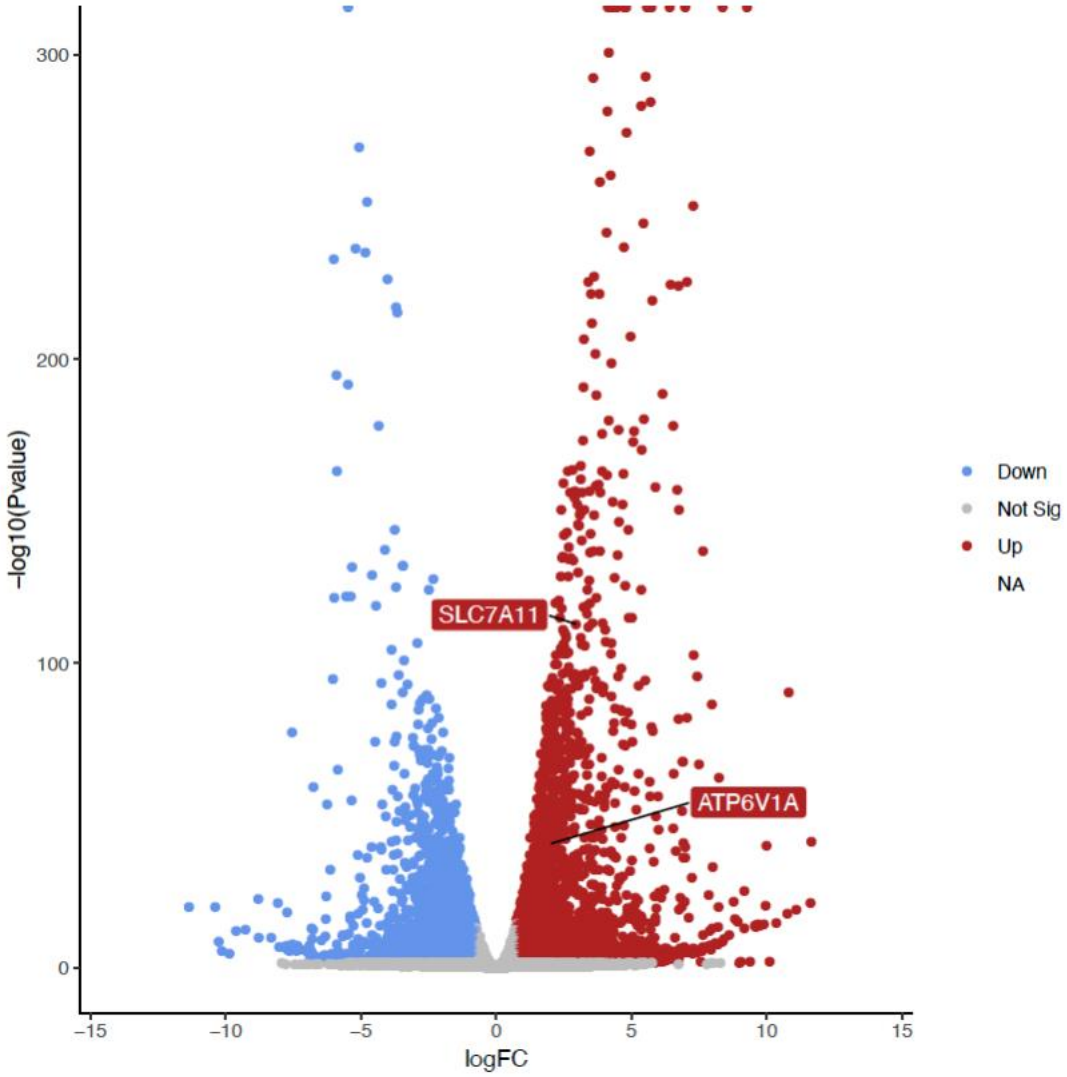
300
200
100
0
−log10(Pvalue)
−15
−10
−5
0
5
10
15
logFC
SLC7A11
ATP6V1A
Down
Not Sig
Up
NA

Figure 3. miR-143-3p is downregulated in *C. burnetii*-infected macrophages. (A) Primary human alveolar macrophages (hAMs) infected with NMII or NMI isolates of *C. burnetii* at 25 multiplicity of infection or uninfected controls were analyzed for miR-143-3p expression using qRT-PCR at 72 hours post-infection. Pairwise comparisons of the expression values in hAMs were done using two-tailed paired t-test followed by Welch's correction (n = 3). (B) In the RNA-Seq experiment, miR-143-3p expression in NMII-infected THP-1 cells compared to uninfected cells was analyzed by DESeq2 (n = 3). Volcanic plot representation of differentially regulated (C) miRNA and (D) mRNAs in NMII infected THP-1 derived macrophages at 72 hpi. Red dots show upregulated while blue corresponds to downregulated gene expression compared to the uninfected control. The x-axis shows the magnitude of fold change ($-0.75 \leq \log2fc \geq 0.75$, $padj \leq 0.05$; n = 3) and y-axis corresponds to statistical significance (-log10 of p value).

A. qPCR assay B. CFU assay

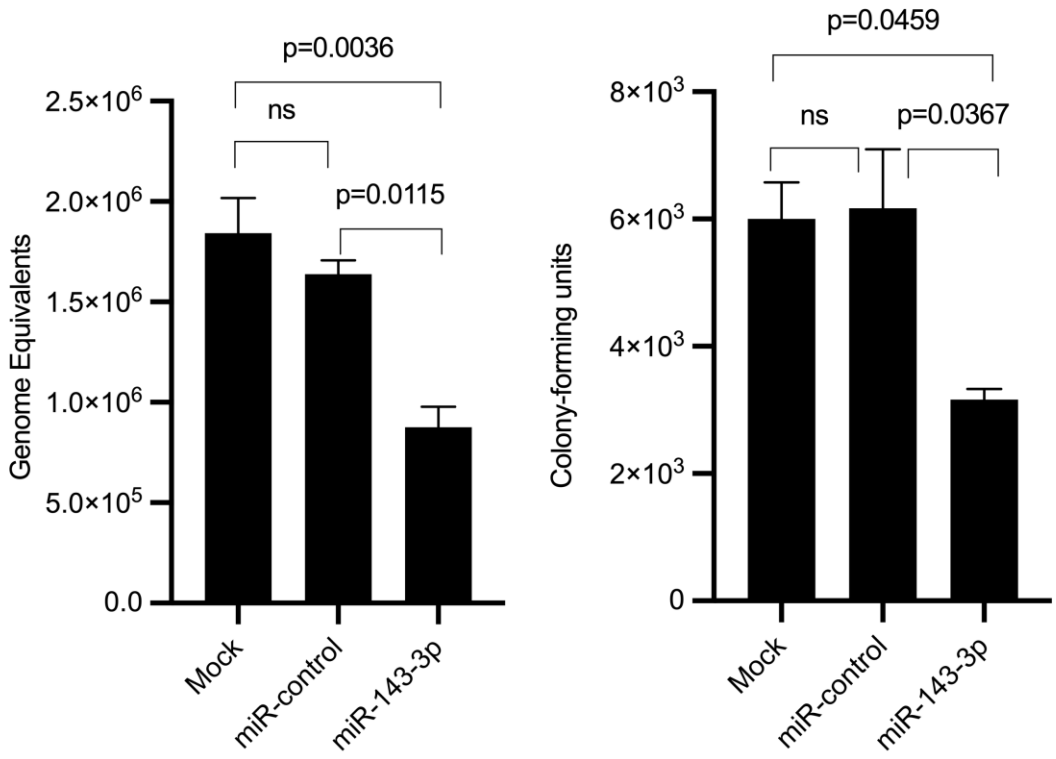

Figure 4. miR-143 inhibits intracellular growth of *C. burnetii*. Quantification of intracellular *C. burnetii* at 48hpi in miR-143-3p-transfected HeLa cells compared to cells transfected with non-specific miRNA (miR-control). Mock-infected cells served as control. Statistical significance was determined using one-way ANOVA followed by Tucky's multiple comparison test (ns: non-significant, n = 3).

miR-143-3p promotes early apoptosis

To test the impact of miR-143-3p on apoptosis, we transfected HeLa cells with either miR-143-3p or a non-specific control miRNA and measured early and late apoptosis using annexin V-PE and eFluor780 staining followed by flow cytometry. We observed that the percentage of early, but not late, apoptotic cells in the miR-143-3p-transfected population was significantly higher than in cells transfected with control miRNA (~15% vs. ~10%; **Figure 5E and G**). However, when the cells were infected with NMII, the percentage of early apoptotic cells in the miR-143-3p-transfected population reduced to ~12%, and it not significantly different from the control-miRNA-transfected cells (~9%) (**Figure 5F and H**).

A. Uninfected + miR-control

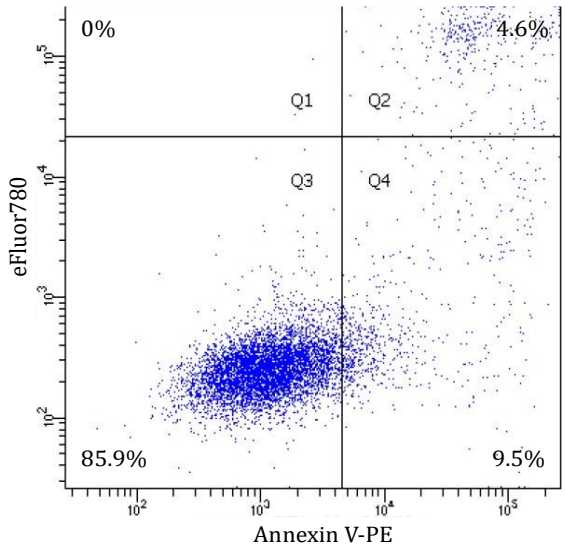

B. Infected + miR-control

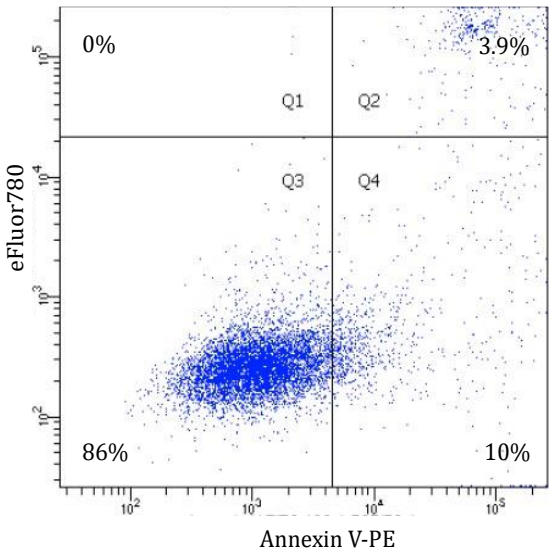

C. Uninfected + miR-143-3p

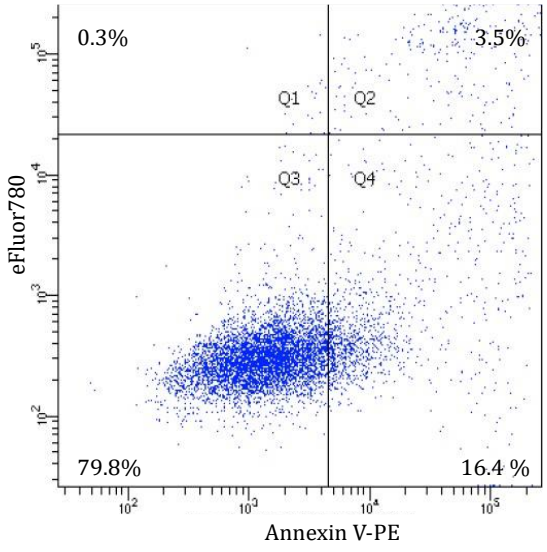

D. Infected + miR-143-3p

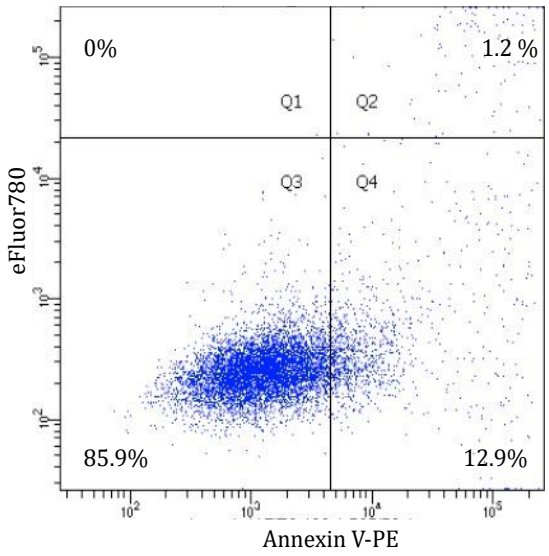

E. Uninfected/early apoptosis

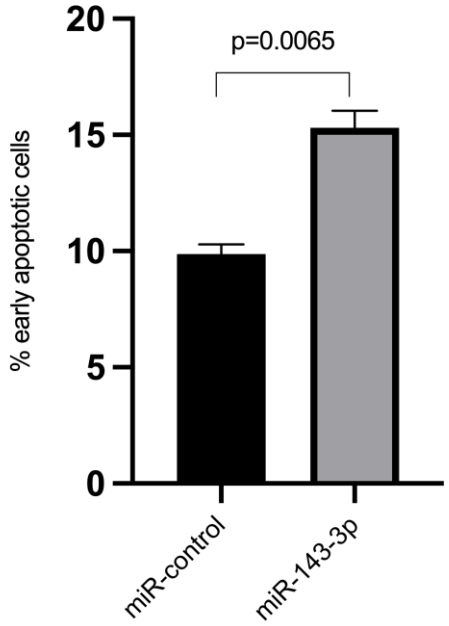

F. Uninfected/late apoptosis

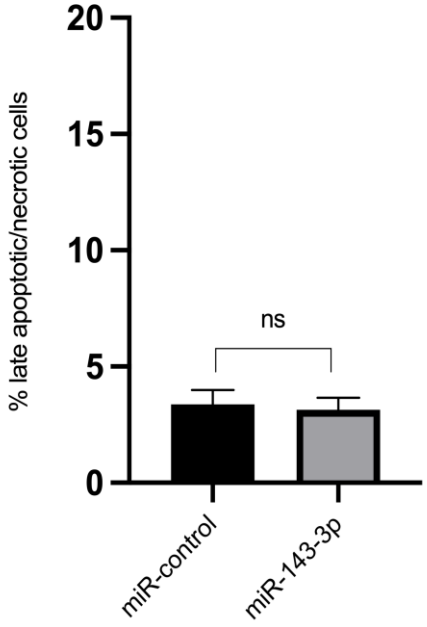

G. Infected/early apoptosis.

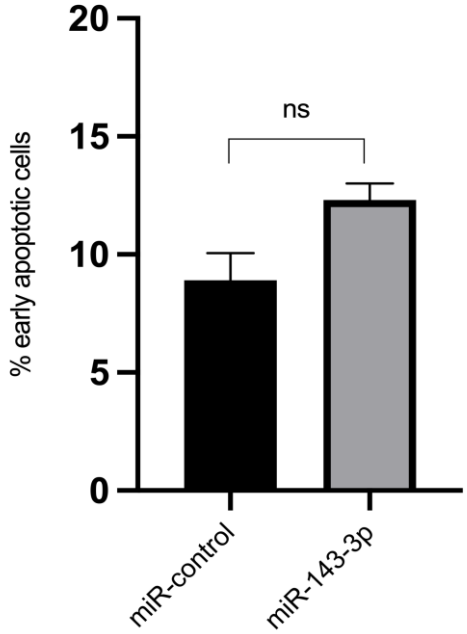

H. Infected/late apoptosis

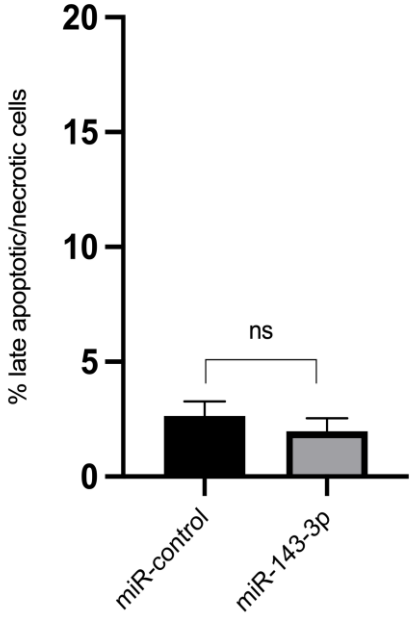

Figure 5. miR-143-3p promotes early apoptosis. Panels A-D show representative flow cytometry density plots. Early apoptotic cells are Annexin V-PE^{+ve}/eFluor780^{-ve} (Q4), whereas late apoptotic cells are Annexin V-PE^{-ve}/eFluor780^{+ve} (Q2). (E, F) Percentage of early and late apoptotic cells in uninfected HeLa cells that were transfected with miR-143-3p or control miRNA (miR-control); (G, H) Percentage of early and late apoptotic cells in *Coxiella*-infected cells that were pre-transfected with miR-143-3p or control miRNA. Pairwise comparisons of number of apoptotic cells were done using two-tailed paired t-test followed by Welch's correction (n = 3).

To begin to understand the miR-143-3p regulatory circuit, we assessed the expression of AKT1 and BCL2, two genes that are regulated by miR-143-3p (28–31) and are central to apoptosis regulation in human macrophages (10, 11). Expression levels of both AKT1 and BCL2 in uninfected cells were significantly reduced in miR-143-3p-transfected cells compared to cells transfected with control miRNA, but infection with *C. burnetii* abrogated the inhibitory effect of miR-143-3p on these genes (**Figure 6)**. Measurement of Akt and Bcl-2, the proteins encoded by the two genes, revealed that while infection neutralized the inhibitory effect of miR-143-3p on Akt, in both uninfected and *Coxiella*-infected cells, the miRNA seems to significantly inhibit Bcl-2 production (**Figure 7)**.

A. Uninfected

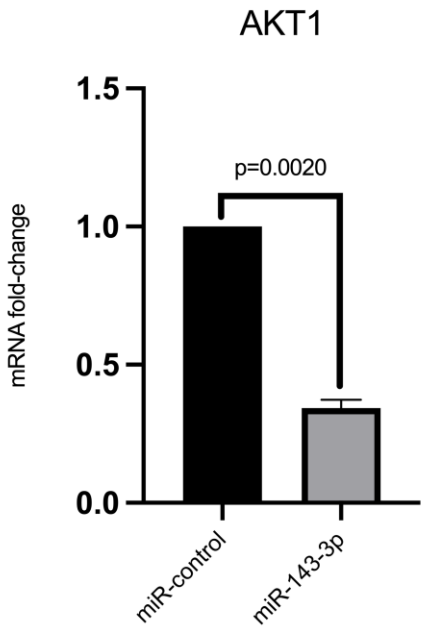

B. Uninfected

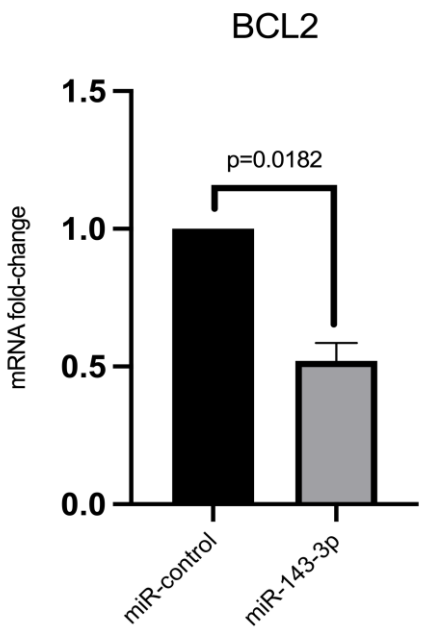

C. Infected

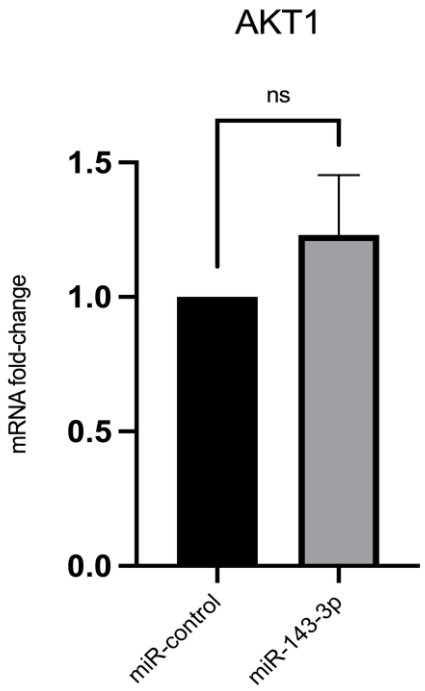

D. Infected

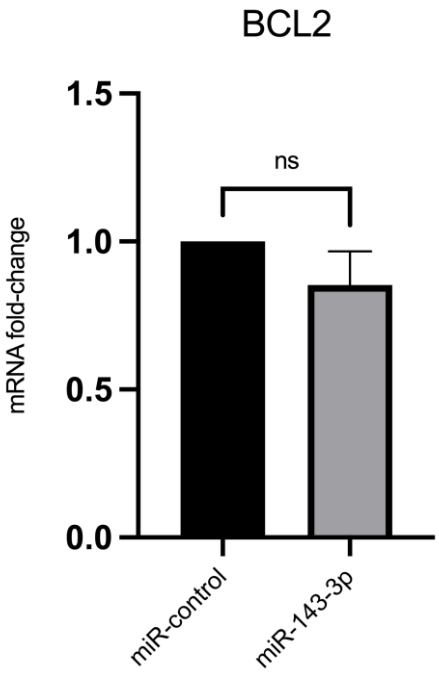

Figure 6. Transfection of HeLa cells with miR-143-3p reduces AKT1 and BCL2 expression. Panels A and B show fold change in AKT1 and BCL2 mRNA expression in uninfected cells when transfected with miR-143-3p compared to cells transfected with control miRNA (miR-control). Panels C and D show fold change in AKT1 and BCL2 mRNA expression in infected cells (48 hpi) pre-transfected with miR-143-3p compared to the miR-control. Pairwise comparisons of the expression values were done using two-tailed paired t-test followed by Welch's correction (n = 3).

A. Uninfected

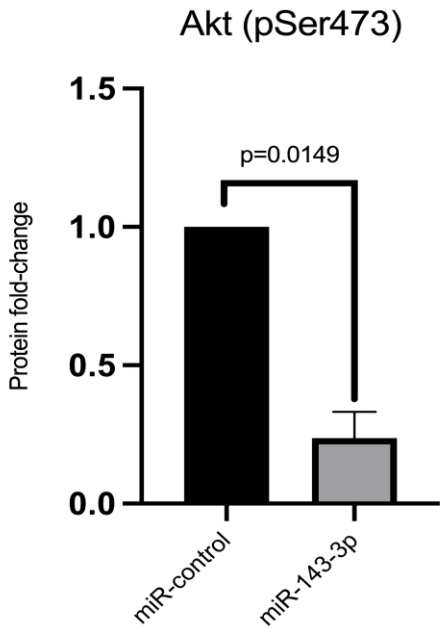

B. Uninfected

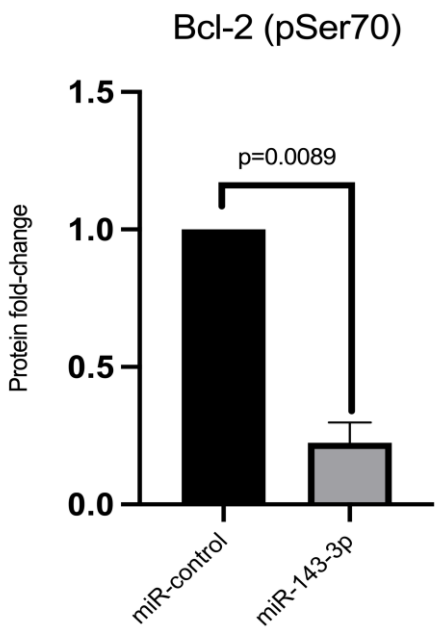

C. Infected

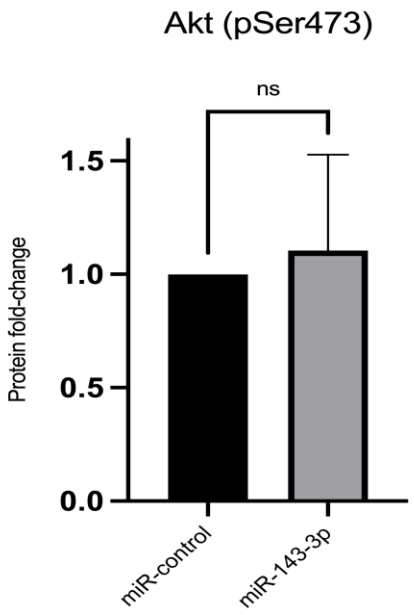

D. Infected

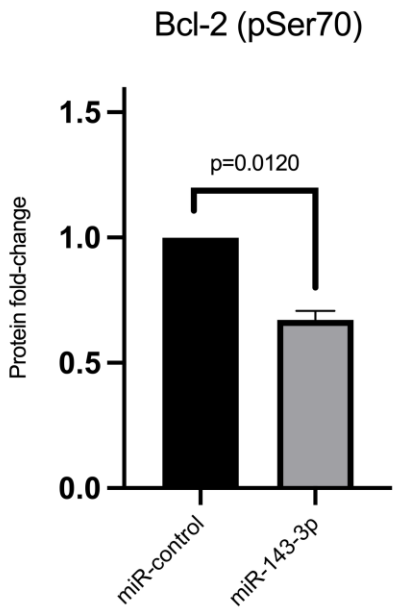

Figure 7. Transfection of HeLa cells with miR-143-3p affects Akt and Bcl-2 production. Panels A and B show fold change in Akt (pSer473) and Bcl-2 (pSer70) protein expression in uninfected cells when transfected with miR-143-3p compared to the cells transfected with control miRNA (miR-control). Panels C and D show fold change in Akt (pSer473) and Bcl-2 (pSer70) protein expression in infected cells (48 hpi) pre-transfected with miR-143-3p compared to the miR-control. Pairwise comparisons of the median fluorescence intensity (MFI) values were done using two-tailed paired t-test followed by Welch's correction (n = 3).

miR-143-3p has potential roles in autophagy and cytokine response

In addition to apoptosis, our analysis of miR-143-3p-targeted pathways indicated that the miRNA could be involved in autophagy and cytokine production **(Table S3),** two processes that are interconnected with the apoptosis pathway and are known to be affected during *Coxiella* infection (32–35). To test this, we measured rapamycin-induced autophagosomal flux in HeLa cells transfected with either miR-143-3p or control miRNA. This analysis showed that in uninfected cells, autophagosomal flux was slightly, but significantly, lower in miR-143-3p-transfected cells compared to the control; however, this phenotype was not observed when the transfected cells were infected with *C. burnetii* (**Figure 8**). To test miR-143-3p's potential role in cytokine response, we measured cytokine levels using multiplex immunoassay in supernatant collected from HeLa cell cultures transfected with miR-143-3p. Of the 20 cytokines and chemokines included in the immunoassay panel, we observed increased production of six proinflammatory proteins [TNF, CXCL8, CCL11 (eotaxin), CXCL10 (IP-10), CXCL1 (GRO alpha), CCL4 (MIP-1 beta)], as well as downregulation of IL6 and CCL2 (MCP-1) (**Figure 9**).

A. Uninfected B. Infected

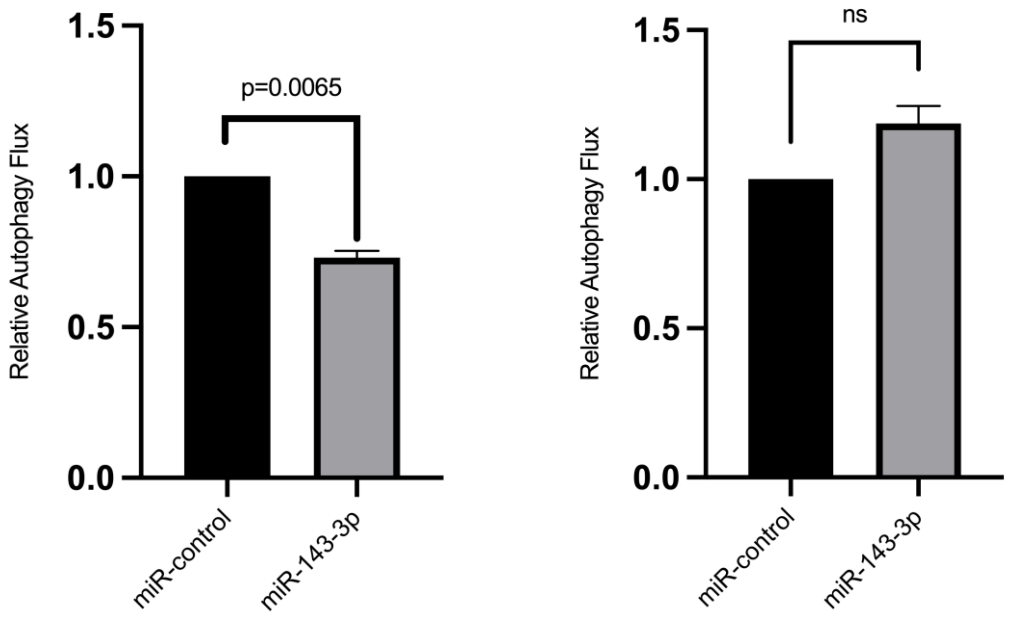

Figure 8. miR-143-3p inhibits autophagic flux. Y-axes show relative autophagy flux reported as average brightness of CYTO-ID green (a cationic tracer that selectively labels autophagic compartments) per cell compared to control. Autophagy was measured in HeLa cells that were transfected with either miR-143-3p or control miRNA (miR-control) and were infected with *C. burnetii* (B) or remained uninfected (A). Pairwise comparisons of average CYTO-ID green brightness per cell on at least 200 cells per well were done using two-tailed paired t-test followed by Welch's correction (n = 3).

A. Cytokines

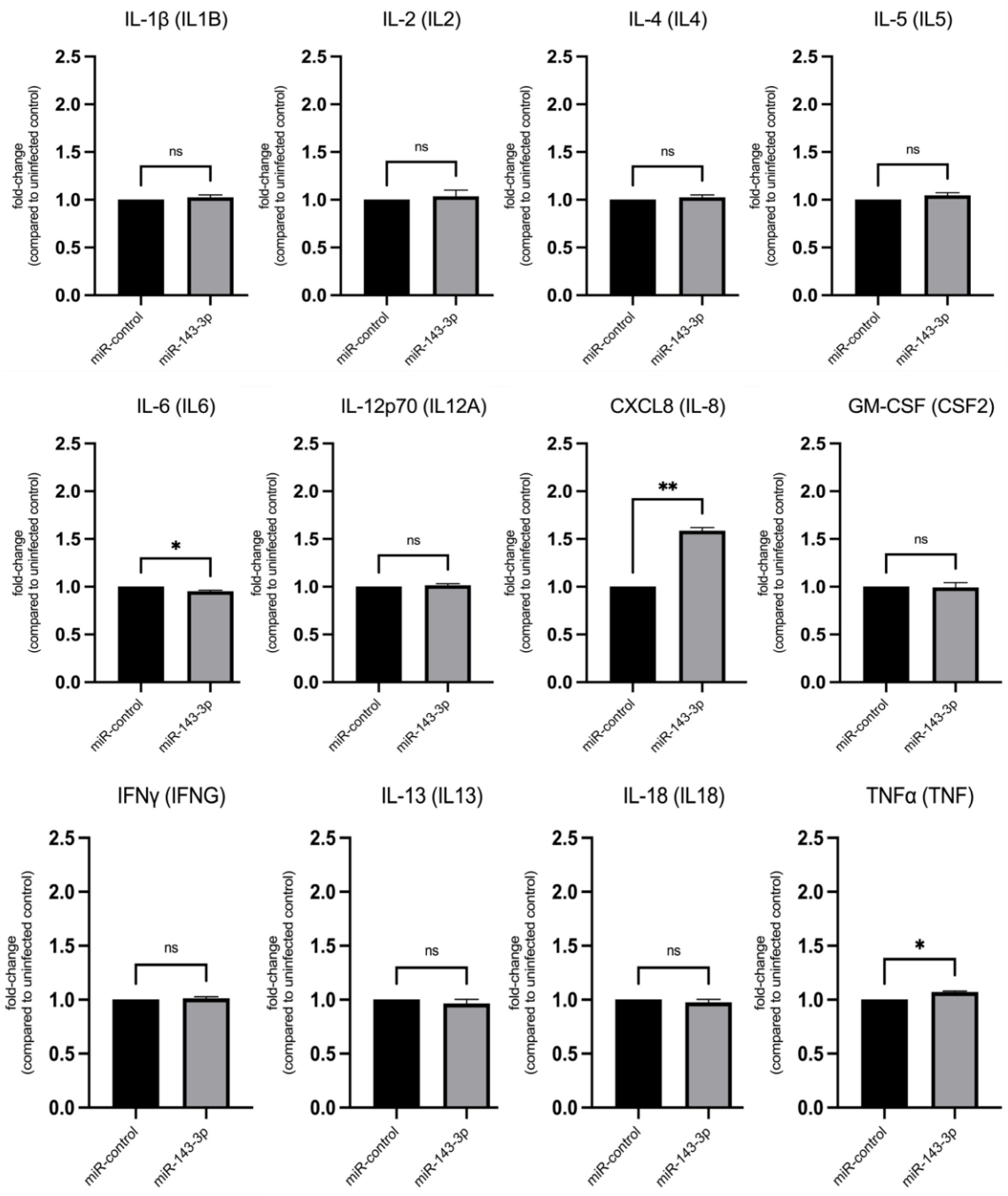
IL-1β (IL1B)
IL-2 (IL2)
IL-4 (IL4)
IL-5 (IL5)
IL-6 (IL6)
IL-12p70 (IL12A)
CXCL8 (IL-8)
GM-CSF (CSF2)
IFNγ (IFNG)
IL-13 (IL13)
IL-18 (IL18)
TNFα (TNF)
fold-change (compared to uninfected control)
2.5
2.0
1.5
1.0
0.5
0.0
ns
*
**
miR-control
miR-143-3p

B. Chemokines

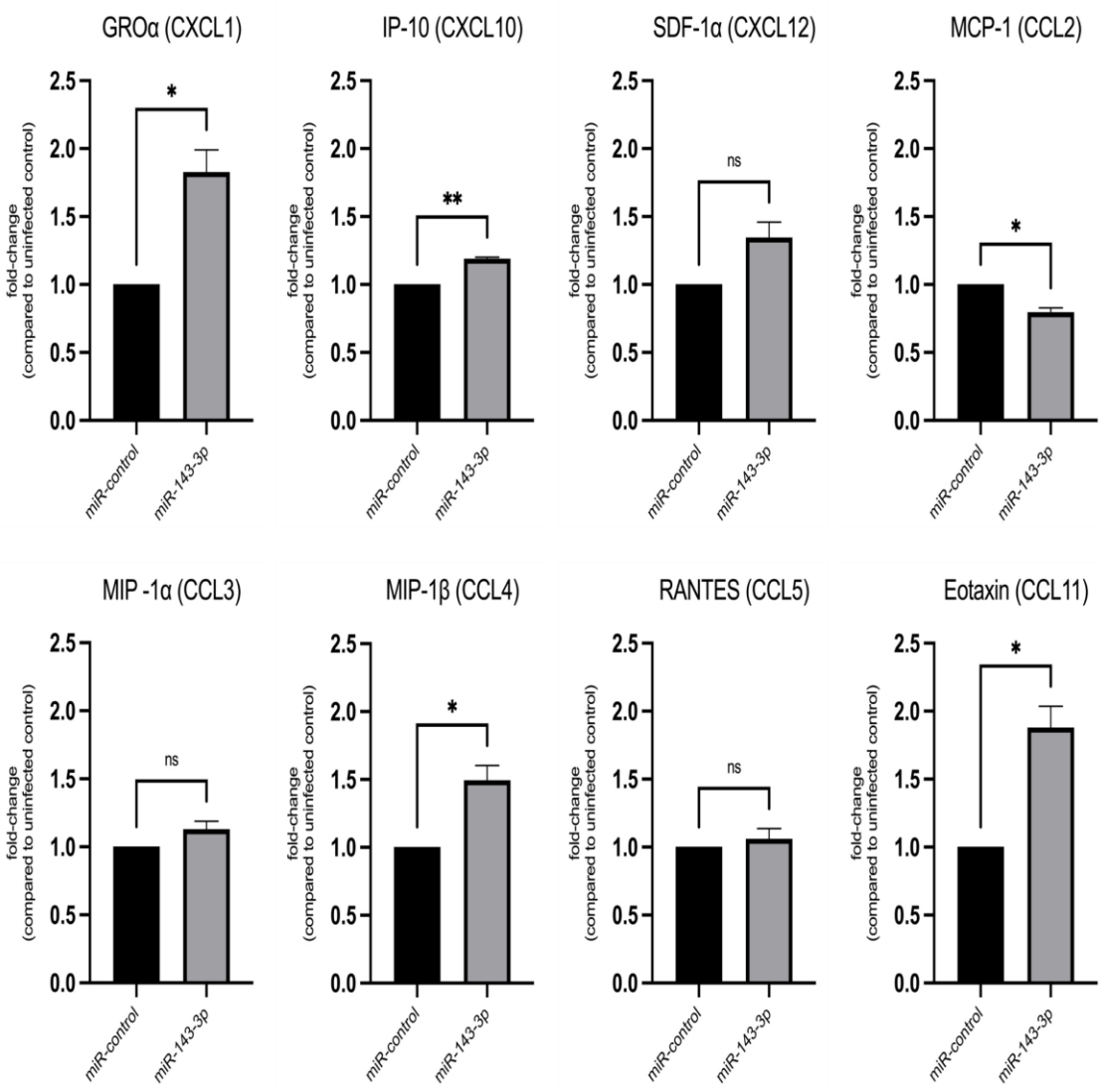

Figure 9. miR-143-3p impacts cytokine response. Y-axis shows the fold-change of (A) cytokines and (B) chemokines secretion by HeLa cells that were transfected with either miR-143-3p or control miRNA (miR-control). Pairwise comparisons of the median fluorescence intensity (MFI) values, that corresponds to the concentrations of cytokines of chemokines, were done using two-tailed paired t-test followed by Welch's correction (*$p \leq 0.05$, **$p \leq 0.01$; $n = 3$).

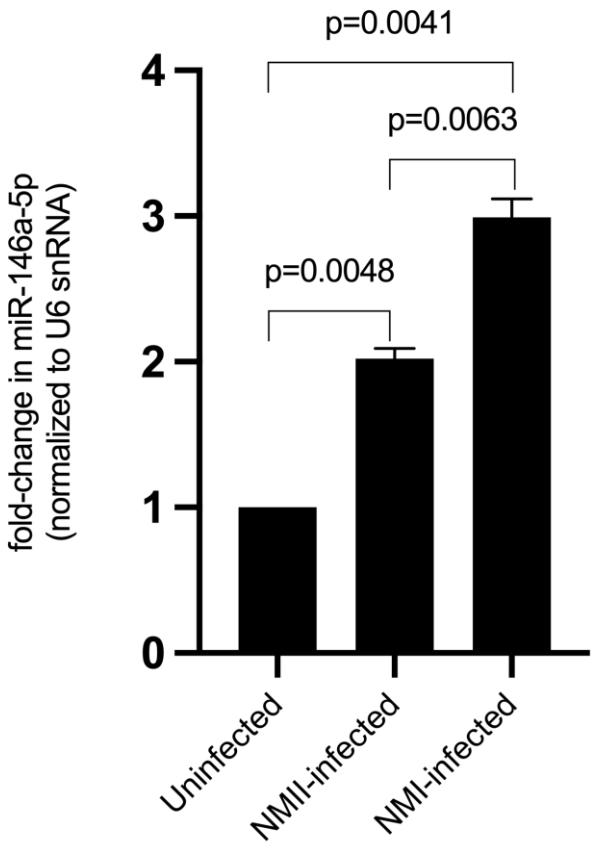

Figure 10. miR-146a-5p expression in primary human alveolar macrophages (hAMs) infected with C. *burnetii*. The y-axis shows the fold-change in miR-146a-5p expression normalized to the expression of U6 small nuclear RNA, an internal control. The x-axis corresponds to the hAMs that are uninfected, infected with NMII or NMI isolate at 25 multiplicity of infection (72 hours post-infection). Pairwise comparisons of the expression values were done using two-tailed paired t-test followed by Welch's correction (n = 3).

A.

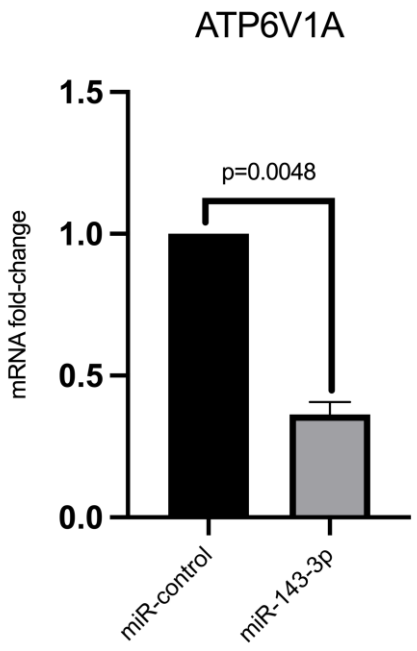
ATP6V1A
mRNA fold-change
1.5
1.0
0.5
0.0
p=0.0048
miR-control
miR-143-3p

B.

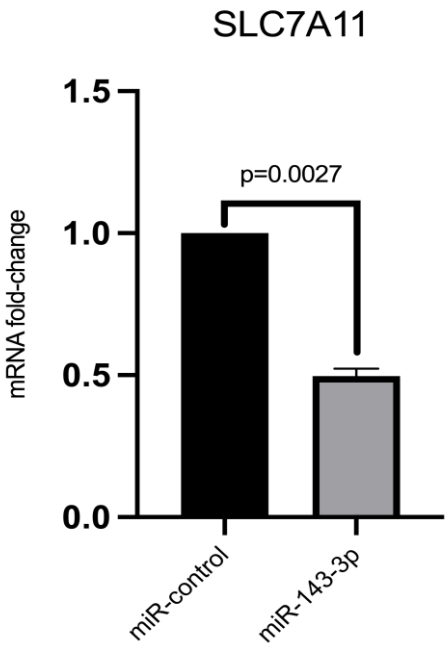
SLC7A11
mRNA fold-change
1.5
1.0
0.5
0.0
p=0.0027
miR-control
miR-143-3p

C.

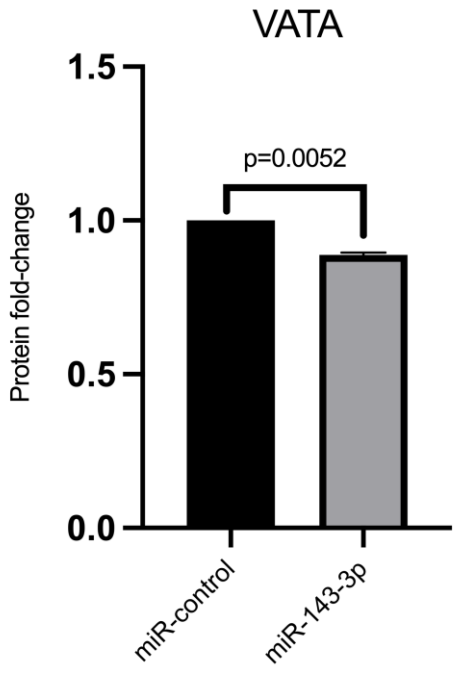
VATA
Protein fold-change
1.5
1.0
0.5
0.0
p=0.0052
miR-control
miR-143-3p

D.

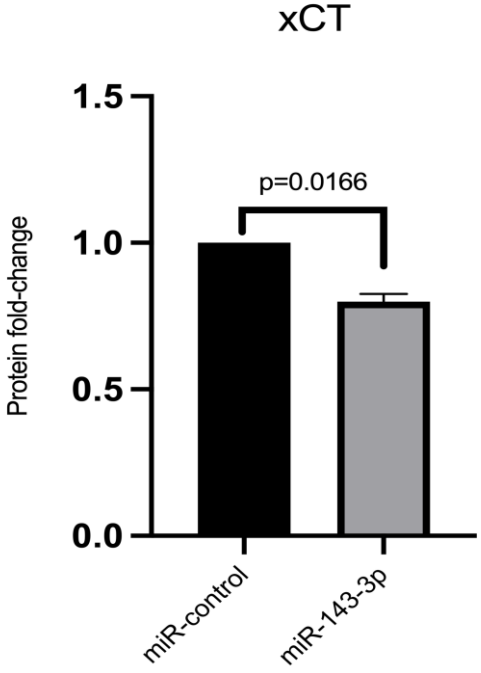
xCT
Protein fold-change
1.5
1.0
0.5
0.0
p=0.0166
miR-control
miR-143-3p

Figure 11. Transfection of HeLa cells with miR-143-3p knockdown v-atpase/ATP6V1A and xCT/SLC7A11 expression. A and B show fold change in ATP6V1A and SLC7A11 mRNA expression in uninfected cells when transfected with miR-143-3p compared to the miRNA negative control (miR-control). C and D show fold change in VATA (ATP6V1A) and xCT (SLC7A11) protein expression in uninfected cells pre-transfected with miR-143-3p compared to the miRNA control measured using quantitative mass-spectrometry. Pairwise comparisons of the raw values were done using two-tailed paired t-test followed by Welch's correction (n = 3).

DISCUSSION

In the present study we show that *C. burnetii* induces the expression of stage-specific sets of host genes with miRNAs likely serving as modulators of host responses. Our data also indicate that the downregulation of miR-143-3p expression observed during *C. burnetii* infection in macrophages likely contributes to the pathogen's intracellular growth. Indeed, overexpression of miR-143-3p reduced bacterial intracellular growth as well as counteracted cellular processes that promote *C. burnetii* survival in HeLa cells. These findings help our understanding of *C. burnetii*-macrophage interactions and could be relevant to infections caused by other intracellular pathogens such as *Anaplasma phagocytophilum* and *Chlamydia trachomatis* (36).

During later stages of infection, *C. burnetii* transitions from the metabolically-active LCV into a dormant SCVs (26, 37, 38). Our data shows that around day 5 post-infection, this developmental transition in *C. burnetii* may induce stage-specific sets of host genes **(Figure 1)**, as shown previously for infections with pathogens such as *C. trachomatis*, *Leishmania major*, and *L. amazonensis* that also have similar biphasic intracellular lifestyles (39, 40). The highest magnitude of host cell response was observed at 3 dpi, pathway enrichment analysis of genes that are the targets of miRNAs at this stage revealed multiple signaling pathways that are known to be involved in *Coxiella* infection such as phosphatidylinositol 3-kinase (PI3K)/protein kinase B (Akt) signaling, autophagy, and inhibition of apoptosis signaling.

Further, many miRNAs identified in this study contribute to host apoptosis regulation in various disease conditions (41–44). For example, miR-16-5p induction can promote host apoptosis in cells infected with Enterovirus 71 (45), and overexpression of

miR-146a-5p, an lipopolysaccharide (LPS)-induced anti-inflammatory miRNA, can inhibit apoptosis by destabilizing p53 (46, 47). A miRNA that was consistently down-regulated during *Coxiella* infection was miR-143-3p. This miRNA is known to inhibit autophagy, and promote apoptosis and pro-inflammatory response by directly inhibiting the expression of pro-survival genes and corresponding proteins such as Bcl-2 (B-cell lymphoma 2), Akt1, Atg2B (Autophagy Related 2B), and HK2 (Hexokinase 2) in a variety of cardiovascular diseases and cancers (30, 48–53). However, its function in host response to intracellular infection is not well understood.

Since our pathway enrichment analysis indicated that PI3K/Akt signaling was activated, we focused on understanding the contribution of miR-143-3p in the modulation of PI3K/Akt signaling network **(Figure 12)**. The PI3K/Akt signaling functions as a key regulator of diverse host cell functions, including autophagy, apoptosis, and inflammation (54). PI3K can activate Akt protein causing multiple downstream effects including mTOR (mechanistic target of rapamycin) activation that serves as a negative regulator of autophagy (55). In addition, activated Akt is known to induce pro-survival proteins such as Bcl-2, and inhibit pro-apoptotic proteins such as Bad (56). These signaling cascades lead to decreased caspase-3 activation and subsequent prevention of intrinsic apoptosis. In order to prevent host apoptosis, intracellular bacterial pathogens such as *Salmonella enterica* Typhimurium, *Legionella pneumophila*, and *M. tuberculosis* activate PI3K/Akt pathway through secreted effectors (57). In case of *C. burnetii,* although activation or phosphorylation of Akt has been reported to coincide with *C. burnetii* replication, effector(s), if any, has not yet been identified (11).

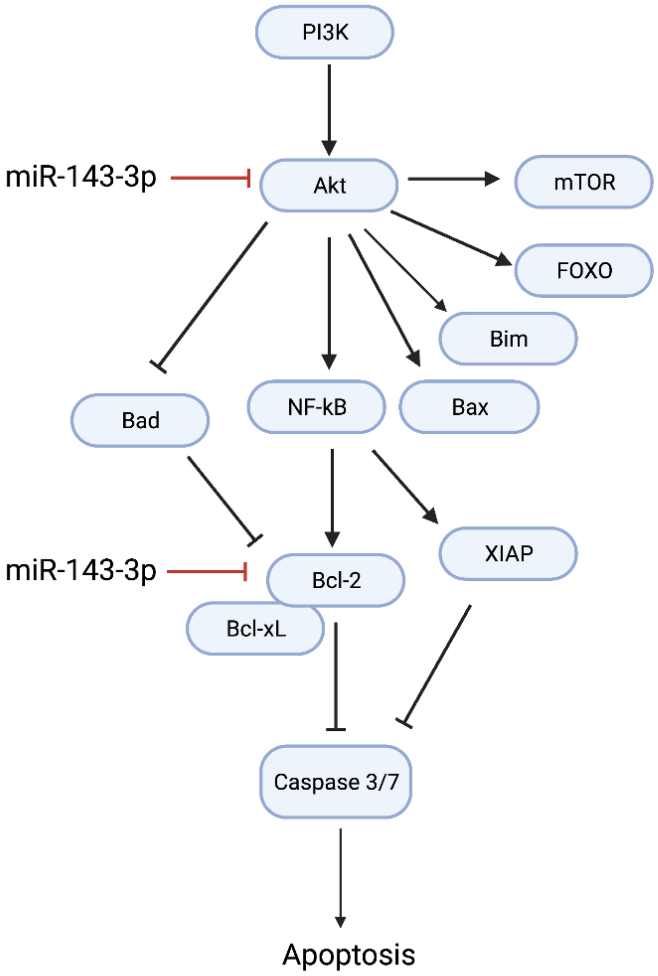

Figure 12. PI3K/Akt signaling network. Activation of PI3K leads to phosphorylation/activation of Akt. Akt activates pro-apoptotic proteins Bad, Bax, Bim, and pro-survival transcription factor NF-κB leading to induction of pro-survival proteins Bcl-2, Bcl-xL, and activation of XIAP. Bcl-2 prevents the release of cytochrome c from mitochondria, thereby preventing a caspase-3 dependent proteolytic cascade leading to apoptosis. Akt, in addition, also activates mTOR and FOXO proteins that can further contribute to apoptosis induction. Overexpression of miR-143-3p can target Akt and Bcl-2 to promote apoptosis.

Besides activating Akt during infection, *C. burnetii* also recruits Bcl-2 to the CCV (10), and secretes effectors to inhibit host apoptosis (6, 12). Interestingly, the transcripts encoding Akt and Bcl-2 contain binding sites for miR-143-3p and have been shown to be targeted by miR-143-3p (28, 29). Our data show that in uninfected HeLa cells that were transfected with miR-143-3p, expression levels of AKT1 and BCL2 both at the mRNA and protein levels were significantly reduced compared to the miRNA negative control. At the same time, miR-143-3p transfection enhanced the percentage of early apoptotic cells in the cells compared to the control suggesting that miR-143-3p induces intrinsic apoptosis by inhibiting the expression of AKT1 and BCL2. In contrast, in infected cells that were transfected with miR-143-3p, the inhibitory effect of miR-143-3p transfection on AKT1 and BCL2 expression was not observed except a moderate inhibition of Bcl-2 at the protein level. At the same time, the difference between percentage of early apoptotic cells in the miR-143-3p-transfected population and control-miRNA-transfected cells in infected cells was not as much as observed in the uninfected cells. Together, these observations suggest that *C. burnetii* infection tends to neutralize the pro-apoptotic effect of miR-143-3p overexpression probably by regulating Akt and Bcl-2. However, the exact mechanism by which the pathogen inhibits the effects of miR-143-3p is not clear.

Previously, lipopolysaccharide (LPS)-stimulated macrophages have been shown to downregulate miR-143-3p expression (58–60). In agreement with this observation, our data show that while miR-143-3p expression was downregulated in cells infected with either NMI or NMII, the degree of downregulation is much more severe in cells infected with NMI, which contains intact LPS, compared to cells infected with the LPS mutant NMII. In addition, expression of miR-146a-5p, a well-known LPS-induced miRNA, in

hAMs infected with NMI was significantly higher than in NMII-infected and uninfected hAMs **(Figure 10)**. Both these findings suggest that LPS of *C. burnetii* may contribute to the modulation of miR-143-3p and miR-146a-5p during *C. burnetii* infection.

Apart from apoptosis, a number of proteins involved in autophagic pathways in intracellular infections are known to be targeted by miRNAs such as miR-146a-5p, miR-125a-5p, and miR-143-3p (52, 66-68). miR-143-3p has been previously shown to target ATG2B to inhibit autophagy (49, 61), and inhibition of autophagy has been shown to reduce intracellular growth of *C. burnetii* and improper CCV maturation (62–64). Therefore, downregulation of miR-143-3p could favor *C. burnetii* growth by the promotion of autophagy and associated proteins such as AKT1, ATG2B, v-ATPase/ATP6V1A and cystine/glutamate antiporter xCT/SLC7A11 that have been known or predicted to be targets of miR-143-3p (16–18, 65–67). In our study on uninfected cells, ATP6V1A and SLC7A11 were found to be downregulated in miR-143-3p transfected cells at the transcript and protein level compared to the miRNA negative control suggesting their involvement in miR-143-3p-mediated inhibition of autophagy **(Figure 11, Table S4)**. At the same time, transfection of miR-143-3p was found to inhibit autophagic flux in uninfected cells compared to the control but not in infected cells. Both of these observations shows that overexpression of miR-143-3p could reduce autophagy that may involve the inhibition of ATP6V1A, SLC7A11, and AKT1 expression.

Inhibition of Akt has also been reported to contribute to a proinflammatory response (68). Further, host inflammatory response is known to be fine-tuned by multiple miRNAs (69, 70). For example, upregulation of miR-146a-5p can promote an

anti-inflammatory phenotype that facilitates the intracellular growth of *M. tuberculosis* in murine macrophages (71). In the case of miR-143-3p, overexpression of the miRNA in intestinal epithelial cells has been shown to reduce IκBα (an inhibitor of NF-κB) and IL-10 levels, and increase the expression of proinflammatory cytokine such as TNF and CXCL8 (49, 72, 73). It is likely that modulation of these miRNAs may benefit *C. burnetii* survival by attenuating the pro-inflammatory host response. Our findings were consistent with the proinflammatory nature of miR-143-3p as the secretion of six proinflammatory or immunomodulatory cytokines/chemokines i.e., IP-10 (CXCL10), CXCL8 (IL8), eotaxin (CCL11), TNFα (TNF), MIP-1β (CCL4), and GROα (CXCL1) were found to be significantly upregulated in cells transfected with miR-143-3p compared to the control. A down-regulated secretion of IL6 and CCL2 in miR-143-3p-transfected cells suggests that miR-143-3p may have additional mechanisms to regulate inflammatory responses in the hosts. It would be interesting to further explore the mechanisms by which the miR-143 regulates the host inflammatory response during *C. burnetii* infection, but collectively our results suggest that downregulation of miR-143-3p may attenuate the expression of proinflammatory cytokine by host cells. In sum, our findings indicate that during *C. burnetii* infection, downregulation of miR-143-3p can benefit the intracellular growth of the pathogen by inhibiting apoptosis and inflammation, and by promoting autophagy.

MATERIALS AND METHODS

Bacterial isolates and infection

Coxiella burnetii Nine Mile RSA439 (Phase II, Clone 4) isolate (NMII) or an isogenic GFP-tagged isolate was cultured in acidified citrate cysteine medium-2 (ACCM-2) for 7

days at 37°C, 5% CO_2, 2.5% O_2 (74) 84). Bacteria were quantified using PicoGreen (75), collected by centrifugation (3000xg,10min, 4°c), resuspended in PBS containing 0.25 M sucrose (PBSS) and stored at –80℃ until further use. Before infection, THP-1 cells (American Type Culture Collection, TIB-202) were differentiated in complete growth medium (RPMI-1640 supplemented with 1 mM sodium pyruvate, 0.05 mM beta-mercaptoethanol, 4500 mg/L glucose, and 10% heat-inactivated fetal bovine serum (FBS)) at 37℃ under 5% CO2 for 24 h using 30 nM phorbol 12-myristate 13-acetate (PMA), followed by 24 h of rest in PMA-free medium to differentiate cells into adherent, macrophage-like cells. Cells were infected with NMII isolate at a multiplicity of infection (MOI) of 25 in serum-free complete RPMI medium for two hours and this time-point was considered to be 0 h post infection (hpi). To remove extracellular bacteria, cells were washed three times with PBS followed by replacement with complete growth medium. The complete growth medium was replaced at 72 hpi. Primary human alveolar macrophages (hAMs) were harvested by bronchoalveolar lavage (BAL) from postmortem human lung donors and infected with NMI (Nine Mile RSA 493) or NMII (Nine Mile RSA439, Phase II, Clone 4) isolate of *C. burnetii* at 25 MOI (76). Unlike NMI that possess a full-length LPS, its derivative NMII has a truncated LPS. hAMs were cultured at 37℃ under 5% CO_2 in Dulbecco's modified Eagle/F-12 (DMEM/F12) medium (Gibco) containing 10% FBS for 72 h post-infection.

Transfection of HeLa cells

Nucleotide sequence of hsa-miR-143-3p was obtained from miRBase 22.1 (77): 5'-UGAGAUGAAGCACUGUAGCUC-3' (accession number MIMAT0000435).

miRCURY LNA miRNA mimic for hsa-miR-143-3p (cat. YM00470035-ADB) and miRNA negative control miRCURY LNA (cat. YM00479902-ADB) were purchased from Qiagen. The negative control is a non-specific miRNA that shows no homology to any known miRNA or mRNA sequences in mouse, rat or human. HeLa cells were reverse transfected as previously described (78). Briefly, 25nM (final concentration) of miR-143-3p mimic or miRNA negative control was mixed and incubated with HiPerFect Transfection Reagent (Qiagen) for 10 min at room temperature to allow formation of transfection complexes. The transfection complex was pre-spotted and uniformly distributed in each well of a 24-well plate. Further, 3.5×10^4 HeLa cells/well were incubated with these transfection complexes for 24 h in OptiMEM media. After 24 h, media was removed, and cells were washed twice with PBS before infection with NMII isolate at MOI of 100 in serum-free DMEM medium for two hours followed by washing and replenishing the cells with serum-containing DMEM medium for subsequent experiments at 48 hpi.

Intracellular growth assay

C. burnetii growth was quantified using qPCR and by quantifying colony-forming units (CFUs) at 48 hpi from HeLa cells that were pre-transfected 24 h before infection with miR-143-3p or miRNA negative control (26, 79). To quantify intracellular bacteria using qPCR, cells were washed, and total DNA was extracted using QIAamp DNA Mini Kit (Qiagen) according to the manufacturer's instructions. 70 ng of total DNA was then subjected to qPCR using CBU_tRNA-Glu-2-specific primers and SYBR Green, as described previously (75). Ct values were converted to the bacterial genome equivalents

(GE) using a standard curve to enumerate bacterial growth, as described previously (75, 80). Since qPCR based quantitation does not differentiate between live and dead cells, we independently quantified viable intracellular bacteria by enumerating CFUs (79, 81). Briefly, infected cells were washed and lysed in ice-cold water for 40 min at 4°C followed by repeated pipetting with a syringe carrying a 25G needle to lyse the remaining cells. The suspension was centrifuged for 10 min at 70 x g (4°C) followed by centrifugation of the supernatant for 1 min at 13,500 x g (4°C). The pellet was resuspended in ACCM-2, serially diluted and was spot-plated on ACCM-2 containing 0.5 mM tryptophan and 0.5% agarose as described by Sanchez et al., 2018 (79). Plates were incubated for 10 days at 37°C, 5% CO_2, and 2.5% O_2 before counting the colonies.

Illumina sequencing, miRNA-target interactions, and pathway analysis

Macrophage-like THP-1 cells infected with NMII (MOI of 25) were analyzed at 8, 24, 48, 72, and 120 hpi for miRNA and mRNA expressions. At respective time-points post-infection, the growth medium was replaced with 1ml of TRI reagent (Life Technologies) and total RNA was extracted and purified by DNase treatment (Invitrogen) as per the manufacturers' instructions. Samples were sequenced using Illumina NovaSeq 6000 for mRNAs and Illumina HiSeq 2500 for miRNAs at Yale Center for Genome Analysis or at Novogene Corporation, Sacramento, CA. Differential gene expression analysis of genes (encoding miRNAs, proteins, or long non-coding RNAs) was conducted using DESeq2 (82) after mapping the sequencing reads to the reference human miRNA (miRbase 22.1) or genome (GRCh38) databases in CLC Genomics Workbench v6.5 (Qiagen). Differentially regulated miRNA and mRNAs were calculated using log2 fold-change (≥

0.75 or ≤ 0.75) and an adjusted p-value ≤ 0.05 compared to uninfected controls. Inverse-expression pairings of differentially regulated miRNAs and mRNAs in THP-1 cells were carried out using Ingenuity Pathway Analysis (IPA, Qiagen) based on known and predicted miRNA-target interactions (MTIs) followed by IPA core analysis of the differentially expressed genes to find enriched pathways and upstream regulators (27).

Quantitative PCR (qRT-PCR)

Differential expression of 84 apoptosis-related miRNAs was confirmed using a qRT-PCR array (Qiagen). Briefly, total RNA extracted from NMII-infected or uninfected THP-1 cells were reverse transcribed using a miScript II RT kit followed by cDNA synthesis from mature miRNAs using HiSpec buffer (Qiagen). Quantitative PCR reactions were carried out on Stratagene Mx3005P according to the manufacturer's instructions. Primers for miR-143-3p (cat. MS00003514, Qiagen) and the endogenous reference small nuclear ribonucleic acid RNU6 (cat. MS00033740, Qiagen) were used to confirm miR-143 expression in hAMs. Raw data from the array were normalized using the global quantitation cycle (Cq) mean of expressed miRNAs, and relative miRNA expression levels were calculated by using the delta-delta Cq method (83).

Expressions of AKT1 and BCL2 were quantified using qRT-PCR on uninfected or infected HeLa cells transfected with either miR-143-3p or control miRNA. Briefly, total RNA was extracted, DNase treated, and cDNA was generated using RevertAid First Strand cDNA Synthesis Kit (Thermo Scientific). To perform qPCR, cDNA template was diluted, and mixed with gene-specific primers and SYBR Green (Applied Biosystems) in a 20ul reaction according to the recommended protocol (Applied Biosystems). The

primers used in this experiment are in the supplementary (**Table S5**). Relative mRNA expression levels were calculated by using the delta-delta Cq method.

Apoptosis assay

Early apoptosis was quantified using flow cytometry on uninfected or NMII-infected HeLa cells that were pre-transfected with miR-143-3p or miRNA negative control 24 h before infection. After 48 h post-infection, cells were treated with trypsin, stained with efluor780 Fixable Viability Dye (Invitrogen) for 30 minutes in dark (4°C), followed by staining with Annexin V-PE (Invitrogen) for 15 minutes as per the recommended protocol (Invitrogen). The cells were immediately assayed for early apoptosis (Annexin V-PE^{+ve}/eFluor780^{-ve}) and late apoptosis (Annexin V-PE^{-ve}/eFluor780^{+ve}) markers using FACSAria Fusion flow cytometer (BD Biosciences). Fluorescence parameters were gated using unstained and single-stained uninfected control cells and a total of 10,000 events were counted for each sample using FACSDiva Software (BD Biosciences).

Autophagic flux assay

CYTO-ID Autophagy Detection Kit 2.0 (ENZ-KIT175, Enzo Life Sciences) was used to quantify autophagic flux on uninfected or NMII-infected HeLa cells that were pre-transfected with miR-143-3p or miRNA negative control at 72 h post-transfection. Before the assay, cells were treated with media containing 200 nM rapamycin for 16-18 hours to induce detectable level of autophagy (84, 85). Post-treatment, cells were washed and incubated for 30 minutes at 37°C in Microscopy Dual Detection Reagent containing CYTO-ID green detection reagent and Hoechst 33342 nuclear stain in 1X assay buffer.

At least 200 cells per well in triplicates were immediately analyzed at 20X magnification with FITC and DAPI filters set in a Keyence fluorescence microscope. The level of autophagic flux was reported as average CYTO-ID green brightness per cell following the manufacturer's instructions using Keyence BZ-X700 software (86, 87).

Multiplex immunoassay

Proteins involved in early apoptosis such as Akt (pS473), BAD (Ser112), Bcl-2 (Ser70), p53 (Ser46), JNK (Thr183/Tyr185), active Caspase-8 (Asp384), and active Caspase-9 (Asp315) were quantitated using 7-Plex Early Apoptosis Magnetic Bead Kit (EMD Millipore). Total cell lysate from uninfected or NMII-infected HeLa cells pre-transfected with miR-143-3p or miRNA negative control was prepared using Lysis Buffer containing protease inhibitors, followed by bicinchoninic acid (BCA) quantitation at 72 h post-transfection. Briefly, 17.5 µg/well of diluted cell lysate was added with 1X magnetic beads at 1:1 ratio in a 96-well plate. The plate was incubated on a plate shaker (4°C, 700 rpm, dark) for 18 hours, followed by washing and incubation with 1X Detection Antibody for 60 min at RT with shaking (700 rpm, dark). The detection antibody was then removed, and samples were incubated for 15 min at room temperature (RT) in the dark with 1X Streptavidin-PE (SAPE), followed by 15 min incubation (RT, dark) with an amplification buffer. SAPE and amplification buffer were removed, and beads were resuspended in a 150 µl assay buffer to analyze median fluorescence intensity (MFI) using a Luminex 200 system.

Cytokine levels were assessed in supernatants collected from HeLa cells pre-transfected with miR-143-3p or miRNA negative control using Th1/Th2 Cytokine &

Chemokine 20-Plex ProcartaPlex Panel 1 (Invitrogen) at 48 h post-transfection. The level of 20 cytokines and chemokines (GM-CSF, IFN gamma, IL-1 beta, IL-2, IL-4, IL-5, IL-6, IL-8, IL-12p70, IL-13, IL-18, TNF alpha, Eotaxin, GRO alpha, IP-10, MCP-1, MIP-1 alpha, MIP-1 beta, RANTES, and SDF-1 alpha) were quantified according to the manufacturer's guidelines. Briefly, supernatants were centrifuged 10,000 x g for 10 minutes to remove particulate matter and stored at -80°C. In a 96-well plate, magnetic beads were added in appropriate wells, washed, and 50 µL of prepared antigen standards, controls, or samples were added. The plate was shaken for 30 min at RT (500 rpm), followed by overnight incubation at 4°C. After incubation, the plate was shaken for 30 min at RT (500 rpm), washed, and incubated with the detection antibody (30 min, RT, 500rpm). Then the plate was washed, incubated with SAPE (30 min, RT, 500rpm), followed by washing and addition of 120 µL of reading buffer to analyze MFI in a Luminex 200 instrument.

Quantitative mass spectrometry

To determine the proteins can be downregulated by miR-143-3p transfection, total cell lysate from HeLa cells, reverse-transfected with miR-143-3p or control miRNA were collected after 48h post-transfection in triplicates. TMT labeling and mass spectrometry were performed by the OHSU proteomics core facility as described previously (88). Briefly, samples were lysed, sonicated, and heated at 90c for 10 min followed by overnight micro-digestion of each sample using S-trap micro protocol. Peptides were labelled with TMT6-plex reagents, and multiplexed TMT-labeled samples were separated by two-dimensional reversed-phase-reversed-phase (2DRPRP) liquid chromatography on

Orbitrap Fusion Tribrid instrument (Thermo Scientific). Proteins were identified by searching against the human proteome in UniProt, and TMT reporter ion intensities were processed with in-house scripts. Differential protein abundance was determined by the Bioconductor package edgeR.

Data availability

Sequencing reads from this study have been deposited at NCBI Sequence Read Archive (SRA) under the BioProject accession PRJNA679931.

ACKNOWLEDGEMENTS

This work was supported in part by National Institutes of Health grants AI123464 and AI133023 to RR.

REFERENCES

1. Minnick MF, Raghavan R. 2012. Developmental biology of *Coxiella burnetii*. *Adv Exp Med Biol* 984:231–248.
2. Dragan AL, Voth DE. 2019. *Coxiella burnetii:* International pathogen of mystery. *Microbes Infect* 22:100-110.
3. Larson CL, Martinez E, Beare PA, Jeffrey B, Heinzen RA, Bonazzi M. 2016. Right on Q: genetics begin to unravel *Coxiella burnetii* host cell interactions. *Future Microbiol* 11:919–939.
4. Newton P, Thomas DR, Reed SCO, Lau N, Xu B, Ong SY, Pasricha S, Madhamshettiwar PB, Edgington-Mitchell LE, Simpson KJ, Roy CR, Newton HJ. 2020. Lysosomal degradation products induce *Coxiella burnetii* virulence. *Proc Natl Acad Sci USA* 117:6801-6810.
5. Friedrich A, Pechstein J, Berens C, Lührmann A. 2017. Modulation of host cell apoptotic pathways by intracellular pathogens. *Curr Opin Microbiol* 35:88–99.
6. Eckart RA, Bisle S, Schulze-Luehrmann J, Wittmann I, Jantsch J, Schmid B, Berens C, Lührmann A. 2014. Antiapoptotic activity of *Coxiella burnetii* effector protein AnkG is controlled by p32-dependent trafficking. *Infect Immun* 82:2763–2771.
7. Bisle S, Klingenbeck L, Borges V, Sobotta K, Schulze-Luehrmann J, Menge C, Heydel C, Gomes JP, Lührmann A. 2016. The inhibition of the apoptosis pathway by the *Coxiella burnetii* effector protein CaeA requires the EK repetition motif, but is independent of survivin. *Virulence* 7:400–412.

8. Kohl L, Hayek I, Daniel C, Schulze-Lührmann J, Bodendorfer B, Lührmann A, Lang R. 2019. MyD88 Is Required for Efficient Control of *Coxiella burnetii* Infection and Dissemination. *Front Immunol* 10:165.
9. Macdonald LJ, Graham JG, Kurten RC, Voth DE. 2014. *Coxiella burnetii* exploits host cAMP-dependent protein kinase signalling to promote macrophage survival. *Cell* Microbiol 16:146–159.
10. Vázquez CL, Colombo MI. 2010. *Coxiella burnetii* modulates Beclin 1 and Bcl-2, preventing host cell apoptosis to generate a persistent bacterial infection. *Cell Death Differ* 17:421–438.
11. Voth DE, Heinzen RA. 2009. Sustained activation of Akt and Erk1/2 is required for *Coxiella burnetii* antiapoptotic activity. *Infect Immun* 77:205–213.
12. Klingenbeck L, Eckart RA, Berens C, Lührmann A. 2013. The *Coxiella burnetii* type IV secretion system substrate CaeB inhibits intrinsic apoptosis at the mitochondrial level. *Cell Microbiol* 15:675–687.
13. Bartel DP. 2018. Metazoan MicroRNAs. *Cell* 173:20–51.
14. Gebert LFR, MacRae IJ. 2019. Regulation of microRNA function in animals. *Nat Rev Mol Cell Biol* 20:21–37.
15. Vasudevan S, Tong Y, Steitz JA. 2007. Switching from repression to activation: microRNAs can up-regulate translation. *Science* 318:1931–1934.
16. Agarwal V, Bell GW, Nam J-W, Bartel DP. 2015. Predicting effective microRNA target sites in mammalian mRNAs. *Elife* 4.
17. Wang W, Cai Y, Deng G, Yang Q, Tang P, Wu M, Yu Z, Yang F, Chen J, Werz O, Chen X. 2020. Allelic-specific regulation of xCT expression increases

susceptibility to tuberculosis by modulating microRNA-mRNA interactions. *mSphere* 5.

18. Huang T, Huang X, Yao M. 2018. miR-143 inhibits intracellular *Salmonella* growth by targeting ATP6V1A in macrophage cells in pig. *Res Vet Sci* 117:138–143.

19. Janssen HLA, Reesink HW, Lawitz EJ, Zeuzem S, Rodriguez-Torres M, Patel K, van der Meer AJ, Patick AK, Chen A, Zhou Y, Persson R, King BD, Kauppinen S, Levin AA, Hodges MR. 2013. Treatment of HCV infection by targeting microRNA. *N Engl J Med* 368:1685–1694.

20. Koriyama T, Yamakuchi M, Takenouchi K, Oyama Y, Takenaka H, Nagakura T, Masamoto I, Hashiguchi T. 2019. *Legionella pneumophila* infection-mediated regulation of RICTOR via miR-218 in U937 macrophage cells. *Biochem Biophys Res Commun* 508:608–613.

21. Liu N, Wang L, Sun C, Yang L, Sun W, Peng Q. 2016. MicroRNA-125b-5p suppresses *Brucella abortus* intracellular survival via control of A20 expression. *BMC Microbiol* 16:171.

22. Pierce JB, Simion V, Icli B, Pérez-Cremades D, Cheng HS, Feinberg MW. 2020. Computational Analysis of Targeting SARS-CoV-2, Viral entry proteins ACE2 and TMPRSS2, and interferon genes by host microRNAs. *Genes (Basel)* 11.

23. Schulte LN, Westermann AJ, Vogel J. 2013. Differential activation and functional specialization of miR-146 and miR-155 in innate immune sensing. *Nucleic Acids Res* 41:542–553.

24. Tamgue O, Gcanga L, Ozturk M, Whitehead L, Pillay S, Jacobs R, Roy S, Schmeier S, Davids M, Medvedeva YA, Dheda K, Suzuki H, Brombacher F, Guler R. 2019. Differential targeting of c-Maf, Bach-1, and Elmo-1 by microRNA-143 and microRNA-365 promotes the intracellular growth of *Mycobacterium tuberculosis* in alternatively IL-4/IL-13 activated Macrophages. *Front Immunol* 10:421.

25. Millar JA, Valdés R, Kacharia FR, Landfear SM, Cambronne ED, Raghavan R. 2015. *Coxiella burnetii* and *Leishmania mexicana* residing within similar parasitophorous vacuoles elicit disparate host responses. *Front Microbiol* 6:794.

26. Coleman SA, Fischer ER, Howe D, Mead DJ, Heinzen RA. 2004. Temporal analysis of *Coxiella burnetii* morphological differentiation. *J Bacteriol* 186:7344–7352.

27. Krämer A, Green J, Pollard J, Tugendreich S. 2014. Causal analysis approaches in Ingenuity Pathway Analysis. *Bioinformatics* 30:523–530.

28. Wang H, Li Q, Niu X, Wang G, Zheng S, Fu G, Wang Z. 2017. miR-143 inhibits bladder cancer cell proliferation and enhances their sensitivity to gemcitabine by repressing IGF-1R signaling. *Oncol Lett* 13:435–440.

29. Anton L, DeVine A, Sierra L-J, Brown AG, Elovitz MA. 2017. miR-143 and miR-145 disrupt the cervical epithelial barrier through dysregulation of cell adhesion, apoptosis and proliferation. *Sci Rep* 7:3020.

30. Liu M, Jia J, Wang X, Liu Y, Wang C, Fan R. 2018. Long non-coding RNA HOTAIR promotes cervical cancer progression through regulating BCL2 via targeting miR-143-3p. *Cancer Biol Ther* 19:391–399.

31. Liu L, Yu X, Guo X, Tian Z, Su M, Long Y, Huang C, Zhou F, Liu M, Wu X, Wang X. 2012. miR-143 is downregulated in cervical cancer and promotes apoptosis and inhibits tumor formation by targeting Bcl-2. *Mol Med Rep* 5:753–760.

32. Krakauer T. 2019. Inflammasomes, Autophagy, and Cell Death: The Trinity of Innate Host Defense against Intracellular Bacteria. *Mediators Inflamm* 2019:2471215.

33. Latomanski EA, Newton HJ. 2018. Interaction between autophagic vesicles and the *Coxiella*-containing vacuole requires CLTC (clathrin heavy chain). *Autophagy* 14:1710–1725.

34. Gutierrez MG, Vázquez CL, Munafó DB, Zoppino FCM, Berón W, Rabinovitch M, Colombo MI. 2005. Autophagy induction favours the generation and maturation of the *Coxiella*-replicative vacuoles. *Cell Microbiol* 7:981–993.

35. Jansen AFM, Dinkla A, Roest H-J, Bleeker-Rovers CP, Schoffelen T, Joosten LAB, Wever PC, van Deuren M, Koets AP. 2018. Viable *Coxiella burnetii* induces differential cytokine responses in chronic Q fever patients compared to heat-killed *Coxiella burnetii*. *Infect Immun* 86.

36. McClure EE, Chávez ASO, Shaw DK, Carlyon JA, Ganta RR, Noh SM, Wood DO, Bavoil PM, Brayton KA, Martinez JJ, McBride JW, Valdivia RH, Munderloh UG, Pedra JHF. 2017. Engineering of obligate intracellular bacteria: progress, challenges and paradigms. *Nat Rev Microbiol* 15:544–558.

37. Sandoz KM, Popham DL, Beare PA, Sturdevant DE, Hansen B, Nair V, Heinzen RA. 2016. Transcriptional Profiling of *Coxiella burnetii* Reveals Extensive Cell

Wall Remodeling in the Small Cell Variant Developmental Form. *PLoS One* 11:e0149957.

38. Voth DE, Heinzen RA. 2007. Lounging in a lysosome: the intracellular lifestyle of *Coxiella burnetii*. *Cell Microbiol* 9:829–840.

39. Dzakah EE, Huang L, Xue Y, Wei S, Wang X, Chen H, Shui J, Kyei F, Rashid F, Zheng H, Yang B, Tang S. 2021. Host cell response and distinct gene expression profiles at different stages of *Chlamydia trachomatis* infection reveals stage-specific biomarkers of infection. *BMC Microbiol* 21:3.

40. Fernandes MC, Dillon LAL, Belew AT, Bravo HC, Mosser DM, El-Sayed NM. 2016. Dual transcriptome profiling of *Leishmania*-Infected human macrophages reveals distinct reprogramming signatures. *mBio* 7.

41. Aguilar C, Mano M, Eulalio A. 2019. MicroRNAs at the host-Bacteria interface: host defense or bacterial offense. *Trends Microbiol* 27:206–218.

42. Zhou X, Li X, Wu M. 2018. miRNAs reshape immunity and inflammatory responses in bacterial infection. *Signal Transduct Target Ther* 3:14.

43. Das K, Garnica O, Dhandayuthapani S. 2016. Modulation of Host miRNAs by Intracellular Bacterial Pathogens. *Front Cell Infect Microbiol* 6:79.

44. Su Z, Yang Z, Xu Y, Chen Y, Yu Q. 2015. MicroRNAs in apoptosis, autophagy and necroptosis. *Oncotarget* 6:8474–8490.

45. Zheng C, Zheng Z, Sun J, Zhang Y, Wei C, Ke X, Liu Y, Deng L, Wang H. 2017. MiR-16-5p mediates a positive feedback loop in EV71-induced apoptosis and suppresses virus replication. *Sci Rep* 7:16422.

46. Li M, Wang J, Fang Y, Gong S, Li M, Wu M, Lai X, Zeng G, Wang Y, Yang K, Huang X. 2016. microRNA-146a promotes mycobacterial survival in macrophages through suppressing nitric oxide production. *Sci Rep* 6:23351.

47. Pan J-A, Tang Y, Yu J-Y, Zhang H, Zhang J-F, Wang C-Q, Gu J. 2019. miR-146a attenuates apoptosis and modulates autophagy by targeting TAF9b/P53 pathway in doxorubicin-induced cardiotoxicity. *Cell Death Dis* 10:668.

48. Wei J, Ma Z, Li Y, Zhao B, Wang D, Jin Y, Jin Y. 2015. miR-143 inhibits cell proliferation by targeting autophagy-related 2B in non-small cell lung cancer H1299 cells. *Mol Med Rep* 11:571–576.

49. Lin X-T, Zheng X-B, Fan D-J, Yao Q-Q, Hu J-C, Lian L, Wu X-J, Lan P, He X-S. 2018. MicroRNA-143 targets ATG2B to inhibit autophagy and increase inflammatory responses in Crohn's disease. *Inflamm Bowel Dis* 24:781–791.

50. Zhuang M, Shi Q, Zhang X, Ding Y, Shan L, Shan X, Qian J, Zhou X, Huang Z, Zhu W, Ding Y, Cheng W, Liu P, Shu Y. 2015. Involvement of miR-143 in cisplatin resistance of gastric cancer cells via targeting IGF1R and BCL2. *Tumour Biol* 36:2737–2745.

51. Wang Y, Lu Z, Li Y, Ji D, Zhang P, Liu Q, Yao Y. 2014. miR-143 inhibits proliferation and invasion of hepatocellular carcinoma cells via down-regulation of TLR2 expression. *Chinese journal of cellular and molecular immunology* 30:1076–1079.

52. Wang L, Shi Z-M, Jiang C-F, Liu X, Chen Q-D, Qian X, Li D-M, Ge X, Wang X-F, Liu L-Z, You Y-P, Liu N, Jiang B-H. 2014. MiR-143 acts as a tumor

suppressor by targeting N-RAS and enhances temozolomide-induced apoptosis in glioma. *Oncotarget* 5:5416–5427.

53. Yu B, Zhao Y, Zhang H, Xie D, Nie W, Shi K. 2018. Inhibition of microRNA-143-3p attenuates myocardial hypertrophy by inhibiting inflammatory response. *Cell Biol Int* 42:1584–1593.

54. Yudushkin I. 2019. Getting the Akt together: guiding intracellular Akt activity by PI3K. *Biomolecules* 9.

55. Saxton RA, Sabatini DM. 2017. mTOR signaling in growth, metabolism, and disease. *Cell* 168:960–976.

56. Hein AL, Ouellette MM, Yan Y. 2014. Radiation-induced signaling pathways that promote cancer cell survival (review). *Int J Oncol* 45:1813–1819.

57. Eisenreich W, Rudel T, Heesemann J, Goebel W. 2019. How viral and intracellular bacterial pathogens reprogram the metabolism of host cells to allow their intracellular replication. *Front Cell Infect Microbiol* 9:42.

58. Cobos Jiménez V, Bradley EJ, Willemsen AM, van Kampen AHC, Baas F, Kootstra NA. 2014. Next-generation sequencing of microRNAs uncovers expression signatures in polarized macrophages. *Physiol Genomics* 46:91–103.

59. He M, Wu N, Leong MC, Zhang W, Ye Z, Li R, Huang J, Zhang Z, Li L, Yao X, Zhou W, Liu N, Yang Z, Dong X, Li Y, Chen L, Li Q, Wang X, Wen J, Zhao X, Lu B, Yang Y, Wang Q, Hu R. 2020. miR-145 improves metabolic inflammatory disease through multiple pathways. *J Mol Cell Biol* 12:152–162.

60. Narasaki CT, Toman R. 2012. Lipopolysaccharide of *Coxiella burnetii*. *Adv Exp Med Biol* 984:65–90.

61. Zhang W, Chen P, Zong H, Ding Y, Yan R. 2020. MiR-143-3p targets ATG2B to inhibit autophagy and promote endothelial progenitor cells tube formation in deep vein thrombosis. *Tissue Cell* 67:101453.

62. Romano PS, Gutierrez MG, Berón W, Rabinovitch M, Colombo MI. 2007. The autophagic pathway is actively modulated by phase II *Coxiella burnetii* to efficiently replicate in the host cell. *Cell Microbiol* 9:891–909.

63. Dragan AL, Kurten RC, Voth DE. 2019. Characterization of early stages of human alveolar infection by the Q fever agent *Coxiella burnetii*. *Infect Immun* 87.

64. Winchell CG, Graham JG, Kurten RC, Voth DE. 2014. *Coxiella burnetii* type IV secretion-dependent recruitment of macrophage autophagosomes. *Infect Immun* 82:2229–2238.

65. Chung CY-S, Shin HR, Berdan CA, Ford B, Ward CC, Olzmann JA, Zoncu R, Nomura DK. 2019. Covalent targeting of the vacuolar H+-ATPase activates autophagy via mTORC1 inhibition. *Nat Chem Biol* 15:776–785.

66. Mukhopadhyay S, Biancur DE, Parker SJ, Yamamoto K, Banh RS, Paulo JA, Mancias JD, Kimmelman AC. 2021. Autophagy is required for proper cysteine homeostasis in pancreatic cancer through regulation of SLC7A11. *Proc Natl Acad Sci USA* 118.

67. Mauvezin C, Neufeld TP. 2015. Bafilomycin A1 disrupts autophagic flux by inhibiting both V-ATPase-dependent acidification and Ca-P60A/SERCA-dependent autophagosome-lysosome fusion. *Autophagy* 11:1437–1438.

68. Gupta P, Srivastav S, Saha S, Das PK, Ukil A. 2016. *Leishmania donovani* inhibits macrophage apoptosis and pro-inflammatory response through AKT-mediated regulation of β-catenin and FOXO-1. *Cell Death Differ* 23:1815–1826.

69. Contreras J, Rao DS. 2012. MicroRNAs in inflammation and immune responses. *Leukemia* 26:404–413.

70. Lee H-M, Kim TS, Jo E-K. 2016. MiR-146 and miR-125 in the regulation of innate immunity and inflammation. *BMB Rep* 49:311–318.

71. Li S, Yue Y, Xu W, Xiong S. 2013. MicroRNA-146a represses mycobacteria-induced inflammatory response and facilitates bacterial replication via targeting IRAK-1 and TRAF-6. *PLoS One* 8:e81438.

72. Wang Y, Li H, Shi Y, Wang S, Xu Y, Li H, Liu D. 2020. miR-143-3p impacts on pulmonary inflammatory factors and cell apoptosis in mice with mycoplasmal pneumonia by regulating TLR4/MyD88/NF-κB pathway. *Biosci Rep* 40.

73. Liu T, Zhang L, Joo D, Sun S-C. 2017. NF-κB signaling in inflammation. *Signal Transduct Target Ther* 2.

74. Martinez E, Cantet F, Fava L, Norville I, Bonazzi M. 2014. Identification of OmpA, a *Coxiella burnetii* protein involved in host cell invasion, by multi-phenotypic high-content screening. *PLoS Pathog* 10:e1004013.

75. Moses AS, Millar JA, Bonazzi M, Beare PA, Raghavan R. 2017. Horizontally acquired biosynthesis genes boost *Coxiella burnetii*'s physiology. *Front Cell Infect Microbiol* 7:174.

76. Graham JG, Winchell CG, Kurten RC, Voth DE. 2016. Development of an *ex vivo* Tissue platform to study the human lung response to *Coxiella burnetii*. *Infect Immun* 84:1438–1445.

77. Kozomara A, Birgaoanu M, Griffiths-Jones S. 2019. miRBase: from microRNA sequences to function. *Nucleic Acids Res* 47:D155–D162.

78. Ganesan S, Roy CR. 2019. Host cell depletion of tryptophan by IFNγ-induced Indoleamine 2,3-dioxygenase 1 (IDO1) inhibits lysosomal replication of *Coxiella burnetii*. *PLoS Pathog* 15:e1007955.

79. Sanchez SE, Vallejo-Esquerra E, Omsland A. 2018. Use of axenic culture tools to study *Coxiella burnetii*. *Curr Protoc Microbiol* 50:e52.

80. Martinez E, Cantet F, Bonazzi M. 2015. Generation and multi-phenotypic high-content screening of *Coxiella burnetii* transposon mutants. *J Vis Exp* e52851.

81. Hayek I, Fischer F, Schulze-Luehrmann J, Dettmer K, Sobotta K, Schatz V, Kohl L, Boden K, Lang R, Oefner PJ, Wirtz S, Jantsch J, Lührmann A. 2019. Limitation of TCA cycle intermediates represents an oxygen-independent nutritional antibacterial effector mechanism of macrophages. *Cell Rep* 26:3502–3510.e6.

82. Love MI, Huber W, Anders S. 2014. Moderated estimation of fold change and dispersion for RNA-seq data with DESeq2. *Genome biology* 15:1-21.

83. Livak KJ, Schmittgen TD. 2001. Analysis of relative gene expression data using real-time quantitative PCR and the 2(-Delta Delta C(T)) Method. *Methods* 25:402–408.

84. Sachan M, Srivastava A, Ranjan R, Gupta A, Pandya S, Misra A. 2016. Opportunities and challenges for host-directed therapies in tuberculosis. *Curr Pharm Des* 22:2599–2604.

85. Zhou J, Tan S-H, Nicolas V, Bauvy C, Yang N-D, Zhang J, Xue Y, Codogno P, Shen H-M. 2013. Activation of lysosomal function in the course of autophagy via mTORC1 suppression and autophagosome-lysosome fusion. *Cell Res* 23:508–523.

86. Rontogianni S, Iskit S, van Doorn S, Peeper DS, Altelaar M. 2020. Combined EGFR and ROCK inhibition in triple-negative breast cancer leads to cell death via impaired autophagic flux. *Mol Cell Proteomics* 19:261–277.

87. Stankov M, Panayotova-Dimitrova D, Leverkus M, Klusmann J-H, Behrens G. 2014. Flow cytometric analysis of autophagic activity with Cyto-ID staining in primary cells. *Bio Protoc* 4.

88. Plubell DL, Wilmarth PA, Zhao Y, Fenton AM, Minnier J, Reddy AP, Klimek J, Yang X, David LL, Pamir N. 2017. Extended multiplexing of tandem mass tags (TMT) labeling reveals age and high fat diet specific proteome changes in mouse epididymal adipose tissue. *Mol Cell Proteomics* 16:873–890.

Chapter III

Host inflammatory pathways respond to *Coxiella burnetii* infection

Madhur Sachan[1], Amanda Dragan[2], Max Schreyer[1], Daniel E Voth[2], Rahul Raghavan[1,3]*

[1]Department of Biology, Portland State University, Portland, OR, 97201, USA.

[2]Department of Microbiology and Immunology, University of Arkansas for Medical Sciences, Little Rock, AR, 72205, USA.

[3]Department of Biology, The University of Texas at San Antonio, San Antonio, TX, 78249, USA.

Key words: Macrophage, IL-17 signaling, *Coxiella burnetii*, cytokines, single-cell sequencing

ABSTRACT

C. burnetii antagonizes the protective inflammatory response mounted by host alveolar macrophages. For example, the pathogen can block the proinflammatory IL-17 signaling, likely through its secreted effector proteins. In this study, we show that infection with *C. burnetii* Dugway, an avirulent rodent isolate, triggers enhanced host response, including activation of IL-17 signaling, compared to human isolates in primary human alveolar macrophages, suggesting the prompt recognition of the rodent isolate by the human innate immune response. In addition, several pro-survival pathways, including PI3K/Akt signaling and autophagy signaling, were activated, whereas apoptosis signaling was inhibited during infection. We further show that during infection chemokines and cytokines that serve downstream to IL-17 signaling such as CCL3, CCL4, CCL5, CXCL1, and IL1B were induced at the transcription level, and were secreted at a higher level than in uninfected macrophages. This finding indicates that *C. burnetii* can tolerate the activation of host IL-17 signaling and associated pro-inflammatory responses inside the macrophages. Interestingly, single-cell investigation of inflammation-associated pathways suggests that *C. burnetii* infection leads to a range of inflammatory states among the subpopulations of infected macrophages, and some of these subpopulations seem relatively more hospitable for bacterial growth than others.

INTRODUCTION

After bacterial invasion, alveolar macrophages provide the first line of defense against invading pathogens by mounting an effective antibacterial response (1, 2). These monocyte-derived cells secrete distinct cytokines, including TNF-α, IL-1β, and IL-6, to eliminate an invaded pathogen and further recruit other immune cells as part of their initial acute inflammatory response (1, 2). However, intracellular bacterial pathogens such as *Coxiella burnetii* have evolved sophisticated mechanisms to subvert the host immune response (3). *C. burnetii* is the etiological agent of Q fever, a condition that can manifest either as a self-limiting, acute flu-like illness or as a life-threatening chronic disease such as endocarditis (4). Based on the distinct genomic characteristics and disease presentations, different isolates of *C. burnetii* have been classified into different groups (5, 6). NMI, NMII, and Graves isolates of *C. burnetii* are human isolates, whereas *C. burnetii* Dugway is an avirulent rodent isolate. Compared to avirulent *C. burnetii*, virulent isolates such as NMI strongly suppresses IL-1β production and NLRP3 inflammasome activation probably due to different LPS composition or secreted effectors (1, 7, 8).

Shortly after inhalation, *C. burnetii* is phagocytosed by host alveolar macrophages and starts replicating in acidic, *Coxiella*-containing vacuoles (CCVs) that mature after fusion with endolysosomal, autophagic, and secretory vesicles (9). In order to overcome the host antibacterial response, such as induction of a robust pro-inflammatory response, *C. burnetii* is known to subvert host response through its virulence factors (10). For example, *C. burnetii* causes the downregulation of specific inflammatory cytokines

associated with IL-17 signaling by an undefined mechanism that may involve its secreted effector proteins (11). Interestingly, *C. burnetii* produces a T4SS effector termed IcaA that antagonizes NLRP3 inflammasome activation in murine macrophages (7). This "tug-of-war" between the host and pathogen to regulate the inflammatory immune response contributes to either successful infection or pathogen clearance (12, 13). However, the contribution of host protective signaling to *C. burnetii* infection is not well elucidated.

To understand the various immune signaling pathways involved in *C. burnetii* infection, we investigated the transcriptome of *C. burnetii*-infected macrophages. Our data showed that *C. burnetii* Dugway, an avirulent rodent isolate, triggered an enhanced host response compared to human isolates and several pro-inflammatory pathways such as IL-17 signaling were activated in macrophages infected with any of these *C. burnetii* isolates. Further, a single-cell scale investigation suggests that *C. burnetii* induces a range of inflammatory states in different subpopulations of infected macrophages that can contribute to a heterogeneous host response to the pathogen.

RESULTS

C. burnetii Dugway infection elicits an enhanced host response.

To evaluate the macrophage responses to *C. burnetii* infection, we first performed gene-expression profiling using RNA-Seq in primary human alveolar macrophages (hAMs) infected with one of the four isolates of *C. burnetii* at 72 h post-infection (**Table 1**) (5, 14, 15). Our analysis of differentially expressed genes (DEGs) in infected cells compared to uninfected cells ($log2fc \geq 0.75$, $padj \leq 0.05$; $n = 3$) showed that hAMs infected with *C. burnetii* Dugway elicited the highest number of differentially expressed genes (772) compared to hAMs infected with NMII (365), NMI (268) or *C. burnetii* Graves (315) isolates (**Figure 1, Table 2 and S1)**.

Table 1. Features of *C. burnetii* isolates used in this study.

Isolate	**Origin**	**Virulence**	**Disease caused in human**	**Group**
NMI	Montana, tick, 1935 (5, 6)	Virulent	Acute	I
NMII	Montana, tick, 1935 (5, 6)	Avirulent	N/A	II
Dugway	Utah, rodents, 1958 (5, 6)	Avirulent	N/A	VI
Graves	Nova Scotia, human heart valve, 1981 (5, 6)	Virulent	Endocarditis	I

Table 2. Number of differentially expressed genes (log2fc ≥ 0.75, padj ≤ 0.05) in human alveolar macrophages (hAMs) infected with different isolates of *C. burnetii*.

	Total	Upregulated	Downregulated
NMI-infected hAMs	250	116	134
NMII-infected hAMs	332	141	191
Dugway-infected hAMs	672	227	445
Graves-infected hAMs	266	106	160

A.

Downregulated

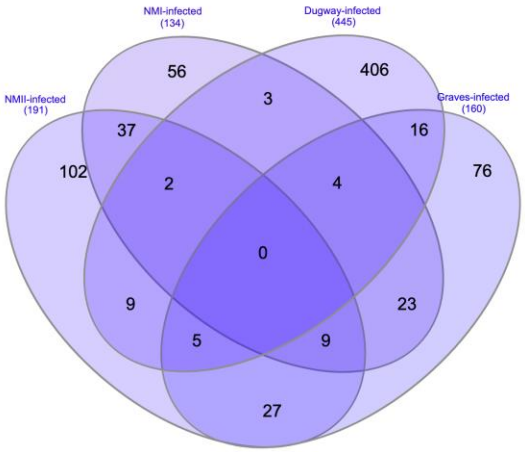

Upregulated

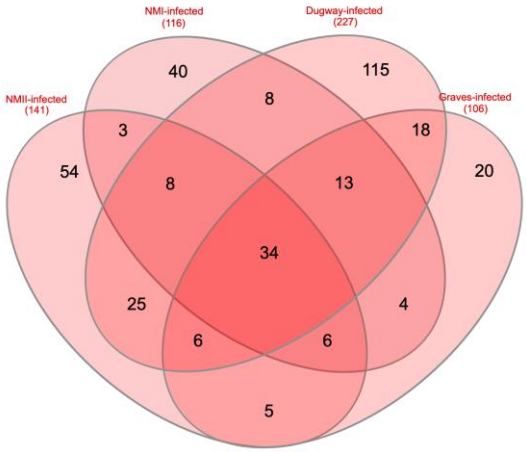

B.

NMI-infected hAMs.

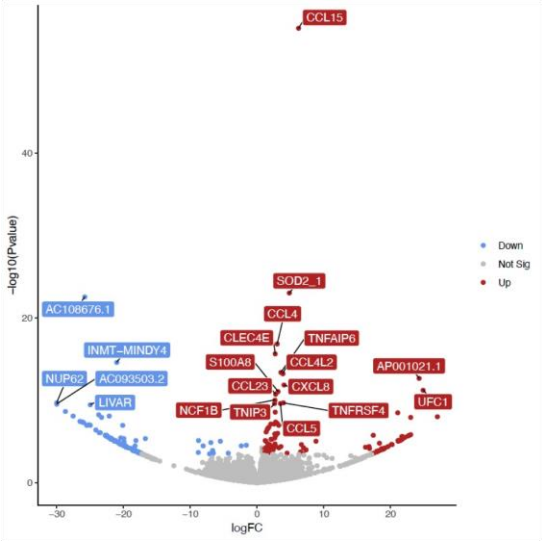

NMII-infected hAMs

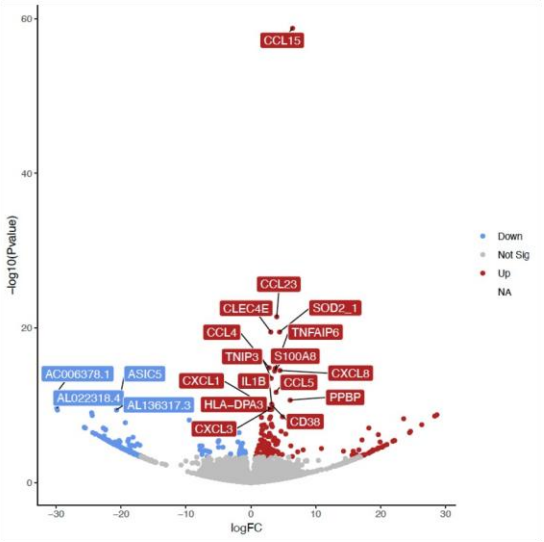

Dugway-infected hAMs. Graves-infected hAMs

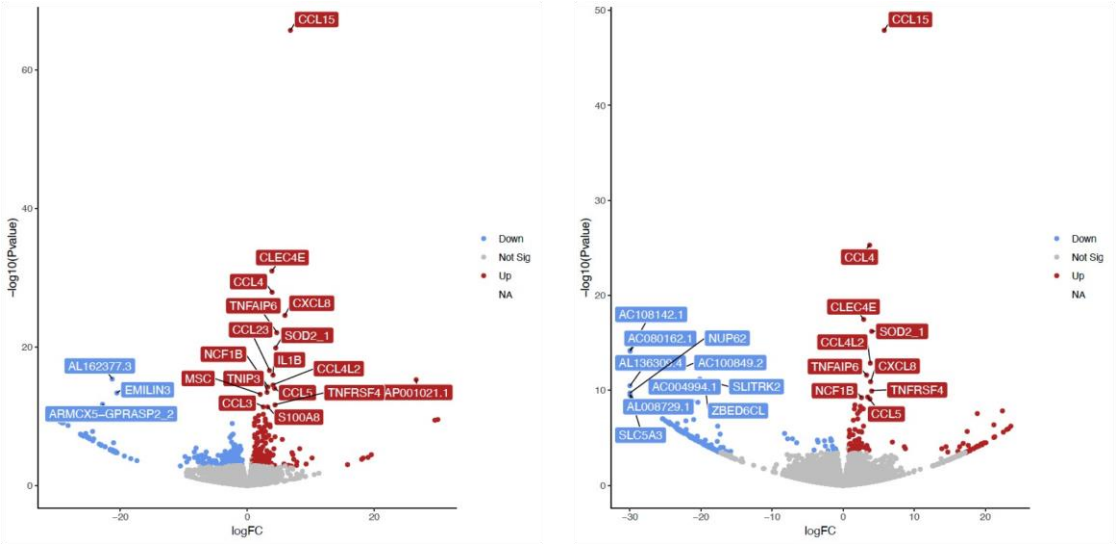

Figure 1. Infection with *C. burnetii* Dugway isolate elicits an enhanced host response compared to hAMs infected with human isolates at 72 hpi. (A) Venn diagram showing overlaps of all significantly up- and down-regulated genes in primary human alveolar macrophages (hAMs) infected with NMII, NMI, Dugway, or Graves isolates of *C. burnetii* compared to uninfected cells ($-0.75 \leq \log2fc \geq 0.75$, $padj \leq 0.05$; n = 3). (B) Volcanic plot representation of differentially expressed genes showing top 20 highest significantly expressed genes in primary human alveolar macrophages infected with NMII, NMI, Dugway, or Graves isolates of *C. burnetii* compared to uninfected cells. Red points show upregulated while blue corresponds to downregulated gene expression compared to the uninfected control. The x-axis shows the magnitude of fold change ($\log2fc \geq 0.75$, $padj \leq 0.05$; n = 3) and y-axis corresponds to statistical significance (-log10 of p value).

Host inflammatory and pro-survival pathways are augmented in *C. burnetii* infection

To elucidate the functional implications of DEGs, we performed pathway enrichment analysis in each of the infections using Ingenuity Pathway Analysis (IPA). This analysis showed activation of pro-inflammatory signaling (including IL-17 signaling, IL-6 signaling, TREM1 signaling, hypercytokinemia/hyperchemokinemia, and differential regulation of cytokine production) in each of the four infections in hAMs compared to uninfected control (z-score $\geq$ 1.5 or $\leq$ -1.5, $p < 0.05$) **(Figure 2, Table 3 and S3)**. Interestingly, IL-17 and IL-6 are known to play a protective pro-inflammatory role against many intracellular pathogens (11, 16–19), therefore activation of IL-17 and IL-6 signaling in *C. burnetii* infected macrophages suggests an early protective immune response.

Similar to data from hAMs, NMII-infected THP-1 cells (as mentioned in Chapter II) show significant activation of many pro-inflammatory pathways **(Figure 3, Table S2)**. These signaling pathways include activation of cytokines-related pathways such as IL-17 signaling, IL-6 signaling, TREM1 signaling, hypercytokinemia/hyperchemokinemia, and differential regulation of cytokine production. THP-1 cells infected with NMII isolate also showed a high degree of overlap in the inflammatory signaling with infected hAMs (**Table S3)**. These observations suggest that THP-1 cells respond similarly to *Coxiella* infection as alveolar macrophages; consequently, we utilized THP-1 cells for subsequent experiments (1, 20). In addition, THP-1 cells showed activation of pro-survival pathways, such as including PI3K/Akt signaling, autophagy, toll-like receptor signaling (21), TGF-β signaling (22), JAK/STAT signaling (23), STAT3 pathway (24), MAPK signaling (25), as well as inhibition of apoptosis signaling (26) that have previously been reported to be involved C. *burnetii* infection. These data also reveals putative roles for a few intracellular

pathogen-influenced signaling pathways such as activation of Wnt/Ca+ pathway and ferroptosis signaling that are unknown in the context of *C. burnetii* infection (27, 28).

A. NMII-infected hAMs

B. NMI-infected hAMs

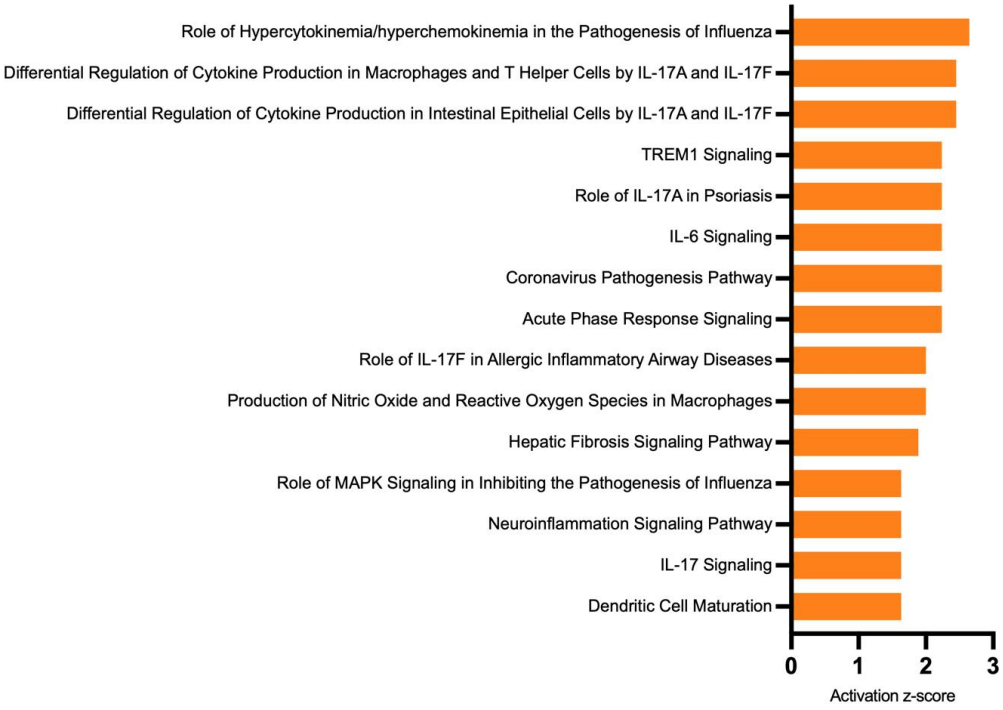

C. Dugway-infected hAMs

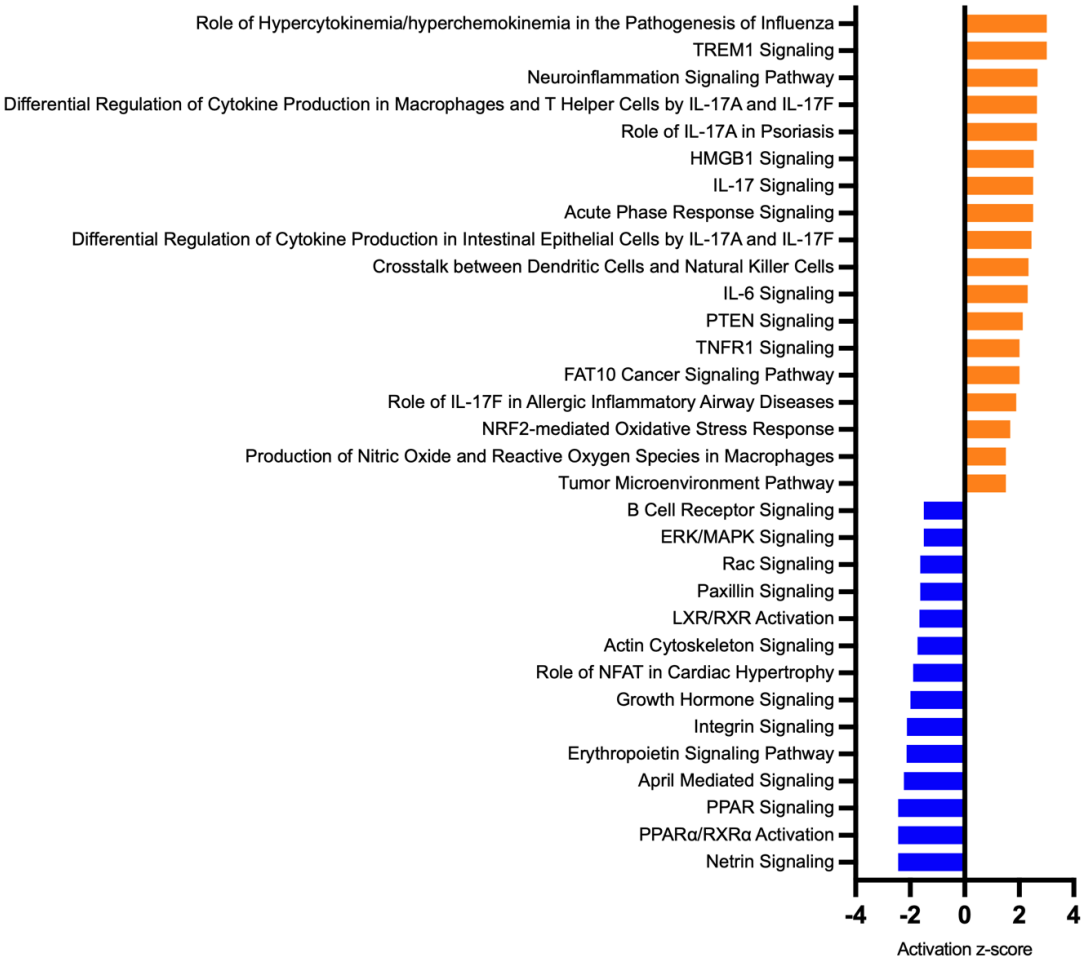

D. Graves-infected hAMs

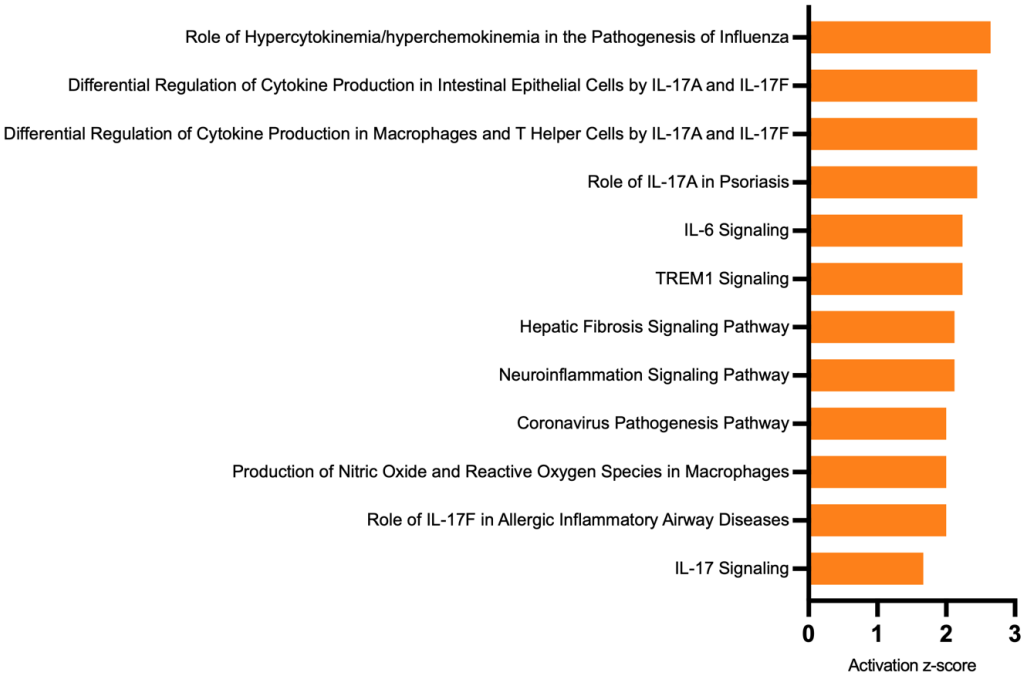

Figure 2. IL-17 signaling is perturbed by each isolate of *C. burnetii*. Pathway enrichment analysis of hAMs infected with (A) NMI, (B) NMII, (C) Dugway, and (D) Graves isolates. Orange bars show a positive z-score (activation) while blue corresponds to a negative z-score (inhibition) in Ingenuity Pathway Analysis ($1.5 < \text{z-score} < -1.5$).

NMII-infected THP-1s

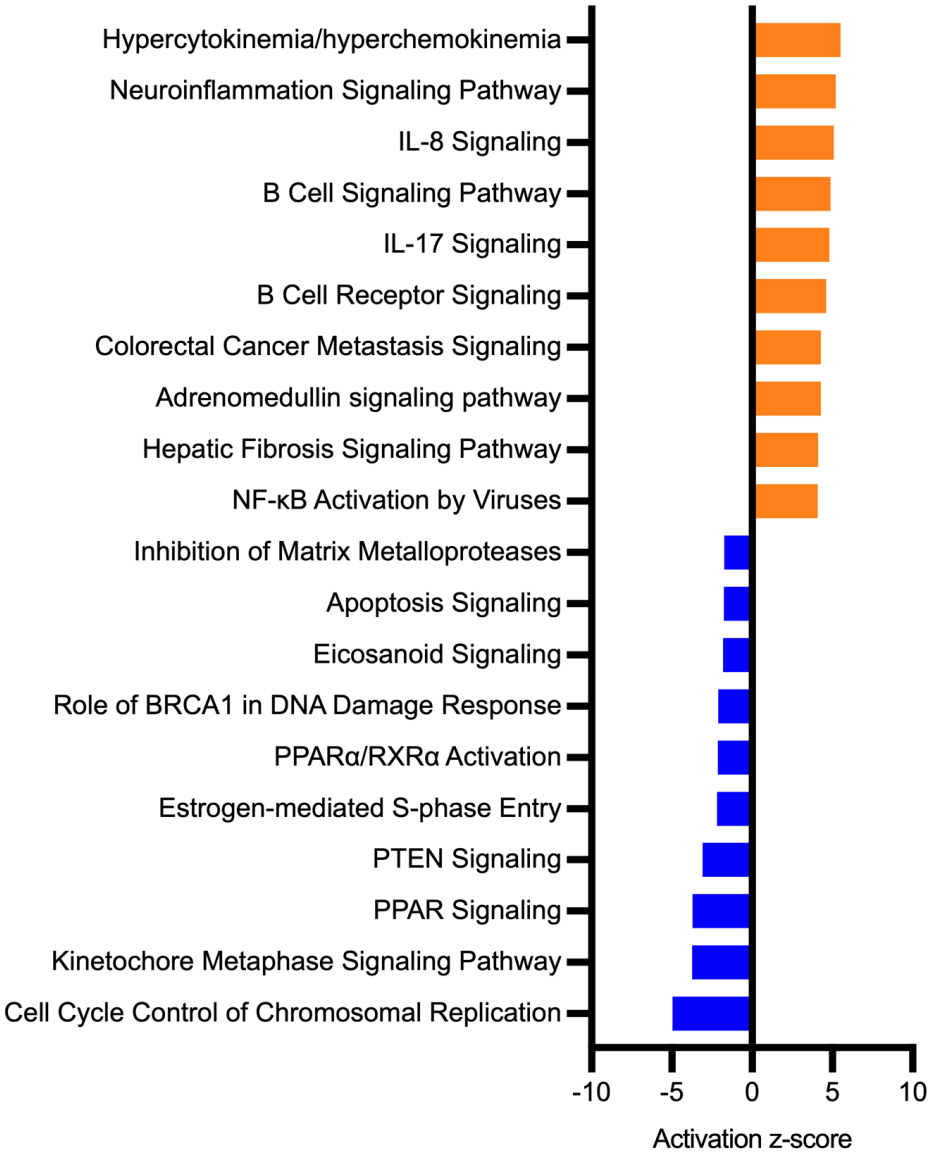

Figure 3. Pathway enrichment analysis of THP-1 infected with NMII isolate shows activation of IL-17 signaling. The figure shows the top 20 enriched pathways in infected cells (Table S3). Orange bars show a positive z-score (activation) while blue corresponds to a negative z-score (inhibition) in ingenuity pathway analysis ($1.5 < \text{z-score} < -1.5$).

Table 3. List of enriched pathways in primary human alveolar macrophages (hAMs) infected with different isolates of *C. burnetii*. Here, the z-score infers the activation states of pathways based on comparison with a model that assigns random regulation directions.

Ingenuity Canonical Pathways	**NMII-hAMs (zScore)**	**NMI-hAMs (zScore)**	**DUG-hAMs (zScore)**	**GRA-hAMs (zScore)**
IL-17 Signaling	2.333	1.633	2.500	1.667
Role of IL-17F in Allergic Inflammatory Airway Diseases	2.449	2.000	1.890	2.000
Role of IL-17A in Psoriasis	2.449	2.236	2.646	2.449
TREM1 Signaling	2.000	2.236	3.000	2.236
IL-6 Signaling	1.633	2.236	2.309	2.236
Differential Regulation of Cytokine Production in Macrophages and T Helper Cells by IL-17A and IL-17F	2.236	2.449	2.646	2.449

Differential Regulation of Cytokine Production in Intestinal Epithelial Cells by IL-17A and IL-17F	2.449	2.449	2.449	2.449
Role of Hypercytokinemia/hyperchemokinemia in the Pathogenesis of Influenza	2.828	2.646	3.000	2.646

IL-17 signaling likely drives the inflammatory response to *C. burnetii* infection

Pathway enrichment analyses of *C. burnetii*-infected macrophages showed that IL-17 signaling is among the top activated signaling pathways in each of the infections **(Figure 3, Table S3)**. IL-17, a member of the IL-17 family of pro-inflammatory cytokines, induces the expression of pro-inflammatory cytokines or chemokines in many cell types (29). Therefore, to understand the effect of IL-17 signaling on the inflammatory response to *C. burnetii*, we performed a pathway reconstruction analysis of this signaling pathway to identify the IL-17 signaling-associated proteins or pathways that may participate in *C. burnetii* infection **(Figure 4)**. We found that genes downstream of IL-17 signaling were consistently upregulated in *C. burnetii*-infected hAMs or THP-1 cells **(Table S1 and S2)**. The upregulated genes encode numerous chemokines (CCL3, CCL4, CCL5, CXCL1, CXCL3, CXCL8) and cytokines (IL1B, EBI3) that can recruit immune cells or mount proinflammatory host response at the site of intracellular bacterial infection in an attempt to control the infection (29–36).

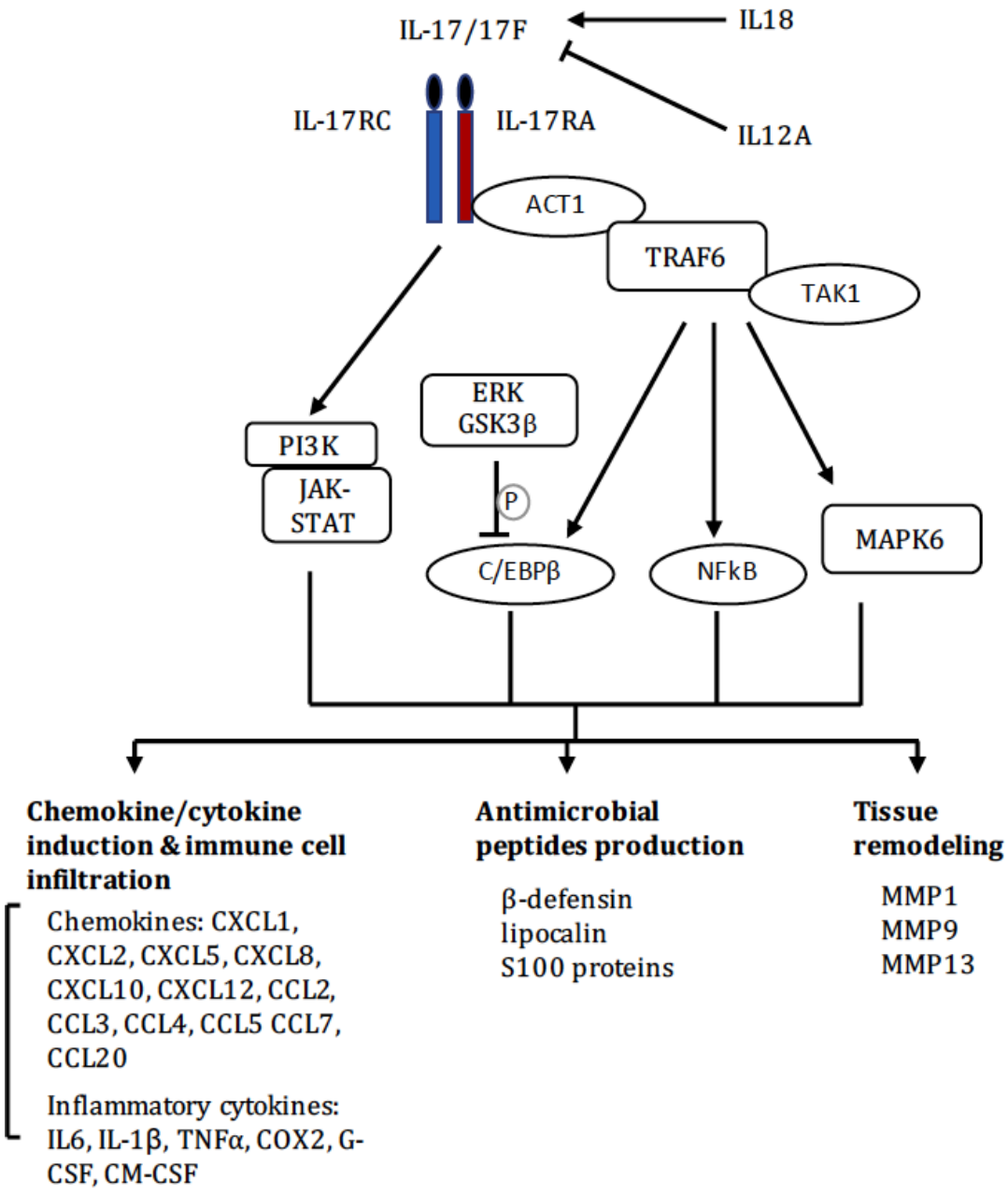
IL-17/17F
IL18
IL12A
IL-17RC
IL-17RA
ACT1
TRAF6
TAK1
ERK
GSK3β
PI3K
JAK-
STAT
P
C/EBPβ
NFkB
MAPK6
Chemokine/cytokine induction & immune cell infiltration
Chemokines: CXCL1, CXCL2, CXCL5, CXCL8, CXCL10, CXCL12, CCL2, CCL3, CCL4, CCL5 CCL7, CCL20
Inflammatory cytokines: IL6, IL-1β, TNFα, COX2, G-CSF, CM-CSF
Antimicrobial peptides production
β-defensin
lipocalin
S100 proteins
Tissue remodeling
MMP1
MMP9
MMP13

Figure 4. IL-17 signaling pathway. IL17A and IL17F form either homodimers or heterodimers that bind to the IL17RA/IL17RC receptor complex to activate downstream signaling cascades. Act1, an interleukin-17-receptor-complex adaptor, activates independent signaling mechanisms by activating different TRAF proteins. Activated TRAF6 triggers NF-κB, MAPK and C/EBPβ pathways. Additionally, IL-17R-Act1 complex leads to the activation of ERK5 via TRAF4. These signaling cascades, in turn, result in induction of chemokines/cytokines, production of antimicrobial peptides, and tissue remodeling. [TRAF: TNF receptor associated factor, ERK: extracellular signal related kinase, PI3K: Phosphoinositide 3-kinases, JAK/STAT: Janus Kinase/Signal Transducer and Activator of Transcription, gsk3β: Glycogen Synthase Kinase 3 Beta, C/EBPβ: CCAAT-enhancer-binding proteins, NF-κB: Nuclear Factor kappa-light-chain-enhancer of activated B cells, MAPK6: Mitogen-Activated Protein Kinase 6].

Infected macrophages show enhanced secretion of several proinflammatory cytokines

To assess the cytokines associated with *C. burnetii* infection, we measured the level of 20 cytokines/chemokines in the supernatants collected from infected and uninfected THP-1 cells **(Figure 5, Table S4)** at 48 h, 72h, and 120 h post-infection (hpi) (37). Additionally, THP-1 cells were separately treated with *Escherichia coli* LPS and ATP for 30 minutes to serve as positive controls. This cytokine secretion assay revealed that at 48 hpi, secretion of CXCL12, CXCL10, CSF2, and IL18 were significantly upregulated in NMII-infected cells compared to uninfected controls. At 72 hpi, the level of CCL3, CCL4, and CXCL10 were upregulated while IL12A was downregulated compared to control. Finally, at 120 hpi, upregulation of CCL2, CCL3, CCL4, CCL5, CXCL1, CXCL10, and IL1B was observed **(Figure 5)**.

A. Cytokines

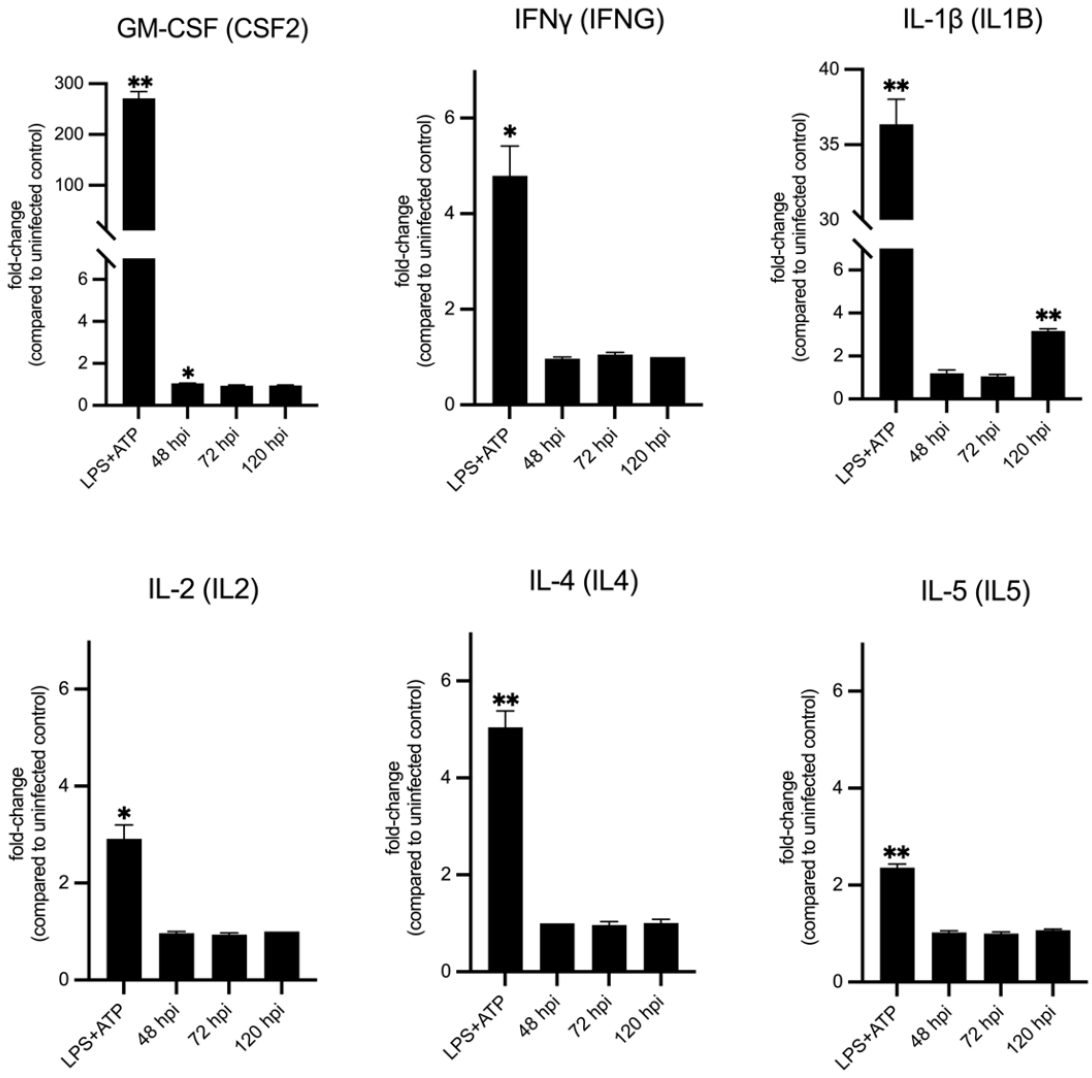
GM-CSF (CSF2)
IFNγ (IFNG)
IL-1β (IL1B)
IL-2 (IL2)
IL-4 (IL4)
IL-5 (IL5)
fold-change
(compared to uninfected control)
LPS+ATP
48 hpi
72 hpi
120 hpi

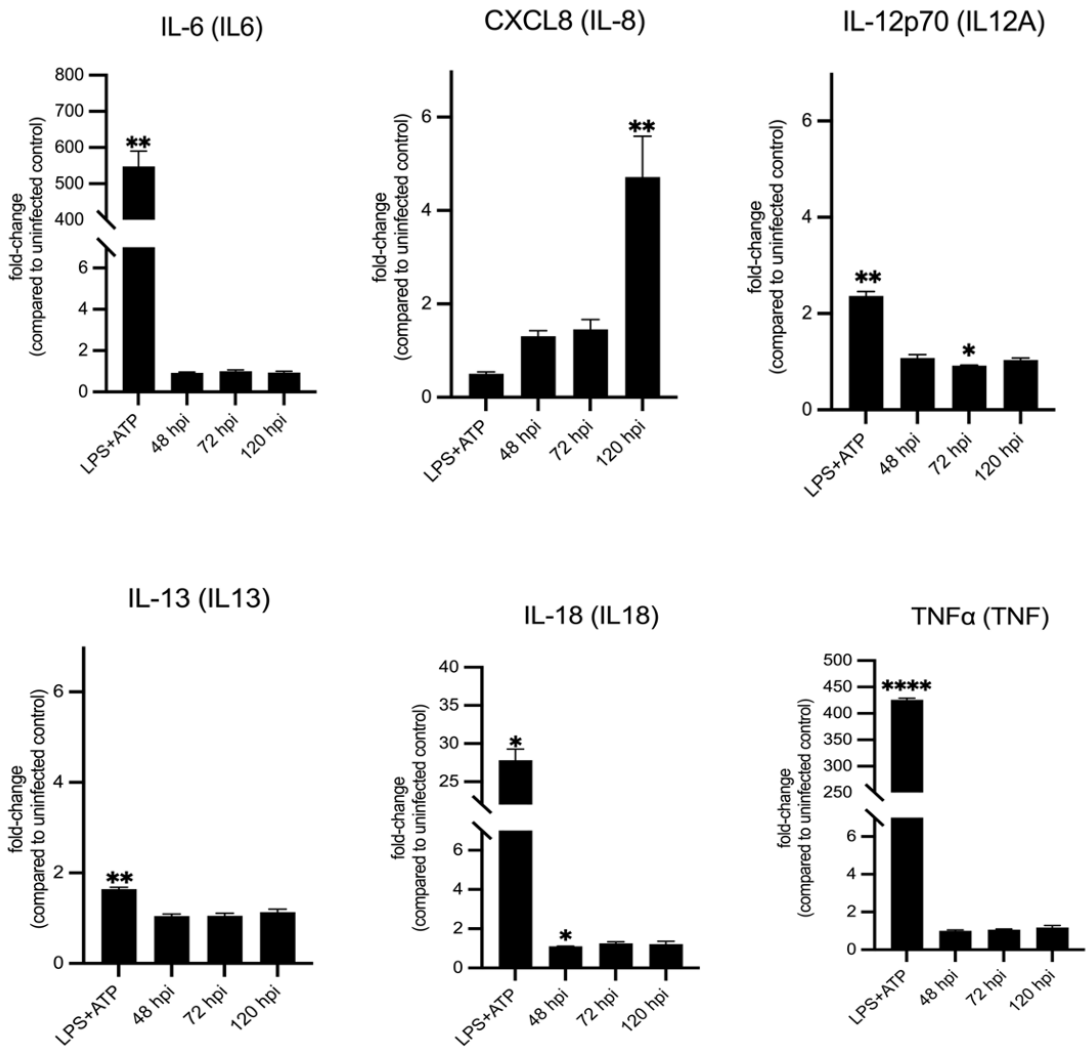
IL-6 (IL6)
CXCL8 (IL-8)
IL-12p70 (IL12A)
IL-13 (IL13)
IL-18 (IL18)
TNFα (TNF)
fold-change
(compared to uninfected control)
LPS+ATP
48 hpi
72 hpi
120 hpi

B. Chemokines

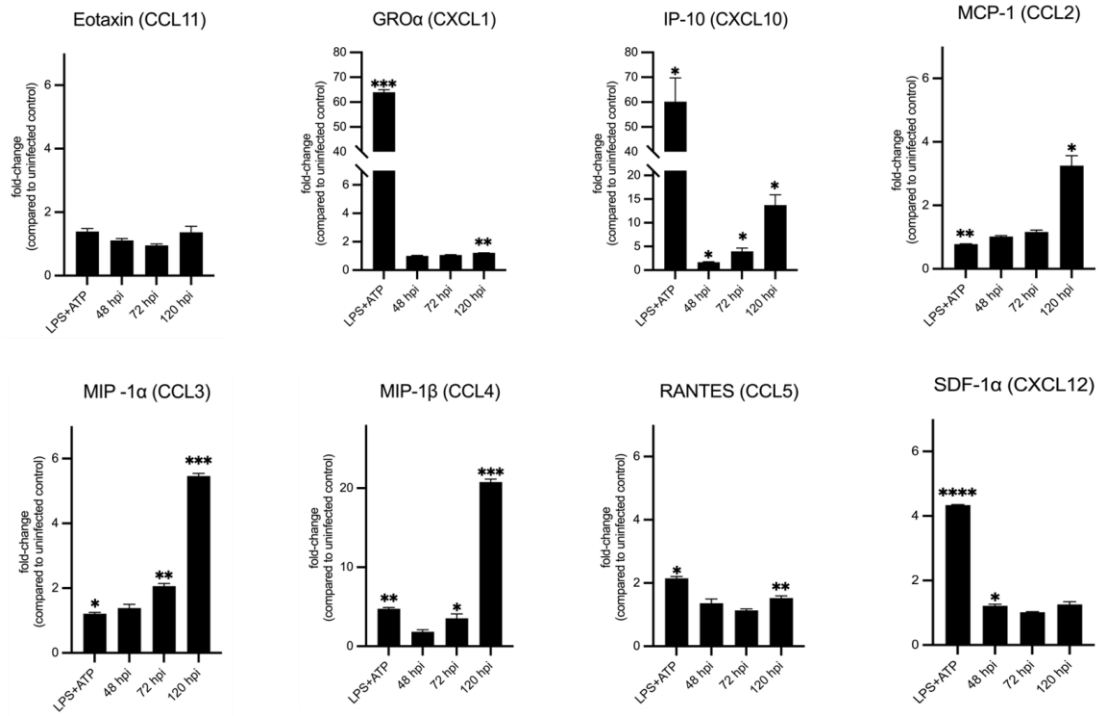

Figure 5. Infected macrophages show enhanced secretion of several proinflammatory cytokines associated with IL-17 signaling. Quantification of (A) 12 cytokines and (B) chemokines released from NMII-infected THP-1 cells was carried out using Th1/Th2 Cytokine & Chemokine 20-Plex ProcartaPlex Panel 1 (Invitrogen). In addition, the cells were separately treated with 200 ng/mL of *E. coli* LPS for 3 h and 5 mM ATP for 30 minutes that served as the positive control for proinflammatory cytokine secretion. Pairwise comparisons of raw expression values were done using two-tailed paired t-test, followed by Welch's correction for each of the 20 cytokines measured in this assay (*$p \leq 0.05$, **$p \leq 0.01$, ***$p \leq 0.001$, ****$p \leq 0.0001$; $n = 3$).

Inflammatory pathways show transcriptional heterogeneity in infected subpopulations

Macrophage infection with *C. burnetii* has previously been shown to result in an atypical macrophage polarization pattern that comprises signatures of both pro-and anti-inflammatory host responses (38). We performed single-cell transcriptome analysis after sorting GFP-tagged *Coxiella*-infected (GFP-pos), bystander (GFP-neg), and uninfected (control) macrophage-like THP-1 populations at 48 hpi (39). Pathway analysis of genes differentially expressed ($\log2fc \geq 0.75$, $p \leq 0.05$) in each subpopulation (cluster) of GFP-pos cells showed a significant difference in the activation states of inflammation-associated pathways unlike the subpopulations of bystander or uninfected cells **(Figure 6, Table S5)**. Interestingly, cluster 7 of GFP-pos cells showed a significant contrast with cluster 2 as several proinflammatory signaling pathways in cluster 7 were activated (positive z-score) relative to all other GFP-pos clusters but the same pathways were inhibited (negative z-score) in cluster 2. A variation in the CXCR4 signaling was found in all three populations, perhaps due to preexisting macrophage heterogeneity (40–43).

A. Infected (GFP-pos) cells

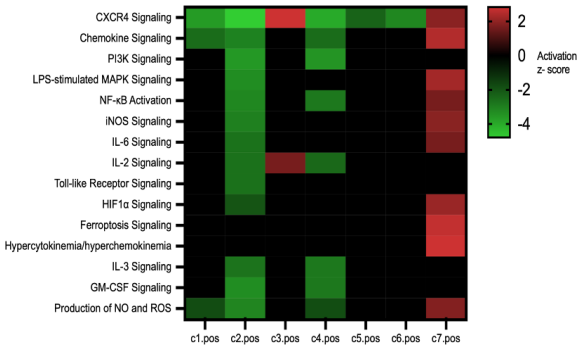

B. Bystander (GFP-neg) cells

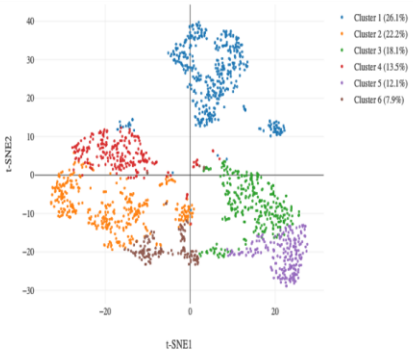

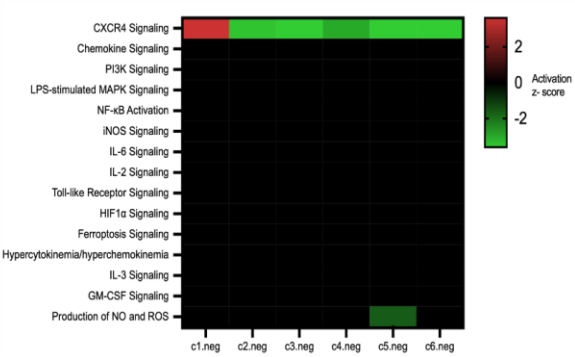

C. Uninfected cells

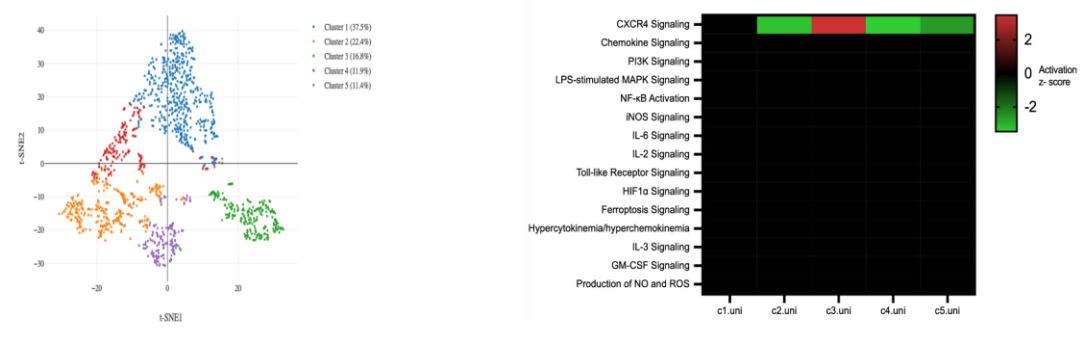

Figure 6. Single-cell analyses show transcriptional heterogeneity within infected cells compared to bystander or uninfected cells. Clustering of cells by t-distributed stochastic neighbor embedding (t-SNE) and pathway enrichment analysis (showing enriched inflammation-associated pathways) revealed transcriptional heterogeneity among ~1000 THP-1 cells at 48 hpi in (A) infected (GFP-pos), (B) bystander (GFP-neg), and (C) uninfected THP-1 cells. The x-axis on the heatmaps show the clusters or subpopulations of the host cells (letter "c" denotes the cluster), and y-axis corresponds to the pathways that are associated with the inflammation. The red blocks show a positive z-score (activation) while green corresponds to a negative z-score (inhibition) in ingenuity pathway analysis ($1.5 < \text{z-score} < -1.5$).

DISCUSSION

In this study, we first performed gene expression profiling to assess the human macrophage response to four different isolates of *C. burnetii*, as shown in **Table 1** (5). Unlike human isolates (NMI, NMII, and Graves), the *C. burnetii* Dugway isolate has a large genome that has not undergone significant levels of genome reduction (44). We found that macrophages infected with human isolates show a similar number of differentially expressed genes compared to uninfected cells. In contrast, *C. burnetii* Dugway, an avirulent rodent isolate, elicited the highest number of differentially expressed genes. Virulent *C. burnetii* has been suggested to escape or antagonize the inflammatory response probably by LPS-mediated shielding of bacterial surface proteins from the immune recognition or through its type IV secretion system (T4SS) effectors (7, 45). Therefore, it appears that *C. burnetii* Dugway isolate fails to suppress the robust host inflammatory response, and being a rodent isolate gets promptly recognized by the human immune response (14). The larger genome size of certain *C. burnetii* isolates has been previously suggested to be associated with reduced virulence compared to others (14). In support of this hypothesis, our data shows that in *C. burnetii* Dugway-infected cells, activation of several host inflammatory pathways is much higher than infection with other human isolates **(Figure 3).** Further, the subtle differences observed in hAMs response to different human isolates could be due to the isolate-specific composition of lipopolysaccharide or secreted effector proteins (46).

Investigation of enriched pathways in *C. burnetii*-infected macrophages showed activation of multiple inflammatory pathways, including IL-17 signaling, among the top enriched pathways that are common to all infections **(Figure 2, Table S3)**. IL-17 is a pro-

inflammatory cytokine that acts in concert with tumor necrosis factor (TNF) and IL-1β and induces the expression of pro-inflammatory cytokines by activating TRAF (TNF receptor associated factor) and PI3K/AKT signaling (16, 29, 47, 48). IL-17 is known to provide a protective immune response against several intracellular pathogens, including *Legionella pneumophila*, *Mycobacterium tuberculosis*, and *Francisella tularensis* (49–51). After the binding of this cytokine to its receptors, Act1, an interleukin-17-receptor-complex adaptor, activates several independent signaling mechanisms by activating TRAF (TNF receptor associated factor) and PI3K/AKT signaling (29, 47) **(Figure 4).** These signaling cascades, in turn, lead to the induction of chemokines/cytokines, production of antimicrobial peptides, and tissue remodeling (29).

Our data suggest that several chemokines and cytokines that serve downstream to IL-17 signaling (CCL3, CCL4, CCL5, CXCL1, and IL1B) were induced at the transcriptional level and were secreted by *Coxiella*-infected macrophages compared to uninfected macrophages. The induction of these genes may either promote a pro-inflammatory response or attract a variety of other immune cells such as T cells, B cells, neutrophils, and dendritic cells to the site of infection to limit the intracellular growth of *C. burnetii* (52–54). Intriguingly, Clemente et al. (11) have previously shown that *C. burnetii* reduces the expression of IL-17 downstream signaling molecules (IL1A, IL1B, TNF, CXCL2, CCL5, and LCN2) compared to T4SS mutant, enabling the pathogen to block IL-17 mediated pro-inflammatory response. Therefore, it seems that despite the strong activation of host pro-inflammatory response, *C. burnetii* might promote its survival through T4SS effector proteins that can antagonize IL-17 signaling or can escape from the effect of immune recognition.

C. burnetii stimulates atypical macrophage polarization with signatures of both the proinflammatory M1 and anti-inflammatory M2 polarization states (38). How the host macrophages account for such heterogeneous polarization in *C. burnetii* infection is poorly understood. Our data show high variability in gene expression and associated pathways in the infected cell populations compared to the bystander and uninfected populations, suggesting that *C. burnetii* infection elicits heterogeneous cellular responses. Intracellular bacteria such as *Salmonella* have been shown to have heterogeneous metabolism and growth rates (phenotypic heterogeneity), shaping the heterogeneous macrophage response (55). Moreover, analysis of inflammation-associated pathways in individual clusters of the infected population indicates that subpopulations of these cells display a spectrum of pro- to anti-inflammatory states that may probably be tied to the phenotypic heterogeneity of the pathogen, as found in the case of *Salmonella*-infected macrophages (56, 57). Activation of inflammation-associated pathways (positive z-score) as shown in cluster 7 of GFP-pos cells **(Figure 6A)** are known to inhibit the growth of intracellular bacterial pathogens and the inhibition of several of these pathways in cluster 2 suggests that some subpopulations of infected macrophages are likely more pathogen-friendly than others (38).

Besides the activation of pro-inflammatory signaling, the pathway enrichment analysis identified several pro-survival pathways known to support *C. burnetii* growth. This analysis also identified a few unexplored pathways in the context of *C. burnetii* infection, such as activation of the Wnt/Ca+ pathway and ferroptosis signaling. For instance, *Ehrlichia chaffeensis,* an obligate intracellular pathogen from the order *Rickettsiales*, secretes tandem repeat protein (TRP) effectors to induce Wnt signaling

pathways that promote phagocytosis (27). The role of ferroptosis during infection is not well understood; however, during infection with *Mycobacterium tuberculosis*, induction of ferroptosis has been shown to drive tissue necrosis, possibly to allow the bacteria to spread to other cells (28). Most aspects of *C. burnetii* infection are not clearly understood, including how the pathogen spreads from one cell to another; hence, a functional investigation of these pathways could advance our understanding of host-*C. burnetii* interactions.

MATERIALS AND METHODS

Bacterial isolates and infection

Primary human alveolar macrophages (hAMs) were harvested by bronchoalveolar lavage (BAL) from postmortem human lung donors and infected with NMI, NMII, Dugway, or Graves isolates at 25 MOI (multiplicity of infection), as previously described (58). hAMs were cultured at 37°C under 5% CO_2 in Dulbecco's modified Eagle/F-12 (DMEM/F12) medium (Gibco) containing 10% FBS for 72 h post-infection, at which point they were harvested for analyzing gene expression. *C. burnetii* Nine Mile RSA439 (Phase II, Clone 4) isolate (NMII) or an isogenic GFP-tagged isolate (59) was cultured in acidified citrate cysteine medium-2 (ACCM-2) for 7 days at 37°C, 5% CO_2, 2.5% O_2 (60). Bacteria were quantified using PicoGreen (61), concentrated by centrifugation (3000xg, 10min, 4°c), and resuspended in PBS containing 0.25 M sucrose (PBSS) and stored at –80°C until further use. Before infection, THP-1 cells (American Type Culture Collection, TIB-202) were differentiated in complete RPMI medium i.e. RPMI-1640 medium supplemented with 1 mM sodium pyruvate, 0.05 mM beta-mercaptoethanol, 4500 mg/L glucose, and

10% heat-inactivated fetal bovine serum (FBS) at 37°C under 5% CO_2 for 24 h using 30 nM phorbol 12-myristate 13-acetate (PMA), followed by 24 h of rest in PMA-free medium to differentiate cells into adherent, macrophage-like cells. Cells were infected with NMII at a multiplicity of infection (MOI) of 25 in serum-free medium for two hours and this time-point was considered to be 0 h post-infection (hpi). To remove extracellular bacteria, cells were washed three times with PBS followed by replacement with complete growth medium. This medium was replaced with the fresh complete growth medium at 72 hpi for subsequent experiments.

Illumina sequencing and pathway analysis

hAMs or macrophage-like THP-1 cells infected with *Coxiella burnetii* were analyzed at 72 h post-infection (hpi) to quantify gene expression. At this time-point, the growth medium was replaced with 1ml of TRI reagent (Life Technologies), and total RNA was extracted, and DNase treated (Invitrogen) as per manufacturer's instructions. Samples were sequenced using the Illumina NovaSeq 6000 platform at Yale Center for Genome Analysis, New Haven, CT. Differential gene expression analysis was performed using CLC Genomics Workbench v6.5 (Qiagen) and DESeq2 (62) after mapping the sequencing reads to the reference human genome (GRCh38) databases in CLC Genomics Workbench v6.5 (Qiagen). Differentially regulated genes were calculated using log2 fold-change ≥ 0.75 and an adjusted p-value ≤ 0.05 as cutoffs, compared to uninfected controls. Core analysis of the differentially expressed genes to find the enriched pathways was performed using Ingenuity Pathway Analysis (IPA, Qiagen) (63).

Cytokine secretion assay

PMA-differentiated THP-1 cells were infected with NMII at an MOI of 25. In addition, the cells were separately treated with 200 ng/mL of *E. coli* LPS for 3h and 5 mM ATP (Adenosine 5′-triphosphate disodium salt hydrate; Sigma-Aldrich) for 30 min as the positive control for proinflammatory cytokine secretion. Cytokine levels were assessed in supernatants collected from THP-1 cells using Th1/Th2 Cytokine & Chemokine 20-Plex ProcartaPlex Panel 1 (Invitrogen) at 48, 72, and 120 hpi. The levels of 12 cytokines [GM-CSF (CSF2), IFNγ (IFNG), IL-1β (IL1B), IL-2 (IL2), IL-4 (IL4), IL-5 (IL5), IL-6 (IL6), CXCL8 (IL-8), IL-12p70 (IL12A), IL-13 (IL13), IL-18 (IL18), TNFα (TNF)] and eight chemokines [(CCL11), GROα (CXCL1), IP-10 (CXCL10), MCP-1 (CCL2), MIP-1α (CCL3). MIP-1β (CCL4), RANTES (CCL5), SDF-1α (CXCL12)] were quantified according to the manufacturer's guidelines. Briefly, supernatants were centrifuged 10,000xg for 10 minutes to remove particulate matter and stored at -80°C till further use. In a 96-well plate, magnetic beads were added in appropriate wells, washed, and 50µL of prepared antigen standards, controls, or samples were added. The plate was shaken for 30 min at RT (500 rpm), followed by overnight incubation at 4°C. After incubation, the plate was shaken again for 30 min at RT (500 rpm), washed with 1X Wash Buffer, and incubated with the detection antibody (30 min, RT, 500 rpm). Then the plate was washed with 1X Wash Buffer, incubated with Streptavidin-Phycoerythrin (SAPE; 30 min, RT, 500rpm), followed by washing and addition of 120 µL of reading buffer to analyze median fluorescence intensity (MFI) within 30 minutes after the addition of reading buffer in a Luminex 200 instrument.

Single-cell sequencing

Fluorescence-activated cell sorting (FACS) of GFP-tagged *Coxiella*-infected and uninfected THP-1 cells was conducted at 48 hpi to separate infected (GFP-pos), bystander (GFP-neg), and uninfected (control) cells in BD FACSAria Fusion instrument. Single cell RNA-seq libraries were generated at Yale Center for Genome Analysis, New Haven, CT from at least 1000 cells each from GFP-pos, GFP-neg, and uninfected samples by capturing individual cells inside gel beads in emulsion (GEM) using single cell 3' v3 chemistry (10X Genomics). Single cell sequencing reads were processed for quality control and analyzed to compare cell clustering and differential gene expression within each population using Cell Ranger 3.1 pipeline (39). Single cell clusters were visualized using tSNE analysis using Loupe Cell Browser (10X Genomics) and log2 fold-change was defined as the ratio of UMI (unique molecular identifier) counts in each cluster relative to all other clusters (log2 fold-change ≥ 0.75 and p-value ≤ 0.05). Differentially regulated genes in each cluster were analyzed using IPA to identify enriched pathways.

Data availability

Sequencing reads from this study have been deposited at NCBI Sequence Read Archive (SRA) under the BioProject accession PRJNA679931.

ACKNOWLEDGEMENTS

This work was supported in part by National Institutes of Health grants AI123464 and AI133023 to RR.

REFERENCES

1. Graham JG, MacDonald LJ, Hussain SK, Sharma UM, Kurten RC, Voth DE. 2013. Virulent *Coxiella burnetii* pathotypes productively infect primary human alveolar macrophages. *Cell Microbiol* 15:1012–1025.
2. Marriott HM, Dockrell DH. 2007. The role of the macrophage in lung disease mediated by bacteria. *Exp Lung Res* 33:493–505.
3. Thakur A, Mikkelsen H, Jungersen G. 2019. Intracellular pathogens: host immunity and microbial persistence strategies. *J Immunol Res* 2019:1356540.
4. Eldin C, Mélenotte C, Mediannikov O, Ghigo E, Million M, Edouard S, Mege J-L, Maurin M, Raoult D. 2017. From Q fever to *Coxiella burnetii* infection: a paradigm change. *Clin Microbiol Rev* 30:115–190.
5. Hendrix LR, Samuel JE, Mallavia LP. 1991. Differentiation of *Coxiella burnetii* isolates by analysis of restriction-endonuclease-digested DNA separated by SDS-PAGE. *J Gen Microbiol* 137:269–276.
6. Beare PA, Samuel JE, Howe D, Virtaneva K, Porcella SF, Heinzen RA. 2006. Genetic diversity of the Q fever agent, *Coxiella burnetii*, assessed by microarray-based whole-genome comparisons. *J Bacteriol* 188:2309–2324.
7. Cunha LD, Ribeiro JM, Fernandes TD, Massis LM, Khoo CA, Moffatt JH, Newton HJ, Roy CR, Zamboni DS. 2015. Inhibition of inflammasome activation by *Coxiella burnetii* type IV secretion system effector IcaA. *Nat Commun* 6:10205.

8. Schoenlaub L, Cherla R, Zhang Y, Zhang G. 2016. *Coxiella burnetii* avirulent Nine Mile phase II induces caspase-1-dependent pyroptosis in murine peritoneal B1a B cells. *Infect Immun* 84:3638–3654.
9. Larson CL, Martinez E, Beare PA, Jeffrey B, Heinzen RA, Bonazzi M. 2016. Right on Q: genetics begin to unravel *Coxiella burnetii* host cell interactions. *Future Microbiol* 11:919–939.
10. Dragan AL, Voth DE. 2019. *Coxiella burnetii:* International pathogen of mystery. *Microbes Infect* 22:100-110.
11. Clemente TM, Mulye M, Justis AV, Nallandhighal S, Tran TM, Gilk SD. 2018. *Coxiella burnetii* blocks intracellular interleukin-17 signaling in macrophages. *Infect Immun* 86:e00532-18.
12. Rana A, Ahmed M, Rub A, Akhter Y. 2015. A tug-of-war between the host and the pathogen generates strategic hotspots for the development of novel therapeutic interventions against infectious diseases. *Virulence* 6:566–580.
13. Krakauer T. 2019. Inflammasomes, autophagy, and cell death: the trinity of innate host defense against intracellular bacteria. *Mediators Inflamm* 2019:2471215.
14. Long CM, Beare PA, Cockrell DC, Larson CL, Heinzen RA. 2019. Comparative virulence of diverse *Coxiella burnetii* strains. *Virulence* 10:133–150.
15. McLaughlin HP, Cherney B, Hakovirta JR, Priestley RA, Conley A, Carter A, Hodge D, Pillai SP, Weigel LM, Kersh GJ, Sue D. 2017. Phylogenetic inference of *Coxiella burnetii* by 16S rRNA gene sequencing. *PLoS One* 12:e0189910.
16. Chamoun MN, Blumenthal A, Sullivan MJ, Schembri MA, Ulett GC. 2018. Bacterial pathogenesis and interleukin-17: interconnecting mechanisms of

immune regulation, host genetics, and microbial virulence that influence severity of infection. *Crit Rev Microbiol* 44:465–486.

17. Li Y, Wei C, Xu H, Jia J, Wei Z, Guo R, Jia Y, Wu Y, Li Y, Qi X, Li Z, Gao X. 2018. The immunoregulation of Th17 in host against intracellular bacterial infection. *Mediators Inflamm* 2018:6587296.
18. Rose-John S, Winthrop K, Calabrese L. 2017. The role of IL-6 in host defence against infections: immunobiology and clinical implications. *Nat Rev Rheumatol* 13:399–409.
19. Del Valle DM, Kim-Schulze S, Huang H-H, Beckmann ND, Nirenberg S, Wang B, Lavin Y, Swartz TH, Madduri D, Stock A, Marron TU, Xie H, Patel M, Tuballes K, Van Oekelen O, Rahman A, Kovatch P, Aberg JA, Schadt E, Jagannath S, Mazumdar M, Charney AW, Firpo-Betancourt A, Mendu DR, Jhang J, Reich D, Sigel K, Cordon-Cardo C, Feldmann M, Parekh S, Merad M, Gnjatic S. 2020. An inflammatory cytokine signature predicts COVID-19 severity and survival. *Nat Med* 26:1636–1643.
20. Chanput W, Mes JJ, Wichers HJ. 2014. THP-1 cell line: an *in vitro* cell model for immune modulation approach. *Int Immunopharmacol* 23:37–45.
21. Ramstead AG, Robison A, Blackwell A, Jerome M, Freedman B, Lubick KJ, Hedges JF, Jutila MA. 2016. Roles of toll-like receptor 2 (TLR2), TLR4, and MyD88 during pulmonary *Coxiella burnetii* infection. *Infect Immun* 84:940–949.
22. Ghigo E, Capo C, Raoult D, Mege JL. 2001. Interleukin-10 stimulates *Coxiella burnetii* replication in human monocytes through tumor necrosis factor down-modulation: role in microbicidal defect of Q fever. *Infect Immun* 69:2345–2352.

23. Textoris J, Ban LH, Capo C, Raoult D, Leone M, Mege J-L. 2010. Sex-related differences in gene expression following *Coxiella burnetii* infection in mice: potential role of circadian rhythm. *PLoS One* 5:e12190.

24. Hayek I, Fischer F, Schulze-Luehrmann J, Dettmer K, Sobotta K, Schatz V, Kohl L, Boden K, Lang R, Oefner PJ, Wirtz S, Jantsch J, Lührmann A. 2019. Limitation of TCA cycle intermediates represents an oxygen-independent nutritional antibacterial effector mechanism of macrophages. *Cell Rep* 26:3502–3510.e6.

25. Boucherit N, Barry AO, Mottola G, Trouplin V, Capo C, Mege J-L, Ghigo E. 2012. Effects of *Coxiella burnetii* on MAPKinases phosphorylation. *FEMS Immunol Med Microbiol* 64:101–103.

26. Voth DE, Howe D, Heinzen RA. 2007. *Coxiella burnetii* inhibits apoptosis in human THP-1 cells and monkey primary alveolar macrophages. *Infect Immun* 75:4263–4271.

27. Luo T, Dunphy PS, Lina TT, McBride JW. 2015. *Ehrlichia chaffeensis* exploits canonical and noncanonical host Wnt signaling pathways to stimulate phagocytosis and promote intracellular survival. *Infect Immun* 84:686–700.

28. Amaral EP, Costa DL, Namasivayam S, Riteau N, Kamenyeva O, Mittereder L, Mayer-Barber KD, Andrade BB, Sher A. 2019. A major role for ferroptosis in *Mycobacterium tuberculosis*-induced cell death and tissue necrosis. *J Exp Med* 216:556–570.

29. Amatya N, Garg AV, Gaffen SL. 2017. IL-17 signaling: the yin and the yang. *Trends Immunol* 38:310–322.

30. Raimondo A, Lembo S, Di Caprio R, Donnarumma G, Monfrecola G, Balato N, Ayala F, Balato A. 2017. Psoriatic cutaneous inflammation promotes human monocyte differentiation into active osteoclasts, facilitating bone damage. *Eur J Immunol* 47:1062–1074.

31. Cheung PFY, Wong CK, Lam CWK. 2008. Molecular mechanisms of cytokine and chemokine release from eosinophils activated by IL-17A, IL-17F, and IL-23: implication for Th17 lymphocytes-mediated allergic inflammation. *J Immunol* 180:5625–5635.

32. Maertzdorf J, Osterhaus ADME, Verjans GMGM. 2002. IL-17 expression in human herpetic stromal keratitis: modulatory effects on chemokine production by corneal fibroblasts. *J Immunol* 169:5897–5903.

33. Jin W, Dong C. 2013. IL-17 cytokines in immunity and inflammation. *Emerg Microbes Infect* 2:e60.

34. Qian Y, Kang Z, Liu C, Li X. 2010. IL-17 signaling in host defense and inflammatory diseases. *Cell Mol Immunol* 7:328–333.

35. Jones CE, Chan K. 2002. Interleukin-17 stimulates the expression of interleukin-8, growth-related oncogene-alpha, and granulocyte-colony-stimulating factor by human airway epithelial cells. *Am J Respir Cell Mol Biol* 26:748–753.

36. Chung Y, Yamazaki T, Kim B-S, Zhang Y, Reynolds JM, Martinez GJ, Chang SH, Lim H, Birkenbach M, Dong C. 2013. Epstein Barr virus-induced 3 (EBI3) together with IL-12 negatively regulates T helper 17-mediated immunity to *Listeria monocytogenes* infection. *PLoS Pathog* 9:e1003628.

37. Cook DB, McLucas BC, Montoya LA, Brotski CM, Das S, Miholits M, Sebata TH. 2019. Multiplexing protein and gene level measurements on a single Luminex platform. *Methods* 158:27–32.

38. Benoit M, Barbarat B, Bernard A, Olive D, Mege J-L. 2008. *Coxiella burnetii*, the agent of Q fever, stimulates an atypical M2 activation program in human macrophages. *Eur J Immunol* 38:1065–1070.

39. Zheng GXY, Terry JM, Belgrader P, Ryvkin P, Bent ZW, Wilson R, Ziraldo SB, Wheeler TD, McDermott GP, Zhu J, Gregory MT, Shuga J, Montesclaros L, Underwood JG, Masquelier DA, Nishimura SY, Schnall-Levin M, Wyatt PW, Hindson CM, Bharadwaj R, Wong A, Ness KD, Beppu LW, Deeg HJ, McFarland C, Loeb KR, Valente WJ, Ericson NG, Stevens EA, Radich JP, Mikkelsen TS, Hindson BJ, Bielas JH. 2017. Massively parallel digital transcriptional profiling of single cells. *Nat Commun* 8:14049.

40. Isaacson B, Hadad T, Glasner A, Gur C, Granot Z, Bachrach G, Mandelboim O. 2017. Stromal Cell-Derived Factor 1 Mediates Immune Cell Attraction upon Urinary Tract Infection. *Cell Rep* 20:40–47.

41. Holmgren AM, McConkey CA, Shin S. 2017. Outrunning the Red Queen: bystander activation as a means of outpacing innate immune subversion by intracellular pathogens. *Cell Mol Immunol* 14:14–21.

42. Gessain G, Blériot C, Ginhoux F. 2020. Non-genetic heterogeneity of macrophages in diseases-a medical perspective. *Front Cell Dev Biol* 8:613116.

43. Marakalala MJ, Martinez FO, Plüddemann A, Gordon S. 2018. Macrophage heterogeneity in the immunopathogenesis of tuberculosis. *Front Microbiol* 9:1028.

44. Beare PA, Unsworth N, Andoh M, Voth DE, Omsland A, Gilk SD, Williams KP, Sobral BW, Kupko JJ, Porcella SF, Samuel JE, Heinzen RA. 2009. Comparative genomics reveal extensive transposon-mediated genomic plasticity and diversity among potential effector proteins within the genus *Coxiella*. *Infect Immun* 77:642–656.

45. Abnave P, Muracciole X, Ghigo E. 2017. *Coxiella burnetii* lipopolysaccharide: what do we know? *Int J Mol Sci* 18:2509.

46. Voth DE, Howe D, Beare PA, Vogel JP, Unsworth N, Samuel JE, Heinzen RA. 2009. The *Coxiella burnetii* ankyrin repeat domain-containing protein family is heterogeneous, with C-terminal truncations that influence Dot/Icm-mediated secretion. *J Bacteriol* 191:4232–4242.

47. Gu F-M, Li Q-L, Gao Q, Jiang J-H, Zhu K, Huang X-Y, Pan J-F, Yan J, Hu J-H, Wang Z, Dai Z, Fan J, Zhou J. 2011. IL-17 induces AKT-dependent IL-6/JAK2/STAT3 activation and tumor progression in hepatocellular carcinoma. *Mol Cancer* 10:150.

48. Shen F, Gaffen SL. 2008. Structure-function relationships in the IL-17 receptor: implications for signal transduction and therapy. *Cytokine* 41:92–104.

49. Kimizuka Y, Kimura S, Saga T, Ishii M, Hasegawa N, Betsuyaku T, Iwakura Y, Tateda K, Yamaguchi K. 2012. Roles of interleukin-17 in an experimental *Legionella pneumophila* pneumonia model. *Infect Immun* 80:1121–1127.

50. Gopal R, Monin L, Slight S, Uche U, Blanchard E, Fallert Junecko BA, Ramos-Payan R, Stallings CL, Reinhart TA, Kolls JK, Kaushal D, Nagarajan U, Rangel-Moreno J, Khader SA. 2014. Unexpected role for IL-17 in protective immunity against hypervirulent *Mycobacterium tuberculosis* HN878 infection. *PLoS Pathog* 10:e1004099.

51. Lin Y, Ritchea S, Logar A, Slight S, Messmer M, Rangel-Moreno J, Guglani L, Alcorn JF, Strawbridge H, Park SM, Onishi R, Nyugen N, Walter MJ, Pociask D, Randall TD, Gaffen SL, Iwakura Y, Kolls JK, Khader SA. 2009. Interleukin-17 is required for T helper 1 cell immunity and host resistance to the intracellular pathogen *Francisella tularensis*. *Immunity* 31:799–810.

52. Andoh M, Zhang G, Russell-Lodrigue KE, Shive HR, Weeks BR, Samuel JE. 2007. T cells are essential for bacterial clearance, and gamma interferon, tumor necrosis factor alpha, and B cells are crucial for disease development in *Coxiella burnetii* infection in mice. *Infect Immun* 75:3245–3255.

53. Schoenlaub L, Elliott A, Freches D, Mitchell WJ, Zhang G. 2015. Role of B cells in host defense against primary *Coxiella burnetii* infection. *Infect Immun* 83:4826–4836.

54. Elliott A, Peng Y, Zhang G. 2013. *Coxiella burnetii* interaction with neutrophils and macrophages in vitro and in SCID mice following aerosol infection. *Infect Immun* 81:4604–4614.

55. Bumann D. 2019. *Salmonella* single-cell metabolism and stress responses in complex host tissues. *Microbiol Spectr* 7:7-2.

56. Saliba A-E, Li L, Westermann AJ, Appenzeller S, Stapels DAC, Schulte LN, Helaine S, Vogel J. 2016. Single-cell RNA-seq ties macrophage polarization to growth rate of intracellular *Salmonella*. *Nat Microbiol* 2:16206.

57. Avraham R, Haseley N, Brown D, Penaranda C, Jijon HB, Trombetta JJ, Satija R, Shalek AK, Xavier RJ, Regev A, Hung DT. 2015. Pathogen cell-to-cell variability drives heterogeneity in host immune responses. *Cell* 162:1309–1321.

58. Graham JG, Winchell CG, Kurten RC, Voth DE. 2016. Development of an *ex vivo* tissue platform to study the human lung response to *Coxiella burnetii*. *Infect Immun* 84:1438–1445.

59. Martinez E, Cantet F, Fava L, Norville I, Bonazzi M. 2014. Identification of OmpA, a *Coxiella burnetii* protein involved in host cell invasion, by multi-phenotypic high-content screening. *PLoS Pathog* 10:e1004013.

60. Omsland A, Beare PA, Hill J, Cockrell DC, Howe D, Hansen B, Samuel JE, Heinzen RA. 2011. Isolation from animal tissue and genetic transformation of *Coxiella burnetii* are facilitated by an improved axenic growth medium. *Appl Environ Microbiol* 77:3720–3725.

61. Moses AS, Millar JA, Bonazzi M, Beare PA, Raghavan R. 2017. Horizontally acquired biosynthesis genes boost *Coxiella burnetii*'s physiology. *Front Cell Infect Microbiol* 7:174.

62. Love MI, Huber W, Anders S. 2014. Moderated estimation of fold change and dispersion for RNA-seq data with DESeq2. *Genome biology* 15:1-21.

63. Krämer A, Green J, Pollard J, Tugendreich S. 2014. Causal analysis approaches in Ingenuity Pathway Analysis. *Bioinformatics* 30:523–530.

Chapter IV

Gallium-Protoporphyrin IX inhibits *Coxiella burnetii* growth

The findings from this chapter are published as part of the following article:

Brenner AE, Muñoz-Leal S, **Sachan M**, Labruna MB, Raghavan R. 2021. *Coxiella burnetii* and related tick endosymbionts evolved from pathogenic ancestors. *Genome Biol Evol*, Volume 13, Issue 7, July 2021, evab108, https://doi.org/10.1093/gbe/evab108

ABSTRACT

Q fever is a global health threat caused by *Coxiella burnetii*, a highly infectious and environmentally stable intracellular pathogen. Due to the emergence of antibiotic resistance isolates and the need for effective treatment regimens to control chronic *C. burnetii* infections, there is an urgent need to develop new antimicrobial agents against the Q fever agent. Iron acquisition strategies are attractive targets for antimicrobial agents as many intracellular pathogens rely on host iron or iron-containing proteins such as heme during infection. In this study we explored *C. burnetii*'s dependence on heme by treating both axenically grown and intracellular bacteria with gallium-protoporphyrin IX (GaPPIX), a heme analog that can replace heme in heme-containing enzymes. Our results demonstrate that GaPPIX inhibits *C. burnetii* growth at very low concentrations without compromising host cellular viability. The antibacterial activity of GaPPIX warrants further investigation to identify the targets of this molecule and the potential application of heme analogs to treat *C. burnetii* infections.

INTRODUCTION

The Q fever pathogen *Coxiella burnetii* is widespread among livestock worldwide (1). Although antibiotic treatment exists for the acute infection, chronic *Coxiella* infections leading to endocarditis and chronic fatigue syndrome are difficult to treat and require 1.5 to 3 years long doxycycline and hydroxychloroquine treatment. In addition, antibiotic resistance isolates of *Coxiella* are becoming more prevalent (2). Thus, there is an urgent need to develop new anti-*Coxiella* agents (1, 3).

During infection, both intracellular bacterial pathogens and their host cells typically compete for nutrients such as iron and heme, an iron-protoporphyrin molecule, to support their growth and survival (4). Bacterial pathogens have evolved different strategies to scavenge host iron either in its free or bound form, as in hemoglobin and transferrin, to promote their intracellular growth (5). Therefore, bacterial iron and heme acquisition mechanisms have emerged as attractive targets for the development of new antimicrobial agents such as iron chelator and Gallium [Ga(III)], an iron mimic (6–9). For example, DIBI (3-hydroxypyridin-4-one chelator) is an iron chelator that restricts the host iron availability to *Acinetobacter baumannii* and inhibits its growth in mice (10).

Host iron has been shown to support intracellular replication of *C. burnetii*, and this bacterium loses its viability upon iron starvation (11). *C. burnetii* expresses a ferrous iron uptake transporter that can import ferrous iron (11). This ferrous iron is likely released from host iron-containing molecules under acidic conditions (11–13). In addition, *C. burnetii* is not known to harbor genes encoding any iron chelators or a transporter for ferric ions and iron-containing proteins (11).

Gallium (Ga) interferes with bacterial iron utilization because it binds with high avidity to iron-binding proteins to disrupt their functions (14). Unlike iron, Ga cannot reduce under physiological conditions resulting in inhibition of catalytic activities of many iron-containing proteins (15). Due to its ability to affect iron metabolism, Ga and its derivatives have been reported to inhibit the growth of intracellular pathogens, including *Francisella tularensis and Pseudomonas aeruginosa* (9, 16–18). Ga disrupts iron uptake by *Francisella* strains by chelating to iron-binding lactoferrin and transferrin in a murine pulmonary infection model (17). Gallium nitrate and gallium maltolate have been shown to exhibit bacteriostatic effects against ESKAPE pathogens such as *P. aeruginosa* and *Acinetobacter baumannii* (9). Intriguingly, gallium-protoporphyrin IX (GaPPIX), a Ga-containing heme analog, can inhibit *P. aeruginosa* by exerting bactericidal activities and targeting heme-dependent cytochrome (9). Combination of GaPPIX with gallium nitrate shows a synergistic effect against *P. aeruginosa* (19).

In this project, we explored *C. burnetii*'s dependence on heme by treating both axenically grown and intracellular *C. burnetii* with GaPPIX. GaPPIX is known to exploit heme-uptake routes to enter bacterial cells, where it could substitute for heme in heme-containing proteins such as cytochromes, catalases, and peroxidases to perturb vital cellular functions (20, 21). GaPPIX was demonstrated to inhibit *C. burnetii* growth at very low concentrations without compromising host cellular viability, indicating that gallium compounds could potentially be used to treat *C. burnetii* infections.

RESULTS

GaPPIX inhibits *C. burnetii* growth in axenic conditions

To investigate the effect of perturbing the functions of heme-containing proteins in *C. burnetii*, we tested increasing concentrations of GaPPIX on *C. burnetii* grown in the axenic ACCM-2 medium. Measurement of the bacterial growth showed that 250 nM of GaPPIX caused significant inhibition of *C. burnetii* growth in ACCM-2 compared to the mock-treated control. At 72 h post-treatment, 8 µM of GaPPIX resulted in almost 3-fold growth inhibition compared to control **(Figure 1)**.

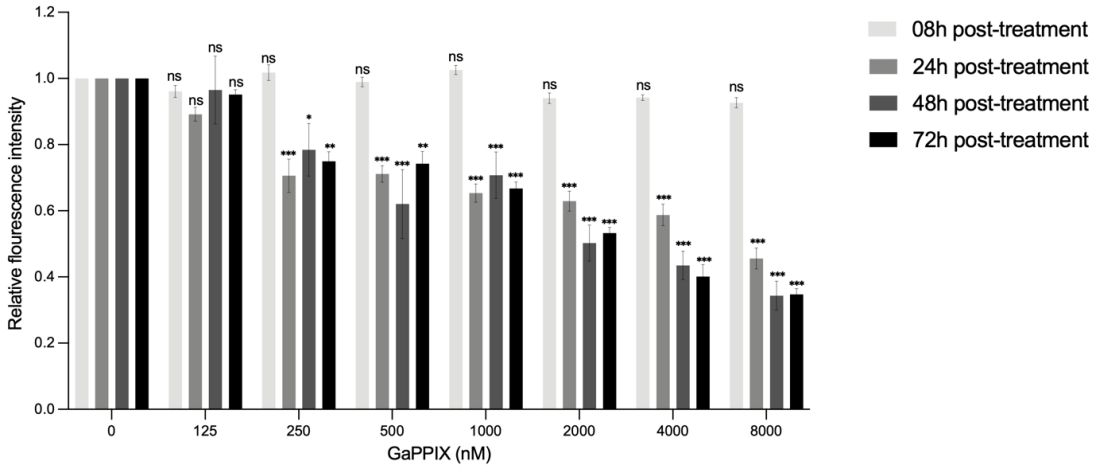

Figure 1. GaPPIX inhibits axenic growth of *C. burnetii*. Bacteria growing in ACCM-2 were exposed to concentrations of GaPPIX shown on x-axis and were quantified using PicoGreen at 8 h, 24 h, 48 h, and 72 h post-treatment. Data shown are mean fluorescence intensity (± SE) compared to the vehicle control (dimethyl sulfoxide, no GaPPIX). Statistical significance was analyzed using two-way repeated measures ANOVA followed by Dunnett's test (*$p \leq 0.01$, **$p \leq 0.001$, ***$p \leq 0.0001$; n = 5).

GaPPIX inhibits intracellular growth of *C. burnetii*

To determine whether GaPPIX has any impact on the growth of *C. burnetii* within macrophages, we measured the effect of several concentrations of GaPPIX on actively replicating *C. burnetii* inside THP-1 cells. Treatment with 2 µM of GaPPIX resulted in significant growth impairment of *C. burnetii* within THP-1 cells at 72 h post-treatment. When exposed to 8 µM of GaPPIX, the growth was reduced ~2.3 fold compared to mock-treated control as measured by qPCR and colony-forming units (CFU) assays. Although the growth inhibition at 8 µM GaPPIX treatment was slightly less compared to axenic medium treated with the same amount of this molecule, *C. burnetii* was found to be susceptible to GaPPIX-mediated growth inhibition.

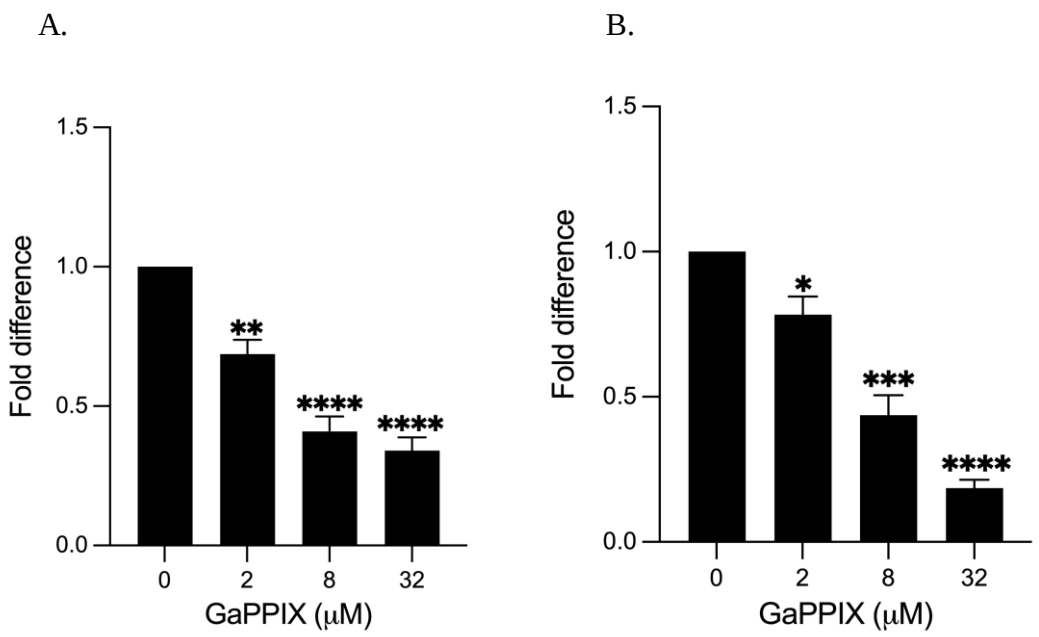

Figure 2. GaPPIX inhibits *C. burnetii* growth within macrophages. At 72h post-treatment with GaPPIX, bacterial growth within THP-1 cells was quantified using (A) qPCR and (B) CFU assays. Intracellular bacterial growth is shown as mean fold difference (± SE) compared to control (no GaPPIX) on x-axes, and y-axes show the concentrations of GaPPIX used in the assays. Statistical significance was analyzed using one-way ANOVA followed by Dunnett's test (*$p \leq 0.05$, **$p \leq 0.01$, ***$p \leq 0.001$, ****$p \leq 0.0001$; n = 3).

GaPPIX is not cytotoxic to macrophages

A cytotoxicity assay was conducted to determine whether GaPPIX-mediated growth inhibition was due to a toxic effect of GaPPIX on the macrophages themselves. This assay quantifies the extracellular lactate dehydrogenase (LDH) released by cells upon damage to the plasma membrane. THP-1 cells were treated with various concentrations of GaPPIX for 24 h, and the levels of released LDH in supernatants was measured. GaPPIX at concentrations of 8, 32, and 128 µM did not significantly reduce the cellular viability of THP-1 cells compared to mock-treated controls. Exposure to 512 µM concentration of GaPPIX was found to be cytotoxic to THP-1 cells indicating that at least a 128 µM concentration of this heme-analogue can be tolerated by the cells.

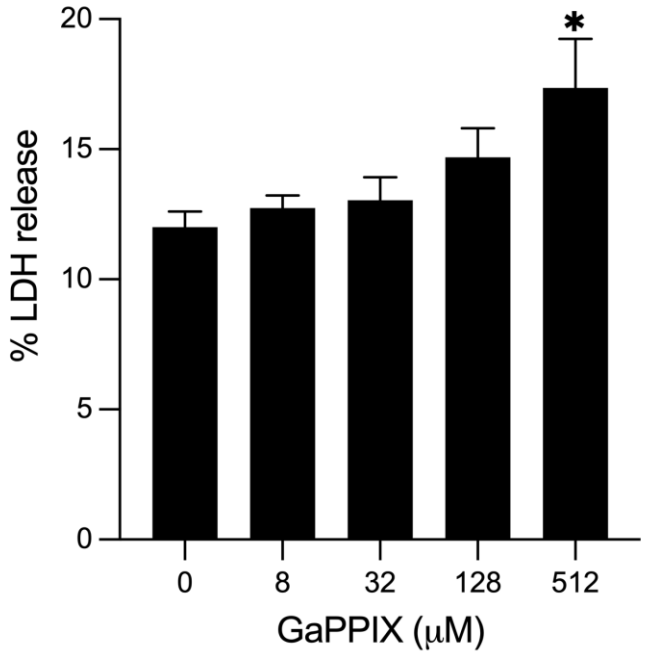

Figure 3. Cytotoxicity assessment of GaPPIX. At 24h post-GaPPIX treatment of THP-1 cells, lactate dehydrogenase (LDH) activity was determined by measuring the level of resorufin formation using an LDH cytotoxicity assay. The cytotoxicity was reported as the percentage LDH released compared to the maximum LDH activity. Data shown as the mean percentage LDH released (± SEM). Statistical significance was analyzed using one-way ANOVA followed by Dunnett's test (*$p \leq 0.05$, $n = 3$).

DISCUSSION

Iron is an essential micronutrient to virtually most organisms, including bacteria. However, access to free iron inside the host is a challenging endeavor faced by intracellular bacterial pathogens as free iron is typically bound to heme or other iron-binding proteins such as transferrin or lactoferrin (22). Pathogens have evolved several mechanisms to obtain iron from their hosts, including (a) high-affinity iron chelators or siderophores, (b) iron transport systems, (c) direct uptake of heme and other bound forms of host iron, (d) expressing the iron acquisition receptors of host iron-containing proteins, and (e) inducing ferritinophagy, a selective form of autophagy causing ferritin degradation to increase the cellular labile iron pool (4, 22, 23).

The iron acquisition strategies in *C. burnetii* are not well elucidated as it does not contain any known siderophore and transporter for ferric ions or iron-containing molecules such as heme (11). But the presence of the genes encoding ferrous iron uptake transporter FeoAB in *C. burnetii* suggests that this pathogen can import ferrous iron released from host iron-containing proteins under acidic conditions that can contribute to the bacterial heme biosynthesis (12). Indeed, *C. burnetii* replication is supported by iron-containing proteins such as hemoglobin, ferritin, and transferrin in the axenic medium (11).

Ga-based compounds target bacterial iron metabolism in a “Trojan horse” type of approach (24). Ga(III) inhibits bacterial growth because it binds to biological complexes that typically bind to Fe(III). However, under physiological conditions, Ga(III) is not reduced to Ga(II), thereby disrupting essential redox-driven biological processes (15).

Therefore, to test the *C. burnetii*'s dependence on perturbing the functions of heme-containing proteins, we exposed the bacterium to GaPPIX, a Ga(III) complex of protoporphyrin IX. We chose GaPPIX over other gallium-based formulations because it could replace heme in cytochromes and other heme-containing enzymes, is known to be bactericidal, and is not toxic to primary human fibroblasts and established cell lines (9, 21, 25). This heme analog was found to be very effective at inhibiting both axenic and intracellular growth of *C. burneti* in a dose-dependent manner without causing cytotoxicity to the host cells at concentrations that inhibit bacterial growth. Although GaPPIX is similar to heme, it is not known whether this similarly can also lead to possible off-target effects due to the presence of host heme-binding proteins.

GaPPIX has been reported to use heme-uptake pathways (7, 12), but *C. burnetii* lacks homologs of known heme transporters. Therefore, it is unclear whether it is the free or protoporphyrin bound Ga that enters into this pathogen and inhibits its growth. Further, a recent study on macrophages infected with *Ehrlichia chaffeensis* showed that *E. chaffeensis* bacterium secretes an effector through type IV secretion system that binds to ferritin and induces ferritinophagy, a process that results in an enhanced cellular labile iron pool that could enhance bacterial proliferation (23). Whether *C. burnetii* secretes an effector to induce iron or heme release from the host iron or heme-containing proteins is unknown. Together, it can be speculated that treatment with GaPPIX may result in the cytosolic release of Ga due to the acidic CCV (26). The released gallium thus may potentially be transported inside the bacterial by the bacterial iron uptake transporter (12).

In addition to the direct inhibition of intracellular pathogens through its Fe(III)-competitive activity, Ga can affect ribonucleotide reductase, mitochondrial activities, ferritin and transferrin receptors, and promote anti-inflammatory activity in different animal models (14, 18, 27). Encouragingly, a recent human trial showed that Ga could improve lung function in people with cystic fibrosis and chronic *Pseudomonas aeruginosa* lung infections, and that the molecule worked synergistically with other antibiotics to inhibit bacterial growth (24). Gallium can result in impaired function of ribonucleotide reductase, mitochondrial activities, and the regulation of ferritin and transferrin receptors. Although further work is required to gauge its off-target effects and impact on the human microbiome, Ga, which the FDA has approved for intravenous administration, and its derivatives, such as GaPPIX, hold great promise as new therapeutic tools against *C. burnetii* (28).

MATERIALS AND METHODS

Axenic susceptibility assay

A 10mM GaPPIX (Frontier Scientific) solution was prepared in dimethyl sulfoxide (DMSO) and was stored at 4°C under dark conditions until further use. *C. burnetii* was cultured in ACCM-2 for 2 days at 37°C, 5% CO_2 and 2.5% O_2, and ~$2x10^7$ genome equivalents were resuspended in fresh ACCM-2 containing 0 nM, 125 nM, 250 nM, 500 nM, 1 mM, 2 mM, 4 mM, or 8 mM GaPPIX in 96-well black-bottom microplates (Greiner Bio-One). Bacterial growth was measured using PicoGreen (Invitrogen) as described previously (12).

Intracellular susceptibility assay

THP-1 human monocytes (ATCC, TIB-202) were cultured in sterile RPMI-1640 medium (Gibco) supplemented with 1 mM sodium pyruvate, 0.05 mM beta-mercaptoethanol, 1% Pen-Strep, and 4500 mg/L glucose with 10% heat-inactivated fetal bovine serum (FBS) at 37°C, 5% CO_2 in 6-well tissue culture plates. Prior to infection, cells were differentiated into macrophages by treating with 30 nM phorbol 12-myristate 13-acetate (PMA) for 24 h, followed by resting in PMA-free RPMI for 24 h. Infection of THP-1 cells with *C. burnetii* was carried out using a 7 days bacterial culture at a multiplicity of infection of 25. After briefly washing the cells with PBS, the bacteria-containing medium was added to each well and the plates were centrifuged at 25 x g for 10 minutes followed by incubation at 37°C, 5% CO_2 for two hours. To remove extracellular bacteria, cells were washed three times with PBS, and replaced with antibiotic-free RPMI and were incubated for 48 h before treating with GaPPIX- (2 μM, 8 μM, and 32 μM) or DMSO- (as control) containing media. After 72 h post-treatment, cells were washed three times with PBS and intracellular bacterial load was measured.

To quantify intracellular bacteria using qPCR, cells were washed, and total DNA was extracted using QIAamp DNA Mini Kit (Qiagen) according to the manufacturer's instructions. 70 ng of total DNA, measured by NanoDrop 2000 (Thermo Scientific), was then subjected to qPCR using CBU_tRNA-Glu-2-specific primers and SYBR Green, as described previously (12). Ct values were converted to the bacterial genome equivalents (GE) using a standard curve, as described previously (12, 29). To validate the qPCR results, we independently quantified intracellular bacteria by enumerating Colony-forming units (CFU) (30, 31). Briefly, infected cells were washed and lysed in ice-cold

water for 40 min at 4°C followed by repeated aspiration with a syringe carrying a 25G needle to lyse the remaining cells. The suspension was centrifuged for 10 min at 70 x g (4°C) followed by centrifugation of the supernatant for 1 min at 13,500 x g (4°C). The pellet was resuspended in ACCM-2, serially diluted and was spot-plated on ACCM-2 containing 0.5 mM tryptophan and 0.5% agarose as described by Sanchez et al., 2018 (30). Plates were incubated for 10 days at 37°C, 5% CO_2, and 2.5% O_2 before counting the colonies.

Cytotoxicity assay

Cytotoxicity was determined by measuring the levels of released lactate dehydrogenase (LDH) within supernatants using an LDH cytotoxicity assay kit (Invitrogen). In brief, 50,000 PMA-differentiated THP-1 cells per well were incubated in triplicate wells in a clear 96-well plate. Following incubation, the cells were washed with PBS and treated with GaPPIX (DMSO, 8, 32, 128, and 512μM) containing RPMI media supplemented with 1% FBS. At 24h post-treatment, the LDH activity was determined using 50 μL each sample medium in a 96-well flat-bottom plate by measuring the level of resorufin formation (Ex/Em = 560/590 nm) in Biotek synergy HT plate reader (Biotek, Winooski, VT) according to the manufacturer's instructions. The cytotoxicity was reported as the percentage LDH detected compared to the maximum LDH activity in the fully lysed cells.

ACKNOWLEDGEMENTS

This work was supported in part by National Institutes of Health grants AI123464 and AI133023 to RR.

REFERENCES

1. Madariaga MG, Rezai K, Trenholme GM, Weinstein RA. 2003. Q fever: a biological weapon in your backyard. *Lancet Infect Dis* 3:709–721.
2. Rolain J-M, Lambert F, Raoult D. 2005. Activity of telithromycin against thirteen new isolates of *C. burnetii* including three resistant to doxycycline. *Ann N Y Acad Sci* 1063:252–256.
3. Kersh GJ. 2013. Antimicrobial therapies for Q fever. *Expert Rev Anti Infect Ther* 11:1207–1214.
4. Cassat JE, Skaar EP. 2013. Iron in infection and immunity. *Cell Host Microbe* 13:509–519.
5. Gomes AC, Moreira AC, Mesquita G, Gomes MS. 2018. Modulation of iron metabolism in response to infection: twists for all tastes. *Pharmaceuticals (Basel)* 11:84.
6. Thompson MG, Corey BW, Si Y, Craft DW, Zurawski DV. 2012. Antibacterial activities of iron chelators against common nosocomial pathogens. *Antimicrob Agents Chemother* 56:5419–5421.
7. Vinuesa V, McConnell MJ. 2021. Recent advances in iron chelation and gallium-based therapies for antibiotic resistant bacterial infections. *Int J Mol Sci* 22.
8. Smith DJ, Lamont IL, Anderson GJ, Reid DW. 2013. Targeting iron uptake to control *Pseudomonas aeruginosa* infections in cystic fibrosis. *Eur Respir J* 42:1723–1736.

9. Hijazi S, Visaggio D, Pirolo M, Frangipani E, Bernstein L, Visca P. 2018. Antimicrobial activity of gallium compounds on ESKAPE pathogens. *Front Cell Infect Microbiol* 8:316.

10. Parquet MDC, Savage KA, Allan DS, Ang MTC, Chen W, Logan SM, Holbein BE. 2019. Antibiotic-resistant *Acinetobacter baumannii* is susceptible to the novel iron-sequestering anti-infective DIBI *in vitro* and in experimental pneumonia in Mice. *Antimicrob Agents Chemother* 63:e00855-19.

11. Sanchez SE, Omsland A. 2020. Critical role for molecular iron in *Coxiella burnetii* replication and viability. *mSphere* 5:e00458-20.

12. Moses AS, Millar JA, Bonazzi M, Beare PA, Raghavan R. 2017. Horizontally acquired biosynthesis genes boost *Coxiella burnetii*'s physiology. *Front Cell Infect Microbiol* 7:174.

13. Brenner AE, Muñoz-Leal S, Sachan M, Labruna MB, Raghavan R. 2021. *Coxiella burnetii* and related tick endosymbionts evolved from pathogenic ancestors. *Genome Biol Evol*. 13:evab108.

14. Chitambar CR. 2016. Gallium and its competing roles with iron in biological systems. *Biochim Biophys Acta* 1863:2044–2053.

15. Bernstein LR. 1998. Mechanisms of therapeutic activity for gallium. *Pharmacol Rev* 50:665–682.

16. Choi S-R, Britigan BE, Moran DM, Narayanasamy P. 2017. Gallium nanoparticles facilitate phagosome maturation and inhibit growth of virulent *Mycobacterium tuberculosis* in macrophages. *PLoS One* 12:e0177987.

17. Olakanmi O, Gunn JS, Su S, Soni S, Hassett DJ, Britigan BE. 2010. Gallium disrupts iron uptake by intracellular and extracellular *Francisella* strains and exhibits therapeutic efficacy in a murine pulmonary infection model. *Antimicrob Agents Chemother* 54:244–253.

18. Bernstein LR, Zhang L. 2020. Gallium maltolate has *in vitro* antiviral activity against SARS-CoV-2 and is a potential treatment for COVID-19. *Antivir Chem Chemother* 28:2040206620983780.

19. Choi S-R, Britigan BE, Narayanasamy P. 2019. Dual inhibition of *Klebsiella pneumo*niae and *Pseudomonas aeruginosa* iron metabolism using gallium porphyrin and gallium nitrate. *ACS Infect Dis* 5:1559–1569.

20. Hijazi S, Visca P, Frangipani E. 2017. Gallium-protoporphyrin IX inhibits *Pseudomonas aeruginosa* growth by targeting cytochromes. *Front Cell Infect Microbiol* 7:12.

21. Stojiljkovic I, Kumar V, Srinivasan N. 1999. Non-iron metalloporphyrins: potent antibacterial compounds that exploit haem/Hb uptake systems of pathogenic bacteria. *Mol Microbiol* 31:429–442.

22. Zughaier SM, Cornelis P. 2018. Editorial: role of iron in bacterial pathogenesis. *Front Cell Infect Microbiol* 8:344.

23. Yan Q, Zhang W, Lin M, Teymournejad O, Budachetri K, Lakritz J, Rikihisa Y. 2021. Iron robbery by intracellular pathogen via bacterial effector-induced ferritinophagy. *Proc Natl Acad Sci USA* 118:23.

24. Goss CH, Kaneko Y, Khuu L, Anderson GD, Ravishankar S, Aitken ML, Lechtzin N, Zhou G, Czyz DM, McLean K, Olakanmi O, Shuman HA, Teresi M,

Wilhelm E, Caldwell E, Salipante SJ, Hornick DB, Siehnel RJ, Becker L, Britigan BE, Singh PK. 2018. Gallium disrupts bacterial iron metabolism and has therapeutic effects in mice and humans with lung infections. *Sci Transl Med* 10:460.

25. Arivett BA, Fiester SE, Ohneck EJ, Penwell WF, Kaufman CM, Relich RF, Actis LA. 2015. Antimicrobial activity of gallium protoporphyrin IX against *Acinetobacter baumannii* strains displaying different antibiotic resistance phenotypes. *Antimicrob Agents Chemother* 59:7657–7665.
26. Sala D, Ciambellotti S, Giachetti A, Turano P, Rosato A. 2017. Investigation of the iron(II) release mechanism of human H-ferritin as a function of pH. *J Chem Inf Model* 57:2112–2118.
27. de Albuquerque Wanderley Sales V, Timóteo TRR, da Silva NM, de Melo CG, Ferreira AS, de Oliveira MVG, de Oliveira Silva E, Dos Santos Mendes LM, Rolim LA, Neto PJR. 2021. A systematic review of the anti-inflammatory effects of gallium compounds. *Curr Med Chem* 28:2062–2076.
28. Bonchi C, Imperi F, Minandri F, Visca P, Frangipani E. 2014. Repurposing of gallium-based drugs for antibacterial therapy. *Biofactors* 40:303–312.
29. Martinez E, Cantet F, Bonazzi M. 2015. Generation and multi-phenotypic high-content screening of *Coxiella burnetii* transposon mutants. *J Vis Exp* e52851.
30. Sanchez SE, Vallejo-Esquerra E, Omsland A. 2018. Use of axenic culture tools to study *Coxiella burnetii*. *Curr Protoc Microbiol* 50:e52.
31. Hayek I, Fischer F, Schulze-Luehrmann J, Dettmer K, Sobotta K, Schatz V, Kohl L, Boden K, Lang R, Oefner PJ, Wirtz S, Jantsch J, Lührmann A. 2019.

Limitation of TCA cycle intermediates represents an oxygen-independent nutritional antibacterial effector mechanism of macrophages. *Cell Rep* 26:3502–3510.e6.

Chapter V. Discussion and future considerations

I. Summary

When challenged with pathogens, host alveolar macrophages typically attempt to control the infection through a spectrum of defense processes, including induction of apoptosis, autophagy, inflammatory response, and nutrients sequestration (1). In the last decade, modulation of microRNAs (miRNAs), a critical component of host regulatory networks, has emerged as an integral part of the host-pathogen interactions that can regulate multiple host defensive or pathogen offensive processes (2). Previously, we have shown that the expression of miRNAs gets perturbed in macrophages infected with *C. burnetii*, an obligate intracellular bacterial pathogen (3). However, whether microRNAs have any functional implication in host-*C. burnetii* interactions is undefined. In the present study, I explored the contribution of miRNAs in *C. burnetii* infection. Further, I studied the potential impact of inflammation and heme-acquisition strategies in *C. burnetii*-infected alveolar macrophages.

My investigation of differentially expressed miRNAs and mRNAs in THP-1 cells infected with NMII isolate of *C. burnetii*, from 8 hours to 5 days post-infection (dpi), showed that this pathogen induces the expression of time-specific sets of host genes. The highest magnitude of host response i.e., number of differentially expressed miRNAs and mRNAs was observed at 3 dpi compared to other time points. It is likely that during later stages of infection, developmental transitions of *C. burnetii* from its metabolically active large cell variants (LCVs) into dormant small cell variants (SCVs) may induce stage-specific sets of host genes (4, 5). Inverse expression pairing of miRNAs with their

potential targets and pathway enrichment analysis of these targets suggests that miRNAs modulation might be an integral host response to *C. burnetii* infection.

Pathway analysis of the targets of miRNAs showed that inhibition of apoptosis is one among many processes that are likely under miRNA regulation. Like several other intracellular pathogens, *C. burnetii* is known to antagonize host apoptosis induction, for example, by activating Akt and recruiting Bcl-2 to the *Coxiella*-containing vacuole (6, 7). Using a qRT-PCR based array, we found that at least 14 apoptosis-related miRNAs likely contribute to apoptosis modulation in *C. burnetii* infection. Among these, *C. burnetii* infection showed downregulation of miR-143-3p and upregulation of miR-146a-5p, probably in response to the lipopolysaccharide (LPS) of *C. burnetii*, as found in other studies with LPS-stimulated macrophages (8–12). Functional studies done by transfection of miR-143-3p mimic on HeLa cells, show that this miRNA could promote apoptosis, inhibit autophagy, and induce the production of pro-inflammatory cytokines. miR-143-3p was observed to reduce the expression of pro-survival proteins such as Akt, Bcl-2, ATP6V1A, and xCT, suggesting that the induction of these proteins is critical for *C. burnetii* survival. Interestingly, we found that miR-143-3p mimic could significantly inhibit the intracellular growth of *C. burnetii* compared to the control. Together, our data show that miRNAs are an integral component of macrophage response to *C. burnetii* infection, and inhibition of miR-143-3p expression during *C. burnetii* infection might facilitate the pathogen's intracellular growth.

The gene expression analysis in NMII-infected THP-1 cells showed the activation of several inflammatory pathways inside the host. To understand the contribution of inflammatory signaling in response to different isolates of *C. burnetii*, we compared the

differentially expressed genes in primary human alveolar macrophages infected with NMI, NMII, Dugway, or Graves isolates as mentioned in Chapter III (13). We showed that infection with Dugway, an avirulent rodent isolate of *C. burnetii*, resulted in more differentially regulated genes than human isolates (NMI, NMII, and Graves) in human alveolar macrophages. Unlike avirulent isolates, virulent *C. burnetii* can escape or antagonize the inflammatory response probably by LPS-mediated shielding of bacterial surface proteins from the immune recognition or through its type IV secretion system (T4SS) effectors (14, 15). Therefore, it appears that avirulent *C. burnetii* Dugway isolate fails to suppress the robust host inflammatory response and being a rodent isolate gets promptly recognized by the human immune response (16).

Several pro-inflammatory and pro-survival pathways, including IL-17 signaling, PI3K/Akt signaling, and autophagy were found to be activated in infected macrophages. To understand the effect of IL-17 signaling on the inflammatory response to *C. burnetii*, we performed a pathway reconstruction of this signaling pathway and found that several genes that are downstream of IL-17 signaling (17) were consistently upregulated in *C. burnetii*-infected macrophages. These genes include chemokines or cytokines (CCL3, CCL4, CCL5, CXCL1, and IL1B) that can recruit immune cells or mount proinflammatory host responses at the site of infection. Cytokine secretion assays confirmed that these molecules were secreted into the culture medium at higher levels than in uninfected macrophages. *C. burnetii* is known to antagonize the IL-17 signaling by reducing expression of IL1B, CCL5, and a few other genes through its T4SS effectors (18). Therefore, it appears that despite the strong activation of host proinflammatory response, including IL-17 signaling, *C. burnetii* can survive inside the macrophages by

antagonizing or escaping from proinflammatory immune response. Interestingly, single-cell investigation of inflammation-associated pathways suggests that *C. burnetii* infection leads to a range of inflammatory states among the subpopulations of infected macrophages, and some of these subpopulations seem relatively more hospitable for the bacterial growth than others.

Lastly, iron sequestration is a well-known macrophage response against intracellular pathogens (1, 19). Many intracellular pathogens rely on host iron-containing proteins such as heme to promote their intracellular survival (20). Despite the limited information available about *C. burnetii'*s iron or heme acquisition strategies, Chapter IV explores *C. burnetii*'s dependence on heme by treating both axenically grown and intracellular bacteria with gallium-protoporphyrin IX (GaPPIX) (21). This heme analog can replace heme in heme-containing proteins such as cytochrome b (22). Although the mechanism by which GaPPIX inhibits *C. burnetii* growth is not defined, these results demonstrate that GaPPIX inhibits *C. burnetii* growth at very low concentrations without compromising host cellular viability.

Collectively, these studies advance our understanding of host-*C. burnetii* interactions. Chapter II reveals that miRNAs, specifically miR-143-3p, have a functional contribution in regulating the host response to *C. burnetii* infection. Chapter III shows the impact of different *C. burnetii* isolates on host inflammatory responses and suggests that some subpopulations of infected macrophages are likely more pathogen-friendly than others. Chapter IV shows that GaPPIX, a heme-analog, inhibits *C. burnetii* growth without compromising cellular viability. Together, these results could contribute to developing novel miRNA or GaPPIX based therapeutic agents and could be applied to

better understanding the virulence strategies of other intracellular pathogens such as *Mycobacterium tuberculosis, Legionella pneumophila,* and *Chlamydia trachomatis* (23–25).

II. Future considerations

The present work points toward several future avenues in the study of host-*Coxiella* interactions. The miRNAs identified in this study could potentially unveil a new area of miRNA-based diagnosis and host-directed therapeutics in Q fever. Future investigations to find whether and how the transfection of miR-143-3p mimic can regulate intracellular growth of virulent *C. burnetii* in an animal model of Q fever would be helpful to enhance our understanding of *Coxiella*'s pathogenesis. Further, our study shows a strong upregulation of miR-146a-5p in the *C. burnetii* infected macrophages compared to the uninfected cells. This miRNA is well known for its anti-inflammatory nature. To investigate its function, we can transfect the macrophages with an inhibitor of miR-146a-5p and assess its impact on inflammation and bacterial growth at different intervals after infection. Such approaches might be helpful to understand how miR-146a-5p potentially fine-tunes the host inflammation and could be beneficial to develop novel therapeutics against acute and chronic *C. burnetii* infection.

Single-cell data suggest that some macrophage subpopulations are more supportive of bacterial growth than others. By utilizing the antibodies against the antigens of dormant (SCVs) or replicative (LCVs) variants of *C. burnetii*, we can assess how the different intracellular state of this pathogen drives the heterogeneity in host immune response. Moreover, GaPPIX, a heme analog, is predicted to interfere with heme-

dependent proteins such as cytochrome b to impair bacterial metabolism. Using inductively coupled plasma mass spectrometry (ICP-MS), the trafficking of total gallium atoms can be measured in the different cellular parts of *C. burnetii*. This approach will be helpful to further understand the molecules and processes associated with bacterial growth inhibition.

REFERENCES

1. Kaufmann SHE, Dorhoi A. 2016. Molecular determinants in phagocyte-bacteria interactions. *Immunity* 44:476–491.
2. Aguilar C, Mano M, Eulalio A. 2019. MicroRNAs at the host-bacteria interface: host defense or bacterial offense. *Trends Microbiol* 27:206–218.
3. Millar JA, Valdés R, Kacharia FR, Landfear SM, Cambronne ED, Raghavan R. 2015. *Coxiella burnetii* and *Leishmania mexicana* residing within similar parasitophorous vacuoles elicit disparate host responses. *Front Microbiol* 6:794.
4. Coleman SA, Fischer ER, Howe D, Mead DJ, Heinzen RA. 2004. Temporal analysis of *Coxiella burnetii* morphological differentiation. *J Bacteriol* 186:7344–7352.
5. Sandoz KM, Popham DL, Beare PA, Sturdevant DE, Hansen B, Nair V, Heinzen RA. 2016. Transcriptional profiling of *Coxiella burnetii* reveals extensive cell wall remodeling in the small cell variant developmental Form. *PLoS One* 11:e0149957.
6. Voth DE, Heinzen RA. 2009. Sustained activation of Akt and Erk1/2 is required for *Coxiella burnetii* antiapoptotic activity. *Infect Immun* 77:205–213.
7. Vázquez CL, Colombo MI. 2010. *Coxiella burnetii* modulates Beclin 1 and Bcl-2, preventing host cell apoptosis to generate a persistent bacterial infection. *Cell Death Differ* 17:421–438.
8. Tamgue O, Gcanga L, Ozturk M, Whitehead L, Pillay S, Jacobs R, Roy S, Schmeier S, Davids M, Medvedeva YA, Dheda K, Suzuki H, Brombacher F, Guler R. 2019. Differential targeting of c-Maf, Bach-1, and Elmo-1 by

microRNA-143 and microRNA-365 promotes the intracellular growth of *Mycobacterium tuberculosis* in alternatively IL-4/IL-13a activated macrophages. *Front Immunol* 10:421.

9. He M, Wu N, Leong MC, Zhang W, Ye Z, Li R, Huang J, Zhang Z, Li L, Yao X, Zhou W, Liu N, Yang Z, Dong X, Li Y, Chen L, Li Q, Wang X, Wen J, Zhao X, Lu B, Yang Y, Wang Q, Hu R. 2020. miR-145 improves metabolic inflammatory disease through multiple pathways. *J Mol Cell Biol* 12:152–162.
10. Cobos Jiménez V, Bradley EJ, Willemsen AM, van Kampen AHC, Baas F, Kootstra NA. 2014. Next-generation sequencing of microRNAs uncovers expression signatures in polarized macrophages. *Physiol Genomics* 46:91–103.
11. Narasaki CT, Toman R. 2012. Lipopolysaccharide of *Coxiella burnetii*. *Adv Exp Med Biol* 984:65–90.
12. Naqvi AR, Zhong S, Dang H, Fordham JB, Nares S, Khan A. 2016. Expression profiling of LPS responsive miRNA in primary human macrophages. *J Microb Biochem Technol* 8:136–143.
13. Beare PA, Samuel JE, Howe D, Virtaneva K, Porcella SF, Heinzen RA. 2006. Genetic diversity of the Q fever agent, *Coxiella burnetii*, assessed by microarray-based whole-genome comparisons. *J Bacteriol* 188:2309–2324.
14. Abnave P, Muracciole X, Ghigo E. 2017. *Coxiella burnetii* lipopolysaccharide: what do we know? *Int J Mol Sci* 18:2509.
15. Cunha LD, Ribeiro JM, Fernandes TD, Massis LM, Khoo CA, Moffatt JH, Newton HJ, Roy CR, Zamboni DS. 2015. Inhibition of inflammasome activation

by *Coxiella burnetii* type IV secretion system effector IcaA. *Nat Commun* 6:10205.

16. Long CM, Beare PA, Cockrell DC, Larson CL, Heinzen RA. 2019. Comparative virulence of diverse *Coxiella burnetii* strains. *Virulence* 10:133–150.
17. Amatya N, Garg AV, Gaffen SL. 2017. IL-17 signaling: the yin and the yang. *Trends Immunol* 38:310–322.
18. Clemente TM, Mulye M, Justis AV, Nallandhighal S, Tran TM, Gilk SD. 2018. *Coxiella burnetii* blocks intracellular interleukin-17 signaling in macrophages. *Infect Immun* 86:e00532-18.
19. Cassat JE, Skaar EP. 2013. Iron in infection and immunity. *Cell Host Microbe* 13:509–519.
20. Vinuesa V, McConnell MJ. 2021. Recent advances in iron chelation and gallium-based therapies for antibiotic resistant bacterial infections. *Int J Mol Sci* 22:2876.
21. Sanchez SE, Omsland A. 2020. Critical role for molecular iron in *Coxiella burnetii* replication and viability. *mSphere* 5:e00458-20.
22. Hijazi S, Visca P, Frangipani E. 2017. Gallium-Protoporphyrin IX inhibits *Pseudomonas aeruginosa* growth by targeting cytochromes. *Front Cell Infect Microbiol* 7:12.
23. Li M, Wang J, Fang Y, Gong S, Li M, Wu M, Lai X, Zeng G, Wang Y, Yang K, Huang X. 2016. microRNA-146a promotes mycobacterial survival in macrophages through suppressing nitric oxide production. *Sci Rep* 6:23351.
24. Herkt CE, Caffrey BE, Surmann K, Blankenburg S, Gesell Salazar M, Jung AL, Herbel SM, Hoffmann K, Schulte LN, Chen W, Sittka-Stark A, Völker U,

Vingron M, Marsico A, Bertrams W, Schmeck B. 2020. A microRNA network controls *Legionella pneumophila* replication in human macrophages via LGALS8 and MX1. *mBio* 11.

25. Benyeogor I, Simoneaux T, Wu Y, Lundy S, George Z, Ryans K, McKeithen D, Pais R, Ellerson D, Lorenz WW, Omosun T, Thompson W, Eko FO, Black CM, Blas-Machado U, Igietseme JU, He Q, Omosun Y. 2019. A unique insight into the MiRNA profile during genital chlamydial infection. *BMC Genomics* 20:143.

APPENDIX

Appendix A: Chapter II Supplementary tables

Table S1. Differentially expressed miRNAs and mRNAs in NMII infected THP-1 derived macrophages

File name: Table II_S1.ods

File size (required software): 589 kb (Microsoft Excel)

Table S2. Inverse expression pairs of differentially expressed miRNAs and mRNAs

File name: Table II_S2.ods

File size (required software): 522 kb (Microsoft Excel)

Table S3. List of enriched pathways that contain miRNAs-target genes

File name: Table II_S3.ods

File size (required software): 27 kb (Microsoft Excel)

Table S4. List of downregulated proteins that were identified by mass spectrometry in miR-143-3p transfected HeLa cells

File name: Table II_S4.ods

File size (required software): 55 kb (Microsoft Excel)

Table S5. List of primers used in this study

File name: Table II_S5.ods

File size (required software): 3 kb (Microsoft Excel)

Appendix B: Chapter III Supplementary tables

Table S1. Differentially expressed genes in hAMs infected with different *C. burnetii* isolates

File name: Table III_S1.ods

File size (required software): 91 kb (Microsoft Excel)

Table S2. Differentially expressed genes in THP-1 cells infected with NMII isolate

File name: Table III_S2.ods

File size (required software): 389 kb (Microsoft Excel)

Table S3. List of enriched pathways in hAMs and THP-1 cells infected with *C. burnetii*

File name: Table III_S3.ods

File size (required software): 36 kb (Microsoft Excel)

Table S4. Cytokine secretion assay in THP-1 cells

File name: Table III_S4.ods

File size (required software): 6 kb (Microsoft Excel)

Table S5. Enriched pathways in infected, bystander and uninfected THP-1 cells

File name: Table III_S5.ods

File size (required software): 23 kb (Microsoft Excel)